DETERMINATION OF VOID FRACTION IN A GAS-LIQUID MIXTURE

BY AN ULTRASONIC TECHNIQUE

by

James Chi-Kung Tai

The velocity of sound at a frequency much greater than resonance in a bubbly air-water mixture has been measured for varying void fractions in a "pool" system. The present investigation was an extension of earlier work by Card. The object in the present work was to find the effect of certain additives in the water (particularly those affecting the surface tension) on the relation between a_m and B. As with Card, the generating frequency was 500 kHz, the gas was air, but the liquids tested included tap water, distilled water, deionized distilled water, tap water of increased surface tension due to the addition of potassium chloride (KCl), tap water of decreased surface tension due to detergent addition and a soap solution.

Compressed air was forced into a column of water (or water plus additive) at various velocities and the resulting void fractions determined by measuring the change in static pressure between two points in the mixture column. The velocity of sound was determined by measuring the time for a pulse of ultrasonic waves to travel between two diametrically opposed crystal transducers. A photographic technique was employed to obtain bubble-size distributions of the mixture of air and distilled water.

A very significant difference in the velocity of sound at the high frequency of 500 kHz compared with existing low-frequency results was found previously by Card; this difference was verified in the present work. Further, the present investigation indicated that there was a dramatic decrease in the curve of acoustic velocity versus void fraction when transition and slug flow developed. There appeared to be a tendency

THE UNIVERSITY OF MANITOBA ELIZABETH DAFOE LIBRARY

for lower acoustic velocities with increasing surface tension in curves of acoustic velocity versus void fraction, although this conclusion is somewhat tentative. A new method of categorizing flow regions was proposed based only on measurements of superficial velocity in the pool versus void fraction.

DETERMINATION OF VOID FRACTION IN A GAS-LIQUID MIXTURE BY AN ULTRASONIC TECHNIQUE

Thesis

Presented to

The Faculty of Graduate Studies

The University of Manitoba

In Partial Fulfillment

of the Requirements for the Degree

Master of Science

by

James Chi-Kung Tai

September 1970

© James Chi-Kung Tai 1971

ABSTRACT

The velocity of sound at a frequency much greater than resonance in a bubbly air-water mixture has been measured for varying void fractions in a "pool" system. The present investigation was an extension of earlier work by Card. The object in the present work was to find the effect of certain additives in the water (particularly those affecting the surface tension) on the relation between a_m and B. As with Card, the generating frequency was 500 kHz, the gas was air, but the liquids tested included tap water, distilled water, deionized distilled water, tap water of increased surface tension due to the addition of potassium chloride (KCl), tap water of decreased surface tension due to detergent addition and a soap solution.

Compressed air was forced into a column of water (or water plus additive) at various velocities and the resulting void fractions determined by measuring the change in static pressure between two points in the mixture column. The velocity of sound was determined by measuring the time for a pulse of ultrasonic waves to travel between two diametrically opposed crystal transducers. A photographic technique was employed to obtain bubble-size distributions of the mixture of air and distilled water.

A very significant difference in the velocity of sound at the high frequency of 500 kHz compared with existing low-frequency results was found previously by Card; this difference was verified in the present work. Further, the present investigation indicated that there was a dramatic decrease in the curve of acoustic velocity versus void fraction when transition and slug flow developed. There appeared to be a tendency

for lower acoustic velocities with increasing surface tension in curves of acoustic velocity versus void fraction, although this conclusion is somewhat tentative. A new method of categorizing flow regions was proposed based only on measurements of superficial velocity in the pool versus void fraction.

ACKNOWLEDGEMENTS

This study was carried out under the direction of Professor G. E. Sims and Professor R. E. Chant, whose advice and support were invaluable.

Thanks are due to Mr. D. C. Card and Mr. I. Robson for their assistance and helpful discussions and to Mr. L. Wilkins of the Mechanical Engineering Machine Shop for his help in modifications to the apparatus.

TABLE OF CONTENTS

LIST OF FIGURES

LIST OF TABLES

NOMENCLATURE

a	velocity of sound
B	void fraction
c	velocity of light in free space
d	diameter of bubbles
K	compressibility
V	ratio of volume of gas to volume of liquid
$\dot{v}''$	superficial gas velocity
w	frequency

Greek Letters

δ	damping constant
ρ	density

Subscripts

0	void fraction measured by column height
1	void fraction measured by pressure drop at tap position 1
2	void fraction measured by pressure drop at tap position 2
g	gas
gr	group
l	liquid
m	gas-liquid mixture
o	resonant
ph	phase
s	signal

CHAPTER 1

INTRODUCTION

The acoustical properties of a liquid are affected by the existence of even very small quantities of gas bubbles, due to the very large difference between the compressibilities of the two phases. Indeed, the velocity of sound through a gas-liquid mixture a_m is a function of the void fraction B where the void fraction is defined as the ratio of the volume of the gas phase to the total mixture volume. This is demonstrated in references [2,15 and 16]. The relationship between a_m and B is applicable in many fields, such as the determination of void fractions in boiling water nuclear reactors [24], underwater tunnels [21], and two-phase flow through nozzles [1].

Many investigators [1,7,12,18,21,23] have measured the acoustic velocity in gas-liquid mixtures as a function of void fraction with sonic frequencies (less than 20 kHz). Some investigators [8,15] have measured the acoustic velocity as a function of frequency extending into the ultrasonic range, but for very low void fractions (of the order of 10^{-4}). Card [2] was the first to report experimental results for the acoustic velocity of a gas-liquid mixture as a function of the void fraction over a wide range of void fractions at an ultrasonic frequency (500 kHz). His report [2,3] indicates that the high-frequency velocity of sound in a bubbly gas mixture is much higher than that obtained at low frequencies.

The present investigation is an extension of Card's work. The object in the present investigation is to find the effect of certain additives in the water (particularly those affecting the surface tension) on the relation between a_m and B. As with Card, the generating frequency is 500 kHz and a "pool" system is used; the gas is again air but liquids tested include tap water, distilled water, deionized distilled water, tap water of increased surface tension due to the addition of potassium chloride (KCl), tap water of decreased surface tension due to detergent addition and a soap solution. A photographic technique is employed to obtain bubble-size distributions of the mixture of air and distilled water.

CHAPTER 2

EXISTING WORK

2.1 Existing theory

The existing theory dealing with the acoustic velocity in a gas-liquid mixture has been developed in references [3,15,19 and 24].

The existence of gas bubbles in a liquid has an effect on the acoustic velocity of the mixture. This is due mainly to the change in the mean compressibility of the mixture caused by the gas bubbles. These gas bubbles begin a damped volume pulsation due to an applied sound field. Some of the applied energy is converted into heat by thermal damping, some is attenuated by viscous effects, and some is re-radiated as new sound waves. These new sound waves interact with the applied sound waves to some extent which depends upon frequency.

The gas-liquid mixture has a resonant frequency w_o, which varies inversely as the mean diameter of the bubles [14,18]. Attenuation is a maximum at the frequency corresponding to the resonant frequency [14,18]. The acoustic velocity and attenuation in a mixture depend upon the void fraction B, the bubble size d, and the applied frequency w. The radial movement of bubbles is nearly in phase with the imposed sound pressure when the applied frequency is much lower than the resonant frequency. If, however, the applied frequency is much greater than the resonant frequency then the displacement of the bubbles lags the applied pressure by approximately 180°.

The ratio of the velocity of sound in the mixture to that in the free liquid (a_m/a_l), depends upon the ratio of density of compressibility of the mixture to those of the free liquid. This may be expressed as:

$$\frac{a_m}{a_l} = [\frac{\rho_m}{\rho_l}\frac{K_m}{K_l}]^{-1/2} \tag{1}$$

For small gas content in a mixture, the density of the mixture is approximately equal to the density of the free liquid. Then

$$\frac{a_m}{a_l} \cong (\frac{K_m}{K_l})^{-1/2} \tag{2}$$

Meyer and Skudrzyk [13] considered the effect of the change in compressibility and obtained the following expression:

$$\frac{a_m}{a_l} = [1 + \frac{B(\frac{a_l}{a_g})^2 \; \frac{\rho_l}{\rho_g}}{[1-B][1-(\frac{w}{w_o})^2 + j\,\frac{w}{w_o}\,\delta]}]^{-1/2} \tag{3}$$

Equation (3) was derived on the assumption that the gas content is low and the density of the mixture is about the same as that of liquid, and that the effect of acoustic interactions* between bubbles has been neglected. In the high-frequency case, where $w/w_o >> 1$, and damping constant δ is less than one (the resonant damping constant given by Devin [6] is less than 0.2, and the maximum value used in literature [15] is 0.5), the real part of equation (3) gives the phase velocity of sound in the mixture for the high frequency case as:

* The term "acoustical interactions" refers to scattering, reflection and re-radiation of waves.

$$\frac{a_{ph}}{a_1} = [1 - \frac{B(\frac{a_1}{a_g})^2 \frac{\rho_1}{\rho_g}}{(1-B)(\frac{w}{w_o})^2}]^{-1/2} \tag{4}$$

The group velocity in a dispersive medium [28,29,30] is given by

$$\frac{1}{a_{gr}} = \frac{d}{dw}(\frac{w}{a_{ph}}) = \frac{1}{a_{ph}} + w\frac{d}{dw}(\frac{1}{a_{ph}}) \tag{5}$$

By substituting equation (4) into equation (5), the group velocity of sound at a very high frequency can therefore be obtained as:

$$\frac{a_{gr}}{a_1} = [1 - \frac{B(\frac{a_1}{a_g})^2 \frac{\rho_1}{\rho_g}}{(1-B)(\frac{w}{w_o})^2}]^{1/2} \tag{6}$$

which is the inverse of the phase velocity. As will be seen later, this equation is of special interest in the present research.

There are four velocities in connection with the propagation of waves; and they are phase velocity, signal velocity, group velocity and velocity of energy transport. These velocities sometimes are difficult to identify because of the distortion of the wave train in a highly dispersive medium. When the applied frequency is well below resonance these four velocities are virtually identical, being real and relatively independent of frequency. In the resonant region they all differ markely. However, at frequencies high above resonance the group velocity, signal velocity and energy velocity are approximately equal but usually less than the phase velocity.

Brillouin [29] has mentioned that forerunners may travel ahead of the main signal but become attentuated to a sufficient degree that their magnitude is negligible compared with the magnitude of the main signal. He defined the signal velocity as the propagation of the front of the main signal. Towne [30] has defined the group velocity as the velocity with which the approximate boundaries of the wave group propagate. However, as mentioned above, at frequencies far from resonance (both higher and lower) these velocities are nearly identical.

In the present work and in Card's work [2], the signal velocity is the one which has been measured. In comparing experimental results with existing theory, relations for theory (e.g. equation (6)) give the group velocity. But again it is stressed that for the frequencies used in the present and in Card's investigation, the group and signal velocities are virtually equal [3].

No theory is known to exist for high-frequency sound waves in a bubbly mixture of high void-fraction.

2.2 Previous experimental work

In this section, the work of Card [2],[3], of which the present work is an extension, will be treated in detail. Card's is the most recent work known to the author. A very good review of work prior to that of Card is given in reference [2].

Card's experimental work was with a "pool" system. Bubbles were generated in the water by forcing compressed air through a sparger, the sparger being fixed at the bottom of a perspex tube. The tube was 3.75 in. in inside diameter, 4.25 in. in outside diameter and 44 in. in length.

The flow of the compressed air was controlled by a set of needle and reducing valves. The flow rate of compressed air was measured by an orifice plate assembly complete with manometers.

Void fractions were determined by measuring the change in hydrostatic pressure between two fixed points in the mixture with an inverted U-tube manometer. Air was contained in the top of U-tube manometer and the manometer was inclined so as to give a sensitive reading of void fraction.

The 500 kHz ultrasonic signal was generated by a Krautkrämer water proof, barium titanate crystal transducer. The signal was received by the same type transducer. The two transducers were mounted diametrically opposite each other through the tube wall. The acoustic velocity of the air-water mixture was determined by measuring the transit time of the signal on a Tetronix storage oscilloscope.

Bubble-size distribution histograms were obtained using a photographic technique.

The most important accomplishment of Card's work was the successful measurement of the acoustic velocity in the two-phase mixture using an ultrasonic technique; these results are shown in Fig. 2.1 for bubbly flow. Also included on the figure is a curve representing the results for the zero-frequency case. The figure shows dramatically the differences in acoustic velocity using low- and high- frequency signal generation. In the low-void-fraction range ($B<0.055$) it is probably valid [3] to compare the observed results with equation (6). Fig. 2.2 shows such a comparison, the experimental data falling within 2% of that predicted by equation (6).

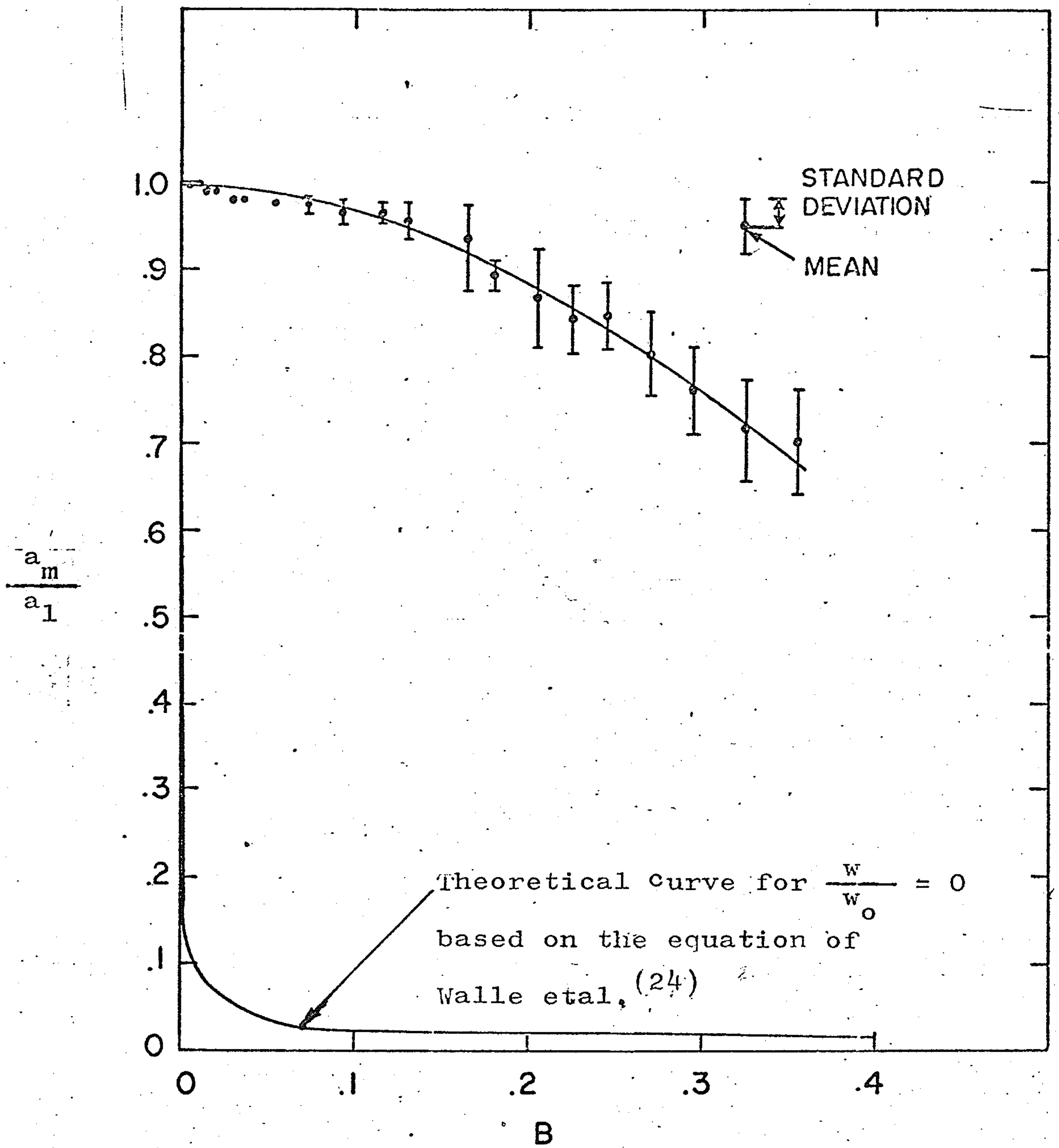

Fig. 2.1 SIGNAL VELOCITY OF SOUND vs VOID FRACTION FOR AIR-WATER MIXTURE AT 500 kHz(Card's work)

Fig. 2.1

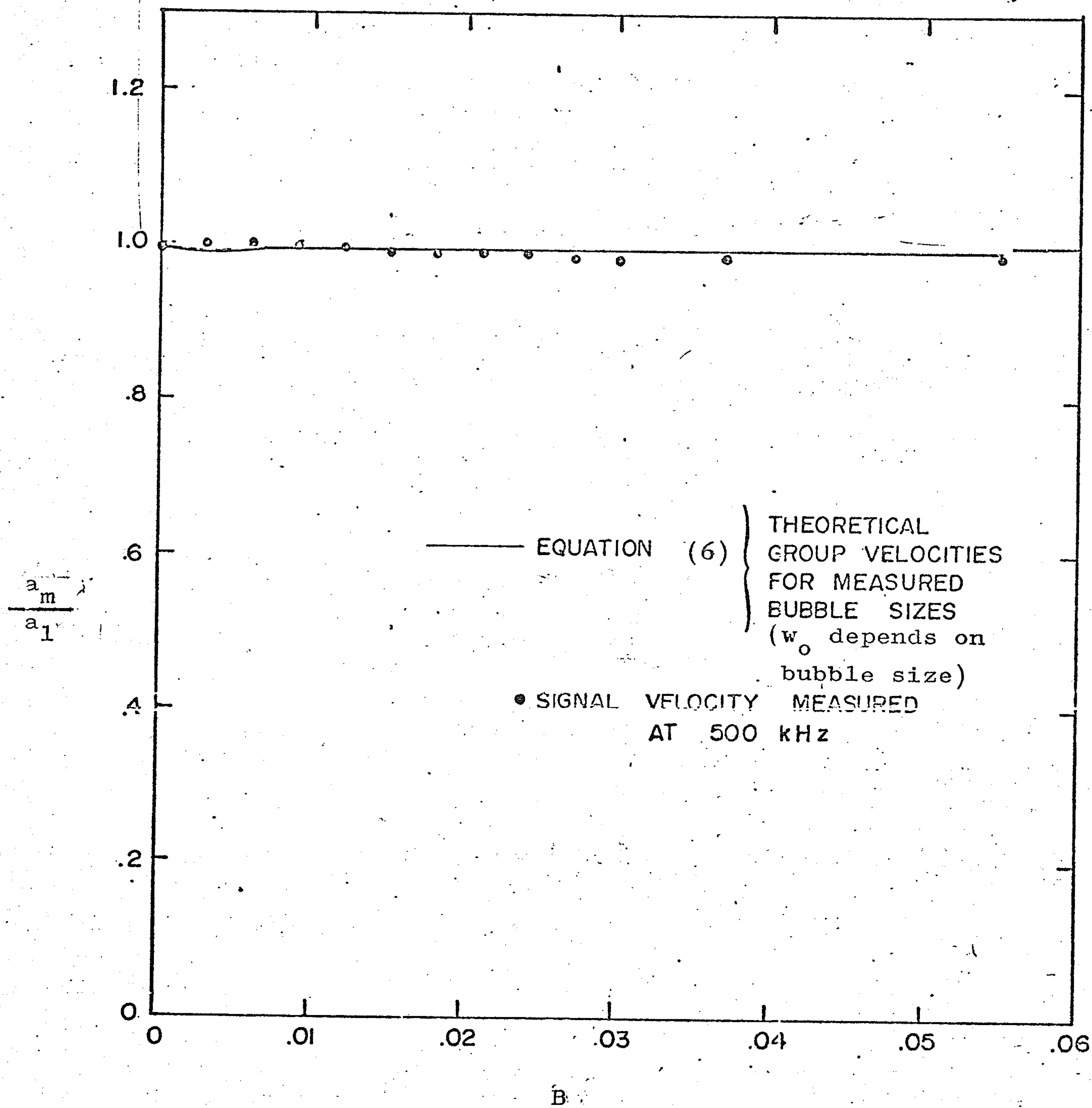

Fig. 2.2 SIGNAL VELOCITY OF SOUND FOR AIR-WATER MIXTURE IN THE LOW VOID FRACTION RANGE(Card's work)

Fig. 2.2

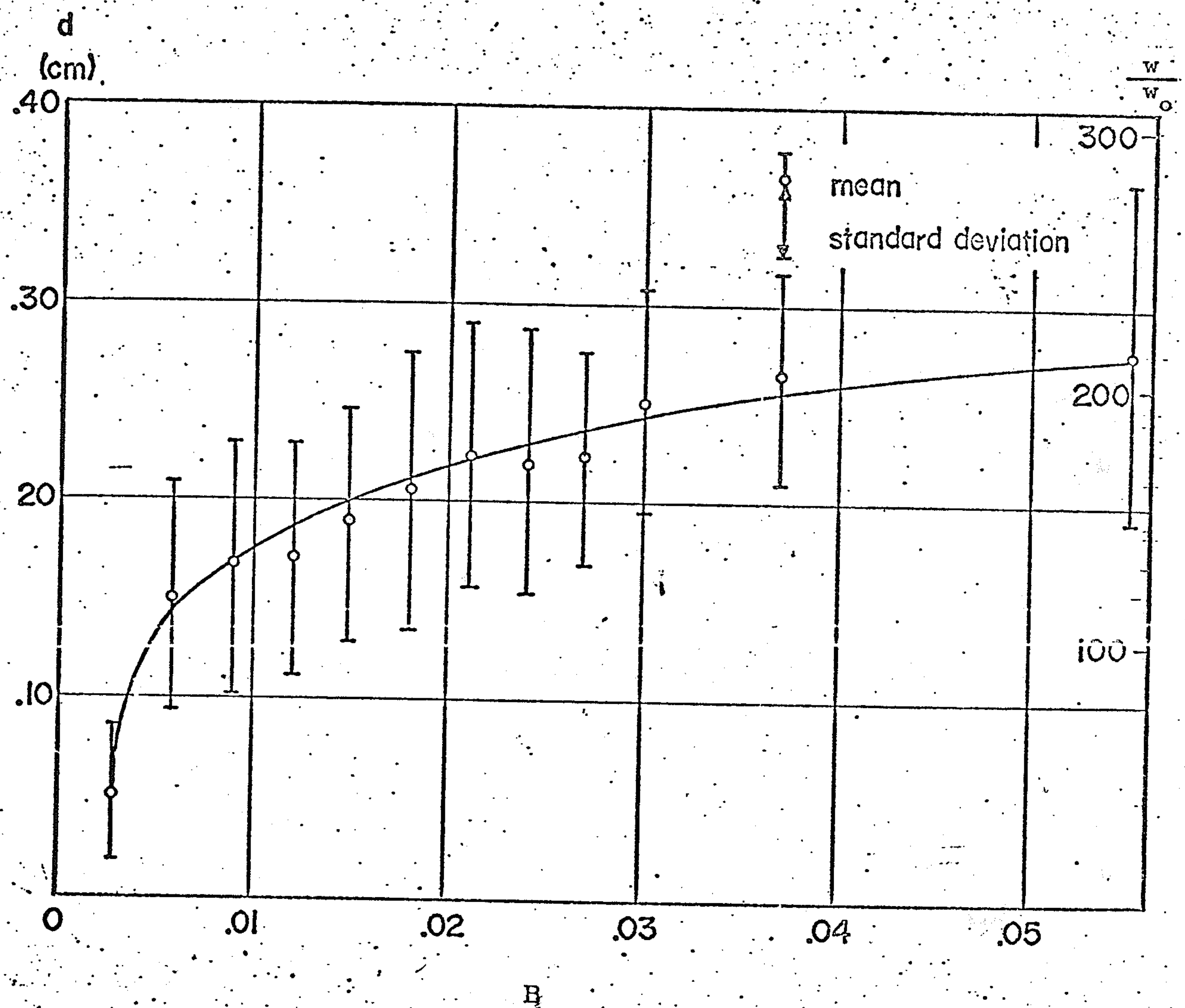

Fig. 2.3 Mean Bubble Diameter and Frequency Ratio versus Void Fraction (Card's work)

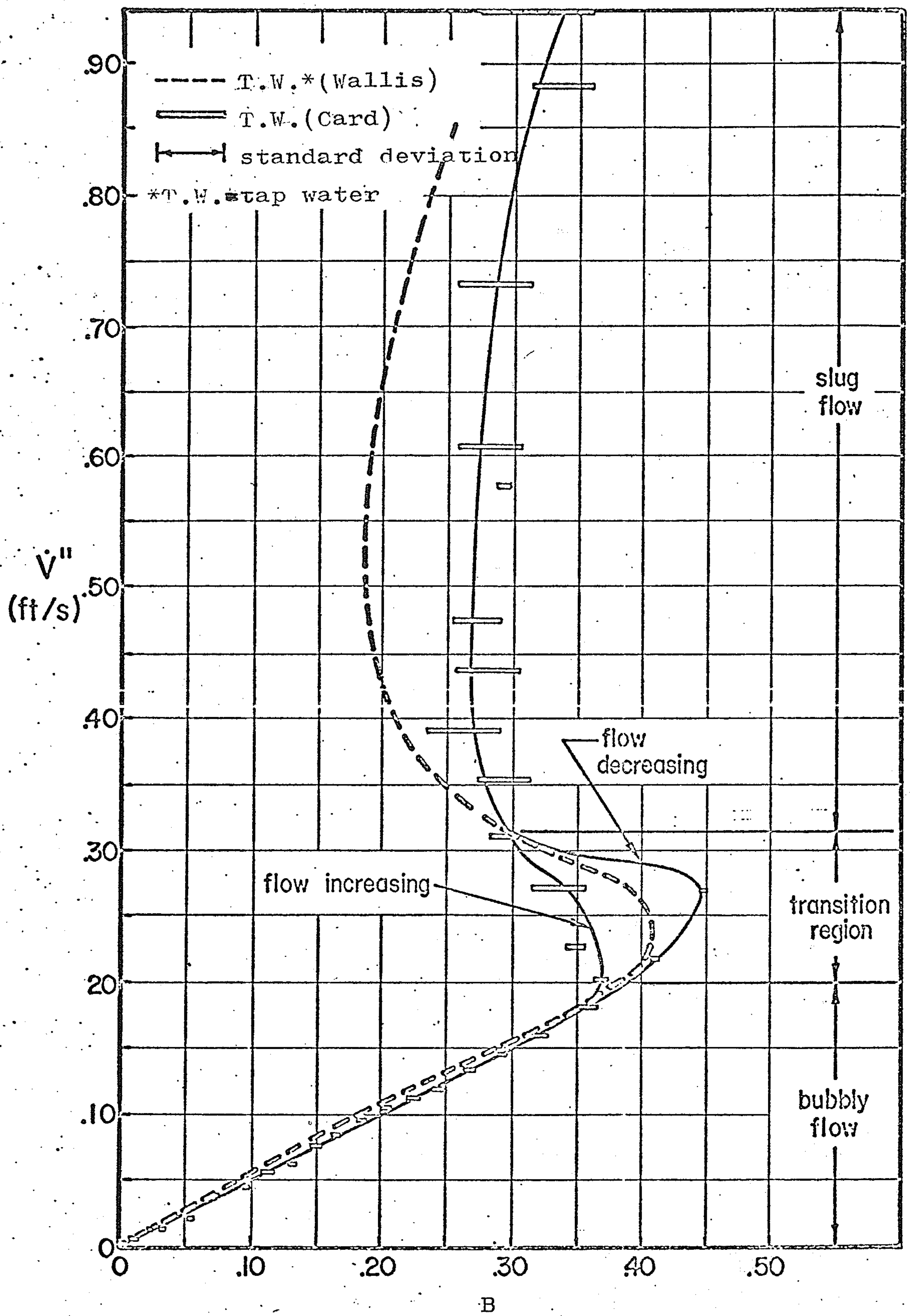

Fig. 2.4 Superficial air velocity versus void fraction(Card)

Fig. 2.4

Card's measurements of bubble sizes for various void fractions are shown in Fig. 2.3 and will be used later in the present work. Card's results of superficial air velocity versus void fraction are shown in Fig. 2.4; the results of Wallis [25] for a similar system are also shown in this figure for comparison purposes. It should be noted that Card's results agree resonably well with Wallis' for $B<0.35$; that in the transition region, B depends on whether the air flow rate is increasing or decreasing; and that the variation of measured void fractions becomes larger in the transition and slug flow regions.

CHAPTER 3

APPARATUS

3.1 Test section

A perspex tube* (3.75 in. in inside diameter, 4.25 in. in outside diameter, 44 in. in length) was used for purposes of:

(i) containing the test liquid,

(ii) measuring the height of the column of gas-liquid mixture, and

(iii) allowing pictures to be taken of the rising bubbles because of its transparency.

The tube was fitted with a perspex plate at the bottom. In this plate was fastened a sparger containing a porous stainless steel plate (maximum diameter of pores was 20 microns), and a drain plug.**

Compressed air tubing was connected to the bottom of the sparger so that the air could enter the liquid in a fairly uniform distribution of bubbles. (The area of the porous surface was 0.935 of the cross-sectional area inside the tube.) The flow rate of compressed air was controlled by a needle and a reducing valve, and was measured by two rotameters. The pressure of air in the system was measured by a manometer. The apparatus is shown in Fig. 3.1. Photographs of the complete apparatus are shown in Figs. 3.2, 3.3, 3.4.

---

* The same tube used by Card in his work except that more taps were fixed on it.

** A more complete description is given in appendix D of Card's thesis [2].

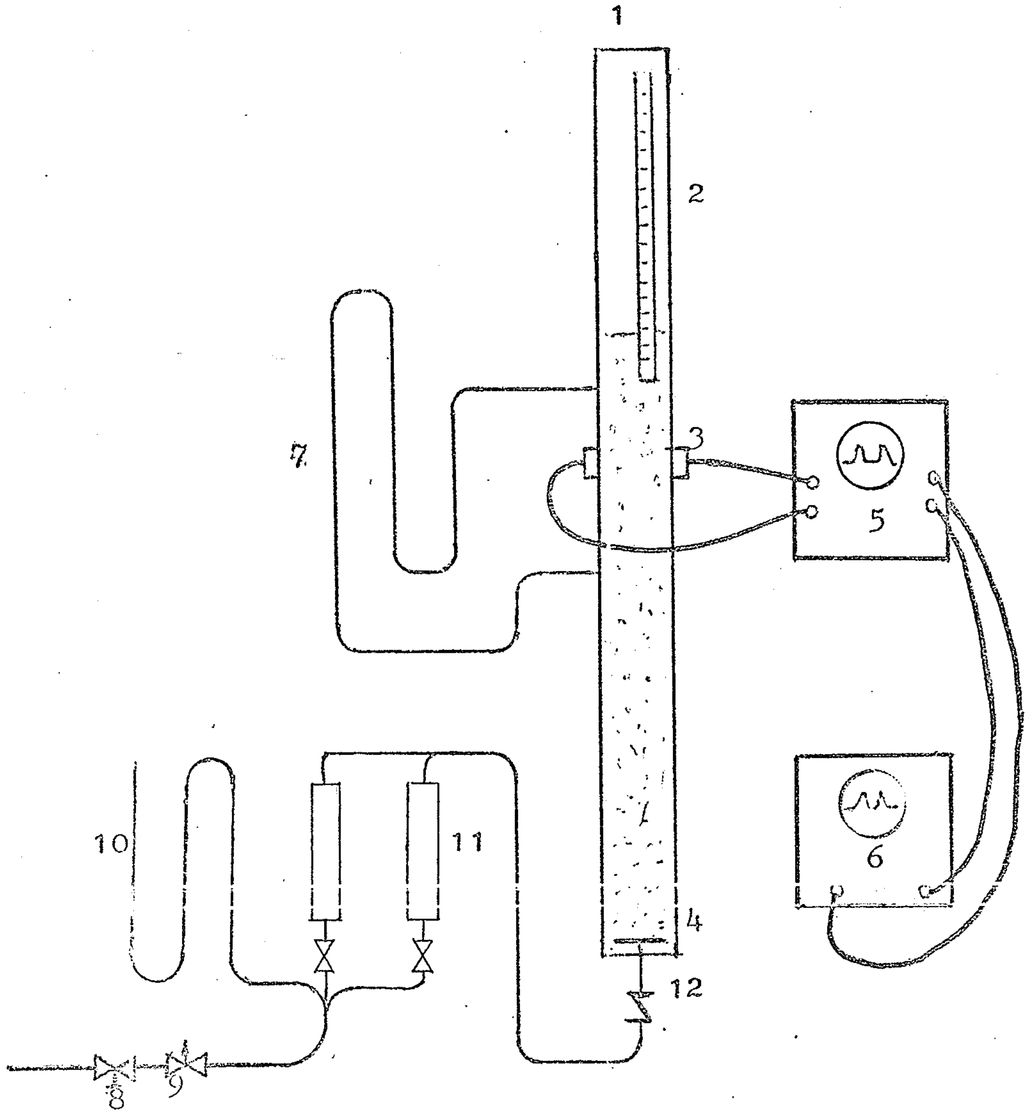

1. perspex tube 2. column height measuring scale
3. plastic probe holder c/w probes
4. sparger c/w porous plate
5. ultrasonic flaw detector
6. storage oscilloscope
7. inclined manometers
8. pressure reducing valve
9. needle valve 10. pressure manometer
11. rotameters 12. check valve

Fig. 3.1 Schematic diagram of apparatus

Fig. 3.1

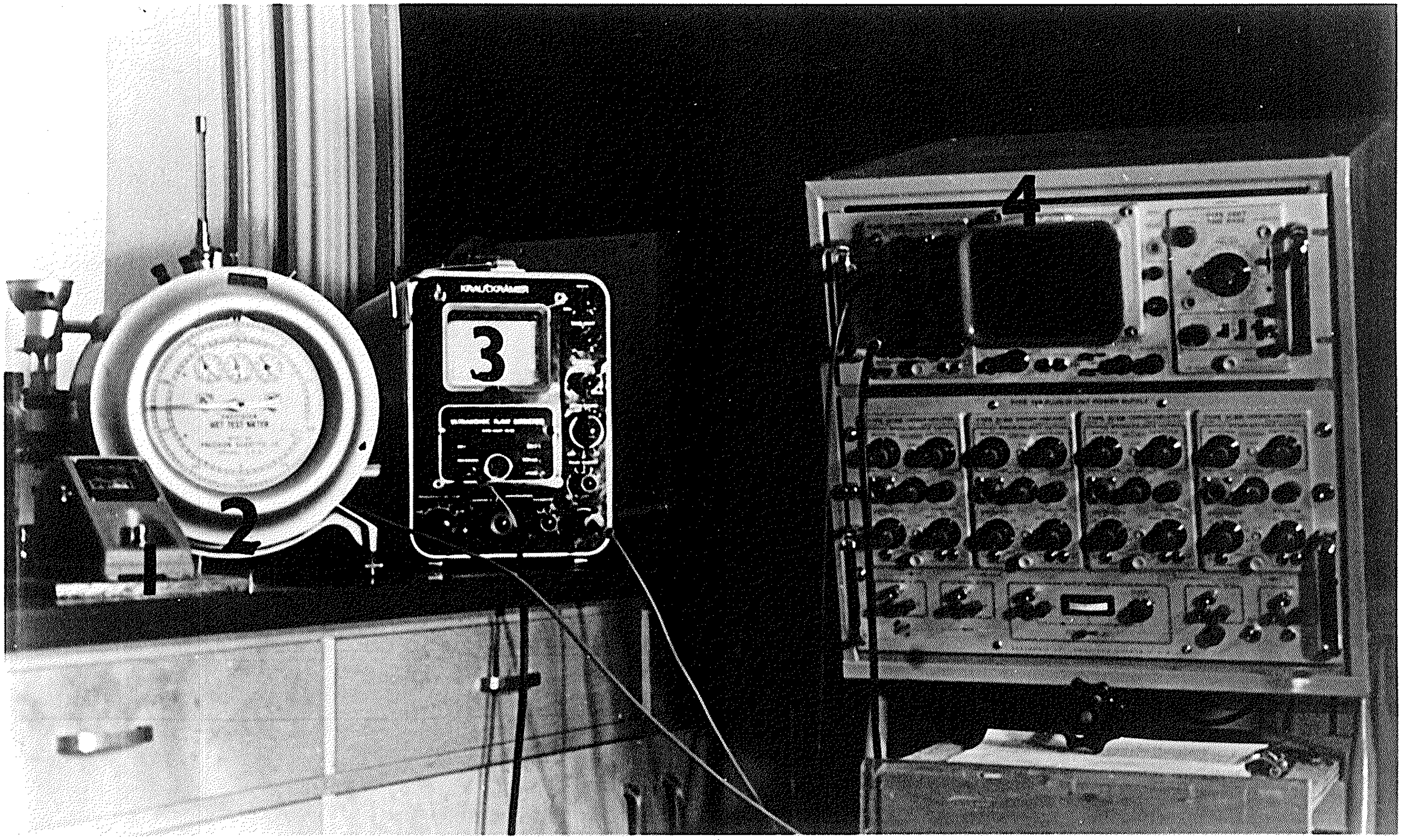

Fig. 3.2

Fig. 3.2 Photograph of apparatus: 1 timer, 2 wet test flow meter, 3 Krautkamer ultrasonic flaw detector, 4 Tektronix RM 564 storage oscilloscope with type 2B67 time base.

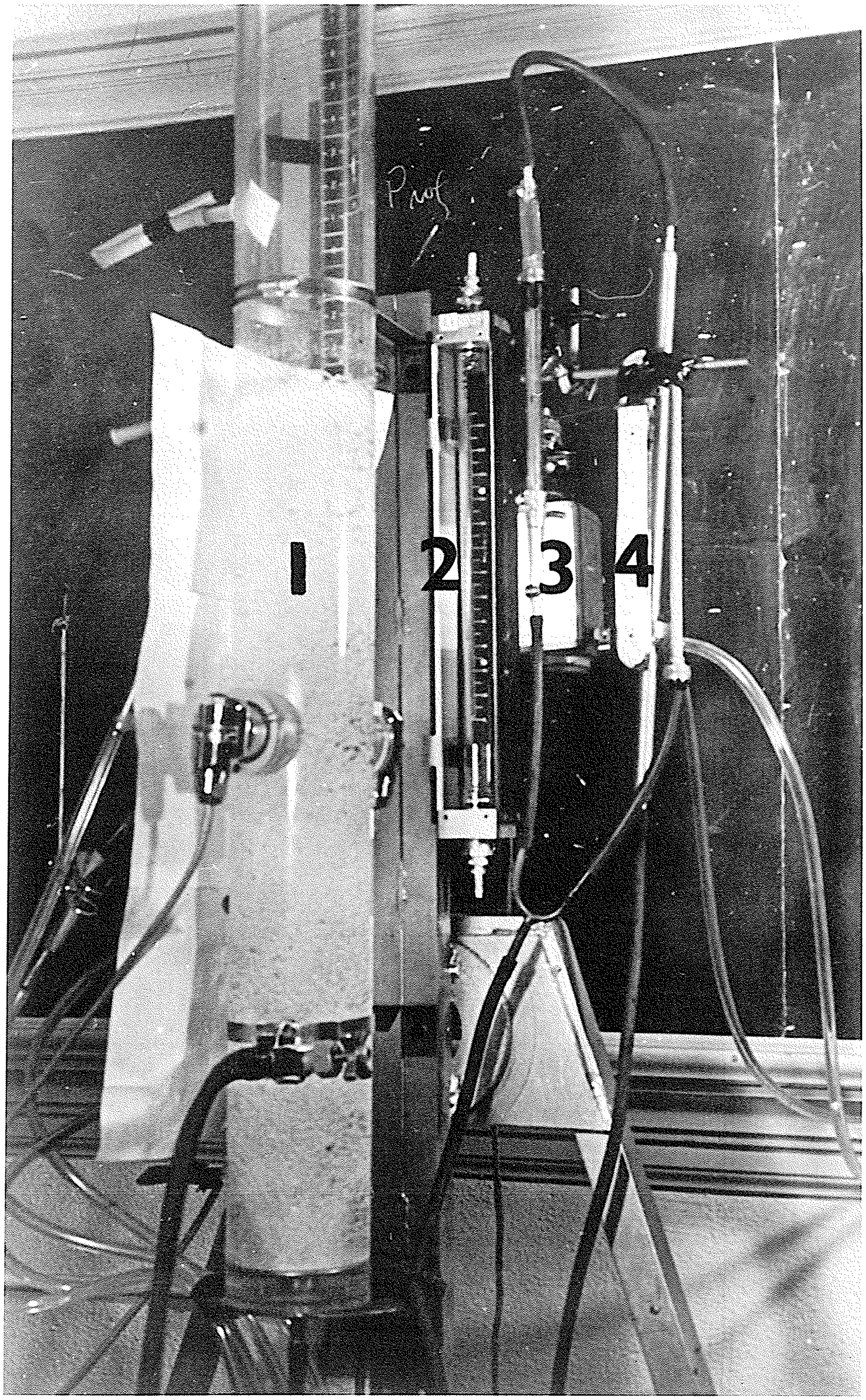

Fig. 3.3 Photograph of apparatus: 1 perspex tube, 2 Brooks R-8M-25-4 rotameter, 3 Brooks R-6-15-8 rotameter, 4 pressure manometer.

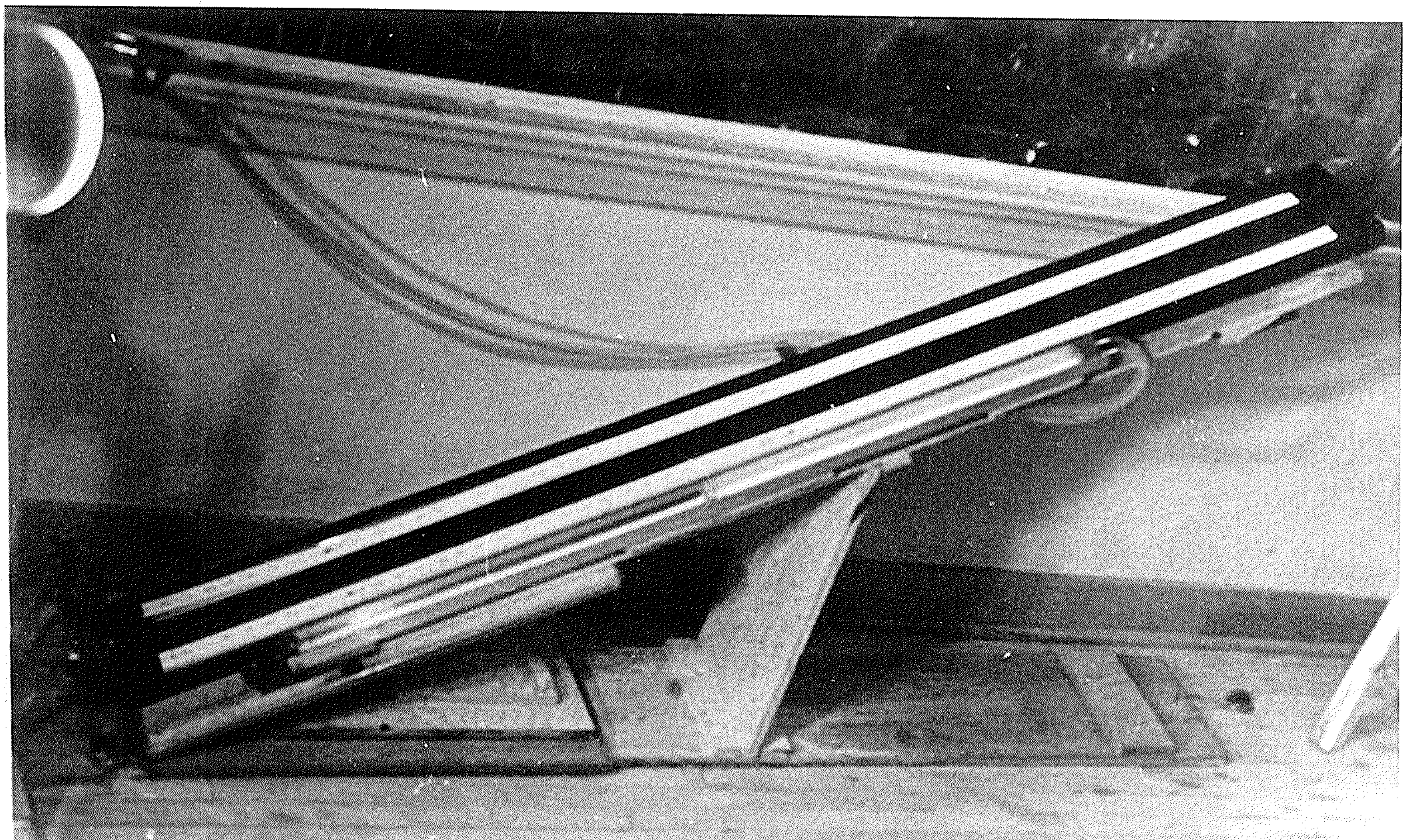

Fig. 3.4

Fig. 3.4 Photograph of inclined inverted U-tube manometer

3.2 Void fraction measurement

3.2.1 Hydrostatic method

Seven pressure taps (1/4 in. inside diameter) were fastened into the tube wall at 3 in., 6 in., 11 in., 16 in., 21 in., 26 in. and 32 in. above the bottom of the tube. Connections from an inverted U-tube manometer could be made to any two of these taps to determine the mean void fraction in that section between the two taps. For comparing the mean void fractions of any two sections under the same experimental condtions and for obtaining a very sensitive reading of void fraction by manometer, two 6 ft. long manometers were chosen, each assembled with two glass tubes, three air-release vents and two rubber syringes for purging the system of air. The top of the U-manometers was filled with Marian oil. These two manometers were fixed on a plate and the plate could be inclined at any angle θ between 0 to 90 degrees; (θ measured from the horizontal) the angle of inclination θ was selected to be 30 degrees for all of the present experiments. The details of construction of the manometer are given in appendix H and the relationships between mean void fraction and measurements taken on the inclined manometers are presented in appendix B.

3.2.2 Column height method

A scale graduated in tenths of inches was fixed against the face of the tube, any level of gas-liquid mixture could therefore be read directly on the scale. The zero level was selected at 30 in. above the sparger. The reading on the scale under test conditions varied from negative 13 in. to positive 15 in.

3.3 Acoustic velocity measurement

Two Krautkamer 500 kHz undamped, waterproof, barium titanate crystal transducers for generating and receiving sound signals were mounted diametrically opposite through the tube wall at a height of 16 in. from the bottom of the tube. These were connected by means of double screened connecting cable to a Krautkämer ultrasonic flaw detector (type USIPIO) which consists of a pulse generator, an amplifier and a cathode-ray tube screen. A Tetronix four beam storage oscilloscope was also connected to this in parallel so that only one sweep of the rapidly changing signal could be observed at any desired time.

At high void fractions the velocity of sound varied with time, due to the changing mixture conditions between the crystals in the test section; it was therefore necessary to take a large number of readings to obtain the mean and the standard deviation of the acoustic velocity for each (nominal) setting of the void fraction.

3.4 Bubble measurement

For obtaining the bubble size distribution and mean bubble diameter, a photographic technique was used. The camera used was a single-lens reflex Ashai Pentax Spotmatic with a through-lens light meter and Macro-Takumar 1:4, 50 mm close-up lens. To achieve maximum enlargement the camera was set up close to the tube, with two 500-watt flood lights for back-lighting as shown in Fig. 3.5. For reducing the glare in the picture, a diffusing screen was mounted behind the tube, between the tube and the flood-lights. As a scale a piece of fine wire of 1 in.

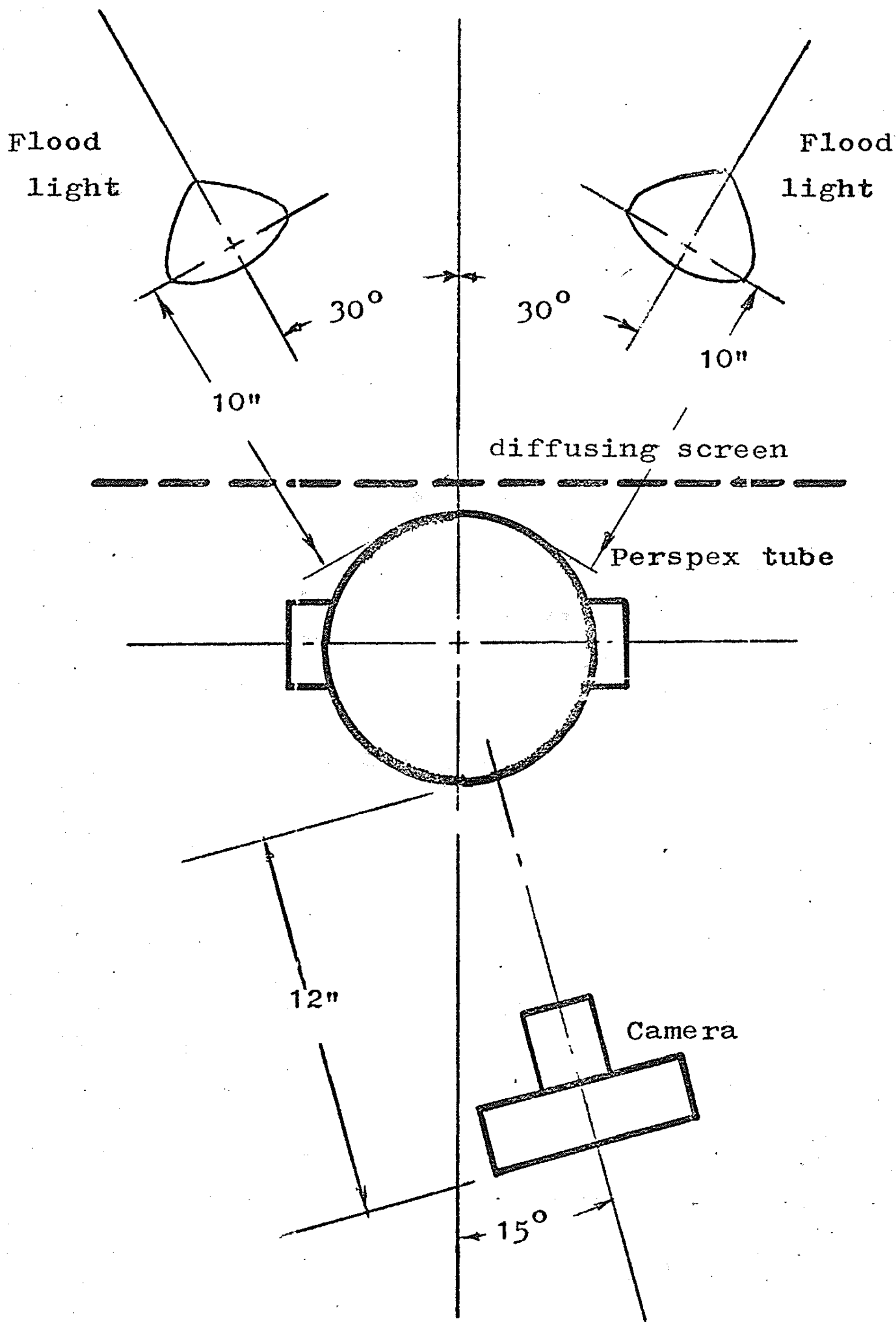

Fig. 3. 5 Camera set-up

Fig. 3.5

length and 0.03 in. diameter was attached to the tube just to the right of the picture area of interest. Also a printed number on a strip of tracing paper was attached to the tube near the scale mark in order to identify each picture. The shutter speed used was 1/1000 second in order to record moving bubbles.

Kodak Plux X(A.S.A. 120) was chosen because it has a finer grain and would thus yield sharper images necessary to discern small bubbles since the frame size of the film is only 24 mm by 36 mm. The film developer was Kodak Microdol X and the prints were made on Kodak Kodabromide F3 double-weight paper. This is a fairly "hard" paper. The images are well defined because of sharpness and contrast.

3.5 Liquids

The various types of water and water plus additives may be described as follows:

1. Distilled water used only once; source was Soils Laboratory of the Civil Engineering Department; used in test no. 1401.

2. Distilled water used five times (all measurements being taken on the fifth time of use); source was Soils Laboratory of the Civil Engineering Department; used in test no. 160.

3. Deionized distilled water (used only once); source was the Physical Chemistry Laboratory of the University of Manitoba; used in test no. 401.

4. Tap water (used only once); source was the mains in the Engineering Building; used in test no. 601.

5. Tap water plus KCl additive; weight of solute was 18.77% giving a surface tension of 76.95 dynes/cm (by calculation); used in test no. 1101.

6. Tap water plus soap solution; used in test no. 1220.

7. Tap water plus detergent (Sunglight); used in test no. 1301.

8. Tap water through which air had been blown for 30 hours; used in test no. 1601; measurements were taken after the 30 hours of blowing.

CHAPTER 4

PROCEDURE

4.1 Preparations

The following preparations were made prior to actual test runs:

1. The trace alignment and linearity of the time base of the Tetronix storage oscilloscope was checked.

2. The perspex tube was kept clean, and before the test liquid was poured into the perspex tube, all the parts which would contact the test liquid were flushed two or three times with the test liquid.

3. The temperature of the test liquid was the same as room temperature before the test liquid was poured into the perspex tube.

4. All instruments were set to operating condition:

(i) the Krautkrämer detector and Tetronix storage oscilloscope were turned on one half hour before use;

(ii) all settings on the Krautkrämer and Tetronix were checked;

(iii) the perspex tube, two rotameters and gas pressure manometer were checked to ensure vertical alignment;

(iv) all settings on the camera and the position of camera and flood-lights were checked before the picture was taken.

5. The mean distance between the faces of the two crystal transducers were measured as shown in Fig. 4.1.

6. The prepared test liquid was filled to the required level.

7. The trapped air was driven out of the manometer system by three air-release vents and two rubber syringes.

8. The test liquid was filled to the required level again.

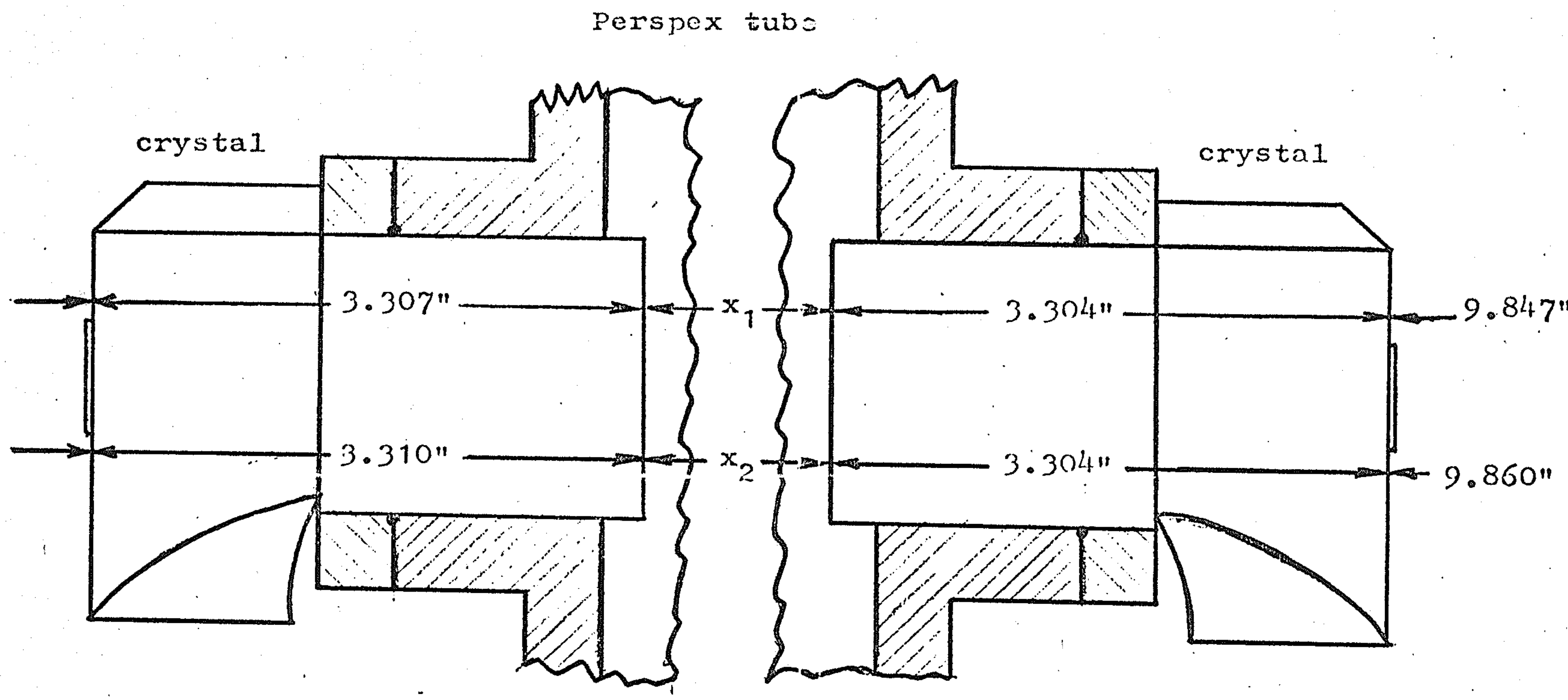

$$x_1 = 9.847'' - 3.307'' - 3.304'' = 3.236''$$

$$x_2 = 9.860'' - 3.310'' - 3.304'' = 3.246''$$

$$\text{mean distance} = \tfrac{1}{2}(\,x_1 + x_2) = \tfrac{1}{2}(\,3.236 + 3.246\,) = 3.241''$$

Fig. 4.1 Measured distance between the two crystals

Fig. 4.1

4.2 Test runs

The procedure for performing a test run was as follows:

1. The acoustic velocity of the test liquid was measured on the oscilloscope. The time data could be read directly from the screen of the scope because there was no variation in the transit time when the void fraction was zero.

2. The air pressure was set to 30 psi on the reducing valve gauge.

3. The air to the sparger was controlled with a needle valve for a series of settings, each flow rate being shown on rotameter.

4. The following readings were then taken:

(i) air pressure of the system at each air flow rate from pressure manometer,

(ii) air-liquid mixture level from the scale on the Perspex tube for each air flow rate; the mean value was taken when, for one air flow rate, there were fluctuations in the level.

(iii) void fractions from both manometers for each air blowing rate; the mean value was taken when the manometer showed variations for one air flow rate,

(iv) a series of time data were taken from the storage oscilloscope for each air flow rate.

The number of series time reading taken depended on the difference from reading to reading. In the very low void fraction range where changes in time were not discernible only few were taken, while in the high void fraction region, where time readings changed markely from reading to reading, thirty to forty readings were taken.

5. For the case of distilled water as the test liquid, a picture of air bubbles was taken at each air flow rate in the void fraction range from 0.0 to 0.053. Each state was assigned a number on the picture.

6. After a test with various air flow rates had been completed and the above steps performed, the flow of compressed air was stopped and the system allowed to reach steady state. The acoustic velocity of liquid was then checked again for the zero void fraction case.

7. After the above step had been done, the liquid was then allowed to drain from perspex tube and an acoustic velocity reading for air was taken for the case of void fraction equal to one.

8. A computer program was then used to calculate:

(i) The acoustic velocity of the test liquid for each test run.

(ii) The acoustic velocity of air-liquid mixture and its standard deviation from two different bases, one based on the mean of time readings, then calculating the velocity with this mean, the other based on velocities, the series of velocities was calculated from the time readings for this void fraction, and then the mean of the velocities was taken. The analogous procedure was used for calculating standard deviations.

(iii) Superficial gas velocity* based on the total inside cross-sectional area of the Perspex tube.

(iv) Void fractions. Three void fractions were obtained and these were:

---

* The superficial gas velocity is defined as the air volumetric flow rate divided by the cross-sectional area of the test section.

B0, calculated from the air-liquid mixture height in the Perspex tube,

B1, calculated from the readings of No. 1 manometer, and

B2, calculated from the readings of No. 2 manometer.

The out-put of these programs, related calculations and rotameter calibration curves are given in appendix C and appendix A.

9. To determine the mean diameter of bubbles for each void fraction in the range of B from 0.0 to 0.053, pictures were taken of the bubbly mixture between the crystals. These pictures were then enlarged to exactly three times of the actual size (Figs. 4.2,4.3,4.4,4.5 and 4.6). Those bubbles with the same sharp image on a picture were considered on a sampling plane (or a focussing plane), and it was assumed that each bubble was an ellipsoid. The number of those bubbles in the sampling area (4.5 in. x 4.5 in.) was counted and the length of semiaxes of each bubble was measured. Then an equivalent diameter of an equivolume sphere was calculated for each ellipsoid using a computer program (appendix D). The data of the equivalent diameter of the bubbles were used as an input to calculate the following using a statistics computer program for each void fraction in the range 0.0 to 0.053:

(i) arithmetic mean of the diameters of bubbles,

(ii) variance,

(iii) standard deviation,

(iv) standard error,

(v) coefficient of variance,

(vi) geometric mean,

(vii) frequency distribution table, and

(viii) histogram plot.

The output of this statistics computer program is given in appendix B. Only items (i), (iii), (vii) and (viii) of the above list (i.e. the most important items) are given in appendix E, but information on the other items is available.

10. The test conditions for the various runs are summarized in Table 1 together with the figure number on which the results appear. For interest and information purposes, the work of Card is included as well.

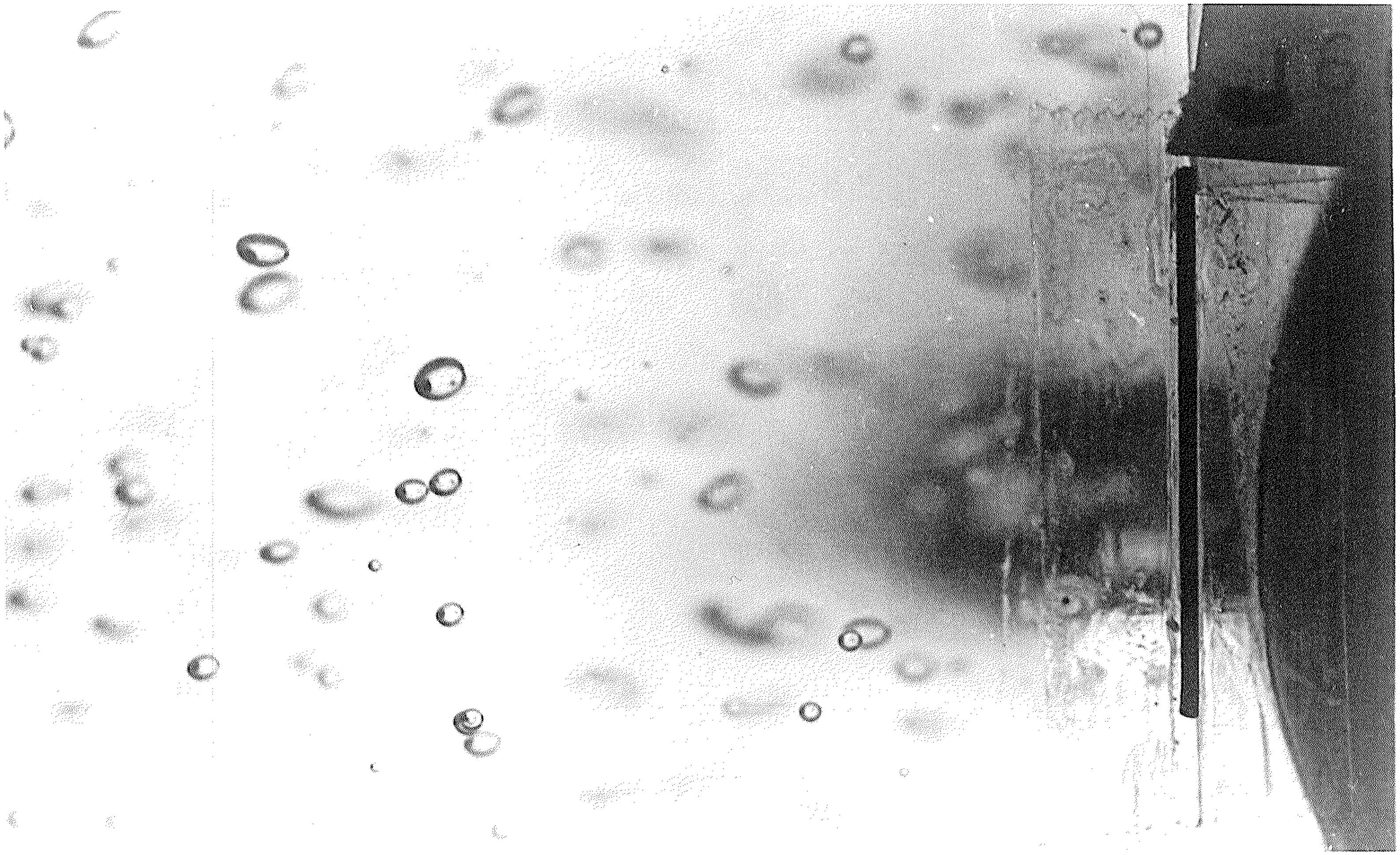

Fig. 4.2

Fig. 4.2 Photograph No. 161, B = 0.006

Fig. 4.3 Photograph No. 164, B = 0.015

Fig. 4.3

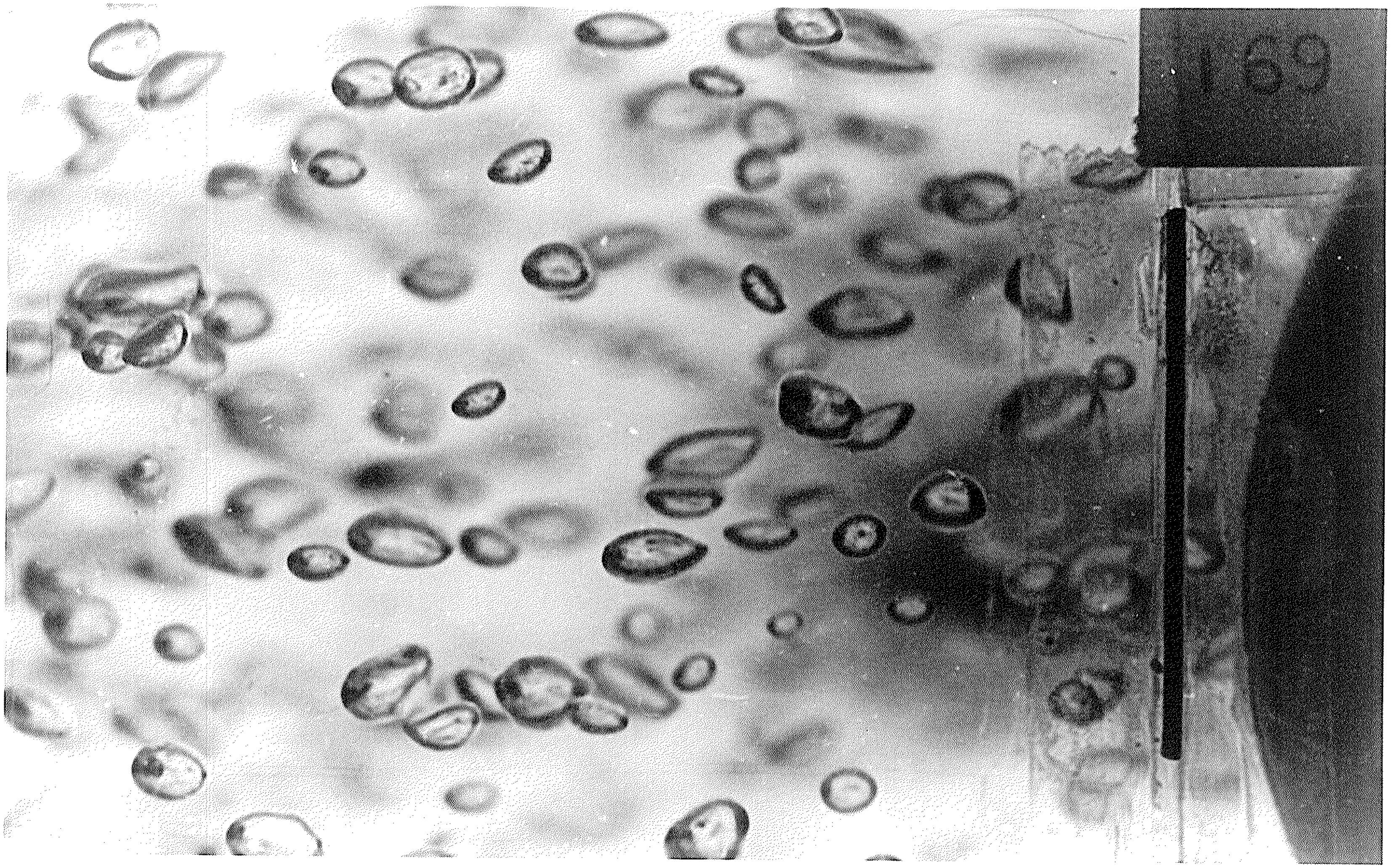

Fig. 4.4

Fig. 4.4 Photograph No. 169, B = 0.031

Fig. 4.5

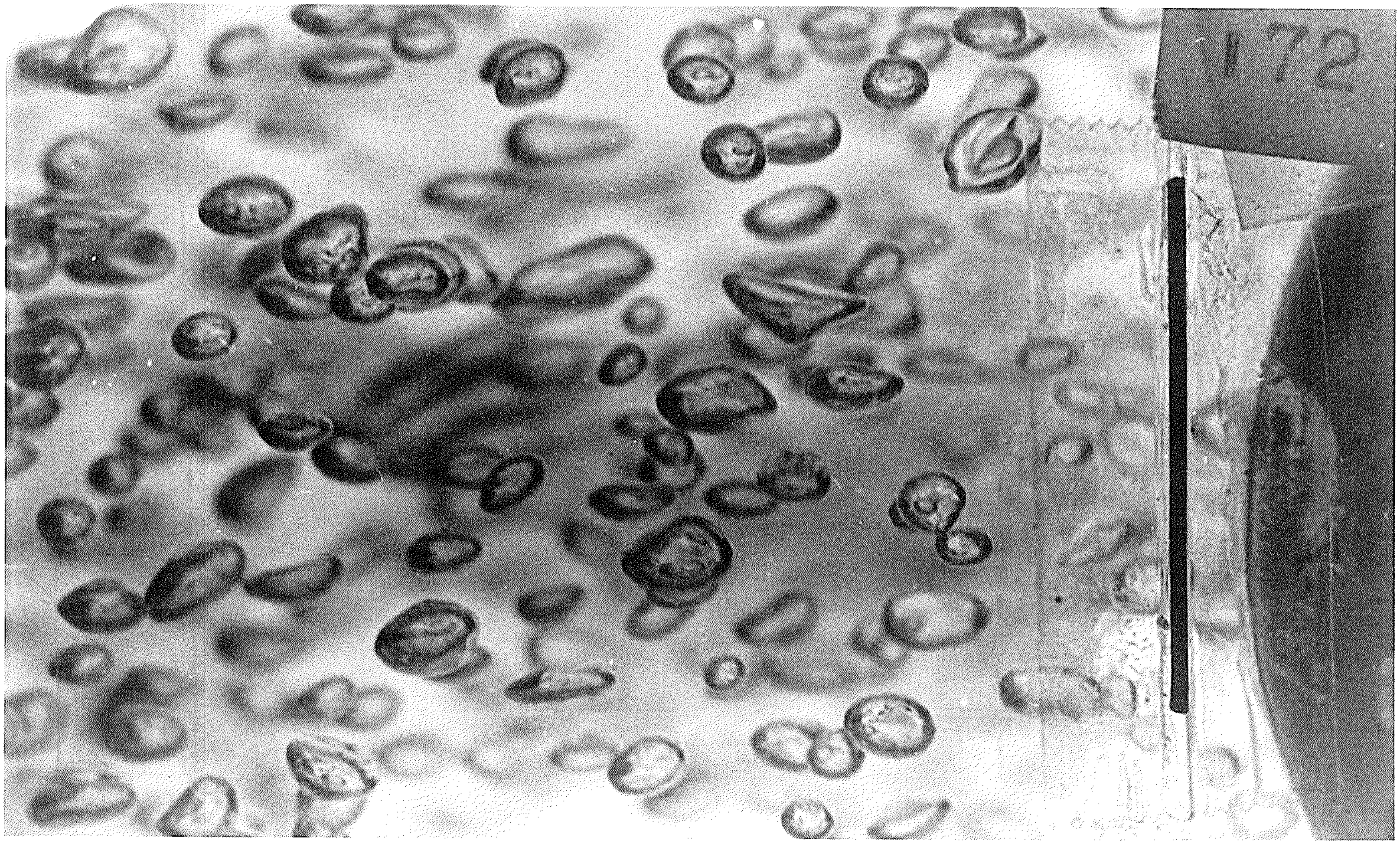

Fig. 4.5 Photograph No. 172, B = 0.044

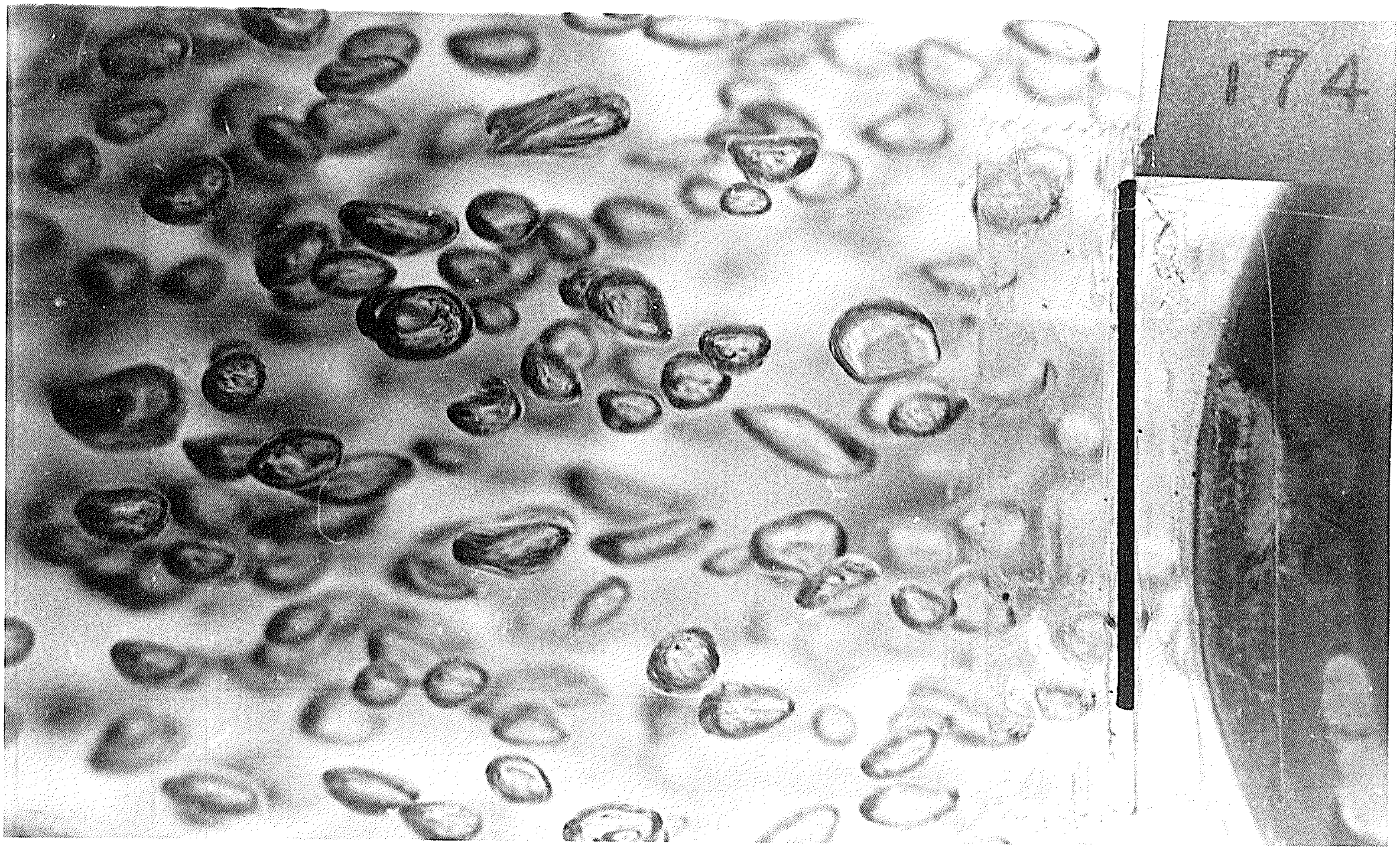

Fig. 4.6

Fig. 4.6 Photograph No. 174, B = 0.053

	Card's Data	Test No. 160	401	601	1101	1220	1301	1401	1601
Liquid used	(1) T.W.	(2) D.W.	(3) D.D.W.	(4) T.W.	T.W.	T.W.	T.W.	D.W.	(7) T.W.
Chemical additive	None	None	None	None	(5) KCl	Soap	Deter-gent	None	None
a_m calculated with different bases		V		V	V			V	
Bubble dias. determined with photographic technique	V	V							
Statistics calculation	V	V							
Histogram of distribution of bubble diameters	V	V							

Table 1. Summary of Test Runs (continued on next page)

			Card's Data	Test No. 160	401	601	1101	1220	1301	1401	1601
Data taken for $\dot{v}''$ versus	B_o	inc.		V	V	V	V			V	V
		dec.			V	V	V			V	V
	B_1	inc.	V	V	V	V	V	V	V	V	V
		dec.	V		V	V	V	V	V	V	V
	B_2	inc.		V	V	V	V			V	V
		dec.			V	V	V			V	V
Data taken & plotted for a_m/a_1 versus	B_o										
	B_1		V			V	V			V	
	B_2			V		V					
Type of tap arrangement (6)			C	A	A	A	B	C	D	B	B
Liquid level (in.) for $\dot{v}'' = 0$				21.75	21.75	21.65	21.65	21.65	7.0	21.65	21.65
Room temperature (°F)			72°	72°	75°	74°	76°	73°	76°	72°	72°
a_1 (m/sec)			1425	1419	1419	1419	1419	1419	1419	1419	1419
a_{air} (m/sec)			345	332	332	332	332	332	332	332	332

Table 1 (cont.) Summary of Test Results (continued on next page)

	Card's Data	Test No.							
		160	401	601	1101	1220	1301	1401	1601
Mean bubble dia. versus B and histogram	V	V							
Fig. No.	2.1, 2.2, 2.3, 2.4	5.3, 5.4, 5.5, 5.6, 5.7	5.8	5.9, 5.10, 5.11	5.12, 5.16, 5.17	5.13	5.14	5.15, 5.16, 5.18	5.19

<u>Remarks</u>

(1) T.W.: tap water
(2) D.W.: distilled water and used for 5 times
(3) D.D.W.: deionized distilled water
(4) The manometer system was cleaned and filled with new Marian oil
(5) Weight % of solute = 18.77; the surface tension = 76.95 dynes/cm
(6) The sketch of tap arrangement of type A,B,C, and D is given in Fig. 5.1
(7) T.W. blown with air for 30 hours

Table 1 (cont.) Summary of Test Results

CHAPTER 5

PRESENTATION AND DISCUSSION OF RESULTS

5.1 Reliability of measurements

The estimated error in the superficial velocity $\dot{V}''$ was 3.2% for $\dot{V}'' > 0.025$ ft/s in bubbly flow and approximately one-half of the transition flow range (measurements on the smaller rotameter) while in slug flow and the upper range of transition flow the error was 4% (measurements on the larger rotameter). The estimated error in the void fraction B was 3% for $B > 0.043$. For $B < 0.043$, the acoustic velocity was relatively insensitive to void fraction; therefore the error in measuring B, which was >3%, could be tolerated. Error analyses for superficial velocity and void fraction appear in appendices A and B respectively.

The error in the acoustic velocity was estimated at 3.2% for single phase and low void fraction conditions and 4.1% for high void fractions. The error analysis is given in appendix F. As a check on the reliability of the acoustic velocity measurements, a comparison was made between the present measured single phase values and corresponding values from the literature [2,20,27]. The data are given in Tables 2 and 3. The maximum deviation from literature values was 3.6%. The difference between Card's water data and present measurements was only 0.4% while the difference in the present and Card's air data was 3.6%. These comparisons would suggest that the present measurements are reliable.

Table 2

Reference Acoustic Velocities

Author	Temperature	a_{water} (m/s)	a_{air} (m/s)
Present Work Test No. 601	23°C	1419 (city water)	332
D. C. Card	22°C	1425 (city water)	345
Calculated*	22°C	1430	344
Stewart and Lindsay	20°C		344
Colladon and Sturm**	8°C	1435 (fresh water Lake Geneva)	
Angerer and Ladenberg**	15°C 22°C		331 (air in open) 339***
Esclangon**	15°C		340 (dry air)
Present Work Test No. 1401	22°C	1419 (distilled)	332
Martini**	19°C	1461 (distilled)	
Present Work Test No. 1101	24°C	1419 (city water + KCl)	332
Present Work Test No. 1220	23°C	1419 (city water + soap solution)	332
Present Work Test No. 1301	24°C	1419 (city water + detergent)	332

* $a = \sqrt{\frac{\gamma P}{\rho}}$ where γ is the ratio of specific heats and P and ρ are the pressure and density at that temperature.

Table 2 (cont.)

** As reported by Wood.

*** With the adjustment $\frac{a'}{a} = \sqrt{\frac{T'}{T}}$

Where: a is the velocity of sound,
T is absolute temperature,
a' is the velocity of sound when the temperature is T'.

Table 3

Comparison of Present Acoustic Velocities With Others

Comparing	for	Difference m/sec	Difference %
Present Work Test No. 601 with D.C. Card	a_{water} (city water)	5.6	0.4%
Present Work Test No. 601 with Calculated	a_{water}	10.6	0.75%
Present Work Test No. 601 with D.C. Card	a_{air}	12.5	3.6%
Present Work Test No. 601 with Calculated	a_{air}	9.6	2.8%
Present Work Test No. 1401 with Angerer & Ladenberg	a_{air}	7	2%
Present Work Test No. 1401 with Martini	a_{water}	41.6	2.75%

5.2 Summary of test runs

Table 1 summarizes the previous (Card) and present experimental results of acoustic velocity as a function of frequency.

5.3 Flow regimes

Three flow regimes are shown on the graphs for eight tests, in Figs. 5.3,8,9,12,13,14,15 and 19; the flow regimes were observed directly in the test. The three regimes have been defined by Wallis [25] as follows:

1. Bubbly flow region: the gas is in the form of discrete small bubbles dispersed uniformly in the liquid.
2. Slug flow region: the gas is in large slugs which occupy most of the flow section.
3. Transition region: in between the bubbly and slug regions there is an area of flow transition.

It is difficult to separate exactly the regions from each other even in a transparent apparatus. Of course these definitions can hardly be applied to testing in a non-transparent apparatus. A new description for flow regimes was also used in present work; it can be applied conveniently to any experiments using transparent or non-transparent apparatus. First B_{max} is defined as the maximum void fraction point and B_s as the point where the decreasing flow trace separated from the increasing flow trace; these can be detected by the present manometer. Therefore, it is convenient to use the B_{max}, B_s and a point $B = 0$ (see Fig. 5.2) to describe four flow regimes as follows:

1. Region 1: the flow increased from $B = 0$ to B_s.

2. Region 2: the flow decreased from B_s to B_{max}.
3. Region 3: the flow decreased from B_{max} to $B = 0$.
4. Region 4: the flow increase from or decreased to B_s.

The sketch of the four flow regimes is given in Fig. 5.2.

The lengths of region 1, 2 and 3, and other characters related to the four flow regimes are listed in Table 4 for each test run. The discussion about the flow regimes will be included in the following section.

5.4 Superficial gas velocity versus void fraction

Results of present work of superficial gas velocity $\dot{V}''$ are plotted against void fraction B, in Figs. 5.3,8,9,12,13,14,15 and 19.

Superficial gas (air) velocity, can be defined as gas (air) flow volume through the area of flow cross section, that is the cross-sectional area of the inside of the tube.

Wallis [25] has derived a theoretical relationship for ideal bubbly flow (his equation (7)) in which the void fraction depends on the superfical velocity, surface tension, liquid and gas densities and gravitational acceleration. It is implicit in this equation (based on empirical evidence) that the system properties such as Reynolds number and viscosity ratio (at least for low-viscosity liquids) are relatively unimportant. Wallis concluded that it is possible only to conduct repeatable measurements of void fraction in ideal bubbly flow (no bubble agglomeration) and ideal slug flow (complete agglomeration); partial agglomeration gives rise to a transition flow pattern which is virtually intractable analytically.

The relationship between $\dot{V}''$ and B gives different traces for increasing and for decreasing air flow rates over part of the range of $\dot{V}''$. This phenomenon was observed by Card [2] in the transition region, but in the present work, it extended into the bubbly and slug flow regions, possibly due to the more sensitive void-fraction measuring apparatus employed. Differences in B between increasing and decreasing air flow rates are described quantitatively in Table 4 which in turn refers to Fig. 5.2. The largest differences (.12) occur in test 1601 for tap water into which air was blown for 30 hours; the results are shown in Fig. 5.19. For other tests the differences in B ranged between 0.02 and 0.085.

Different tap arrangements, as shown in Fig. 5.1, were used to determine the effect of tap arrangement on void fraction measurements. There are small differences (maximum 0.020) between B_1 and B_2 (arrangement types A and B), the difference being especially small in arrangement type B (maximum 0.015). The differences depend on air flow rate; there is no discernible difference, for instance, in the range $B<.053$, which would correspond closely to ideal bubbly flow. Any differences in measured B using B_1 and B_2 would no doubt be due to slight density variations of the mixture with height. Results appear in Figs. 5.3,8,9, 12,15 and 19.

The void fraction B_o measured with column height represents the mean void fraction for the whole column plus the foaming effect. The difference between B_1 and B_o represents the foaming effect; it varied with the flow rate of air and became a constant in region 4. The results appear on Figs. 5.3,8,9,12,15 and 19, and in Table 4. The biggest foaming effect existed in the tap water into which air had been blown for 30 hours, (maximum difference between B_o and B_1 of .18) while for all other tests this effect was approximately the same (approximately 0.06 in void fraction). It is stressed that B_o is not as good a measurement of void fraction as B_1 or B_2 and is presented here mainly for interest. For later plots of acoustic velocity versus void fraction, the most meaningful void fraction measurement is probably B_2 of arrangement type A.

The chemical additive KCl was used in test run no. 1101, the weight percentage of solute being 18.77. The surface tension force increased 3.59 dynes/cm from 72.36 dynes/cm for tap water at 23°C to 76.95 dynes/cm for the test liquid against air [31]. The effect of KCl on tap water can be found by comparing test run no. 1101 (Fig. 5.12) for tap water plus additive with 601 (Fig. 5.9) for tap water, the following observations being relevant:

1. The maximum void fraction of B_1 increased 0.06, or 21.8%.
2. The maximum difference of void fraction between 1 and 2 formed by B_1 increased 0.043, or 102.1%.
3. The forming effect reduced from 0.075 to 0.05.
4. The length of region 1, 2 and 3 all reduced from 0.90, 0.57, 0.33 to 0.80, 0.55, 0.25 ft/s respectively.

Other chemical additives of soap solution and detergent were used in tap water. The effect of soap solution reduced the maximum void fraction of tap water 0.095 or 30.9%, reduced the length of region 1 and 3, also gave the lowest "maximum void fraction" in the present work (see Fig. 5.9 for tap water results and Fig. 5.13 for soap solution results.)

The effect of detergent was to increase the maximum void fraction of tap water 0.035 or 12.7% and the maximum difference of B between 1 and 2 was reduced 0.022 or 52.3% to a value of 0.020, the smallest in the present work.

Three different distilled water conditions were used in the present work: the distilled water used in test run no. 160 was repeatly used five times (measurements being taken on the fifth time), the distilled water in test run no. 1401 was used only once, and the distilled water in test run no. 401 was deionized distilled water (used only once). The repeatly-used distilled water and the deionized distilled water gave a slightly higher "maximum void fraction" of B_1 than the distilled water used only once. Also the maximum difference of void fraction between 1 and 2 formed by loop B_1 of deionized distilled water was larger than the distilled water used only once. These data are given in Table 4 and in Figs. 5.3,8 and 15.

The difference in maximum void fraction of B_1 between test run no. 1401 for distilled water used only once and 601 for tap water is smaller than in Wallis' work. This probably means that the distilled water and tap water used in present work are closer in physical properties than those used by Wallis. These data can be seen in Table 4 and Figs. 5.15 and 9.

Two tests performed here may be compared with Card's results [2]. These are tests no. 601 (tap water) and no. 1601 (tap water through which air was blown for 30 hours); the comparisons are shown in Figs. 5.9 and 5.19 respectively. In both tests at low B (<0.10 for test no. 601 and <0.18 for test no. 1601, at least part of which region would include ideal bubbly flow) and in slug flow there is good correspondence with Card's results; the best agreement with Card's results is with decreasing air flow rates in test no. 1601 (Fig. 5.19). The longer air is blown through the water the more impurities are likely to be introduced into the water. It would therefore appear that the tap water used by Card probably had more impurities in it than test no. 601 here. However, as will be seen shortly, this does not at all affect the acoustic velocity versus void fraction relationship, the most important measurements performed in the present work.

5.5 Bubble size measurement

The photographs taken of the air-distilled water mixture between the two crystals, as mentioned in chapter 4, were enlarged to triple size, and four of them were illustrated in Figs. 4.2,3,4 and 5. The enlarged photographs showed that there appeared to be no bubble agglomeration within the range of B from 0 to 0.053. Therefore, it could be considered that this region is an ideal bubbly flow region.

The histogram of bubble size distribution and other statistical results are shown in appendix E.

The relationship of mean bubble diameter and frequency ratio versus void fraction is shown in Fig. 5.4. The curve of mean bubble diameter or frequency ratio of the present work is a little higher than that of tap water of the previous work when the void fraction is greater than 0.015. One might expect larger bubbles in distilled water due to surface tension effects on the bubble break-off diameter from the porous plate and the ease with which bubbles can agglomerate should they touch.

5.6 Acoustic velocity versus void fraction

The ratio of the acoustic velocity in the mixture to that in the bubble free liquid (a_m/a_l) is plotted against void fraction B for each test run as shown in Figs. 5.5,6,7,10,11,16,17 and 18.

Figs. 5.5,6 and 7 show the a_m/a_l versus B relationship of test run no. 160. The test liquid was distilled water which had been used for five times. Fig. 5.5 shows the results for the low B region (<.053). On the figure also is shown equation (6); measured bubble sizes were used to determine the corresponding values of w_o which were then used in the equation to find the ratio of the group velocity to the bubble-free liquid. It is pointed out [3] that at these high frequencies the signal velocity (measured in these experiments) is virtually identical to the group velocity. It is in this low B region that one would expect the constant-density equation (6) to apply; it is seen that the correspondence between the measurements and the theoretical equation is very good.

The results of test run no. 160 for the whole B range are shown in Fig. 5.6 for both bases of B_1 and B_2. Virtually no difference can be detected in the relationship using these two bases and a single solid line has been drawn in by eye to represent the results. On Fig. 5.7 a comparison is made between the present test run no. 160 results and the tap water results of Card [2]. The solid line in the figure represents Card's results (as well as the circles); it is seen that the solid line can equally well represent the present results. A glance at Fig. 5.3 shows that the $\dot{V}''$ versus B trace for Card's tap water and the present distilled water used five times are not unlike each other, perhaps suggesting that, particularly after using five times, the distilled water had had impurities introduced into it.

Figures 5.10 and 5.11 show a comparison between Card's tap water results and the present tap water results (Fig. 5.10 uses B_1 as the base, Fig. 5.11 uses B_2). First it is noted there is virtually no difference between the two plots. The agreement with Card's results is excellent. This is especially significant since some differences in $\dot{V}''$ versus B between Card's and the present results are apparent in Fig. 5.9. One of the most important features on Figs. 5.10 and 5.11 is the dramatic decrease in a_m/a_1 once transition and slug flow develops. This decrease is also evident in Figs. 5.16,17 and 18.

Figure 5.17 shows results of a_m/a_1 versus B for tap water plus KCl (test run no. 1101). The surface tension is higher with the additive. The results tend to lie below Card's tap water results (solid line), and hence below the present tap water results.

Figure 5.18 shows results for distilled water used once. There appears to be a slight tendency of the data to be above the tap water data. Comparisons among the tap water, tap water plus KCl and distilled water (used only once) are shown in Fig. 5.16. There appears to be a tendency for lower a_m/a_1 with increasing surface tension, although the fair amount of scatter evident makes this observation somewhat tentative.

For a given void fraction, the mean acoustic velocity may be calculated in two ways; one using the mean of the transit time readings, the other calculating the acoustic velocity for each time reading and then taking the mean of these acoustic velocities. This latter method would appear to be slightly preferable, although the quantitative differences between the two methods are extremely small. In the bubbly flow region the largest difference between the two methods was 0.52% (the tabulated results for the two methods is shown in appendix C, Tables C-9, C-10, C-11 and C-12). As Card used the first-mentioned method (mean of times) and as the present work involves extensive comparison with Card's work, mean acoustic velocities based on the mean of times are generally reported in the present work.

5.7 Suggestion for further study

No theory is known to exist for predicting the high frequency velocity in high void fraction mixtures. For these conditions it is necessary to take into account the acoustical interactions between closely spaced bubbles, change of shape of larger bubbles, as well as the decrease in mixture density.

Considerable further work can be done to establish the effect of fluid properties of both liquid and gas phases such as density, acoustic velocity and surface tension (the present work was really just a beginning, as regards the effect of surface tension, compared with what could be done in an extensive study). Possibly the effect of the method of generating the bubbles could be tested using different plates and spargers.

If the work is extended into the forced convection field, additional variables are added, e.g. velocities of each phase, and geometry and orientation of the channel.

The frequency has a pronounced effect on the mixture acoustic velocity; it would prove interesting to use fixed void fraction and variable applied frequency.

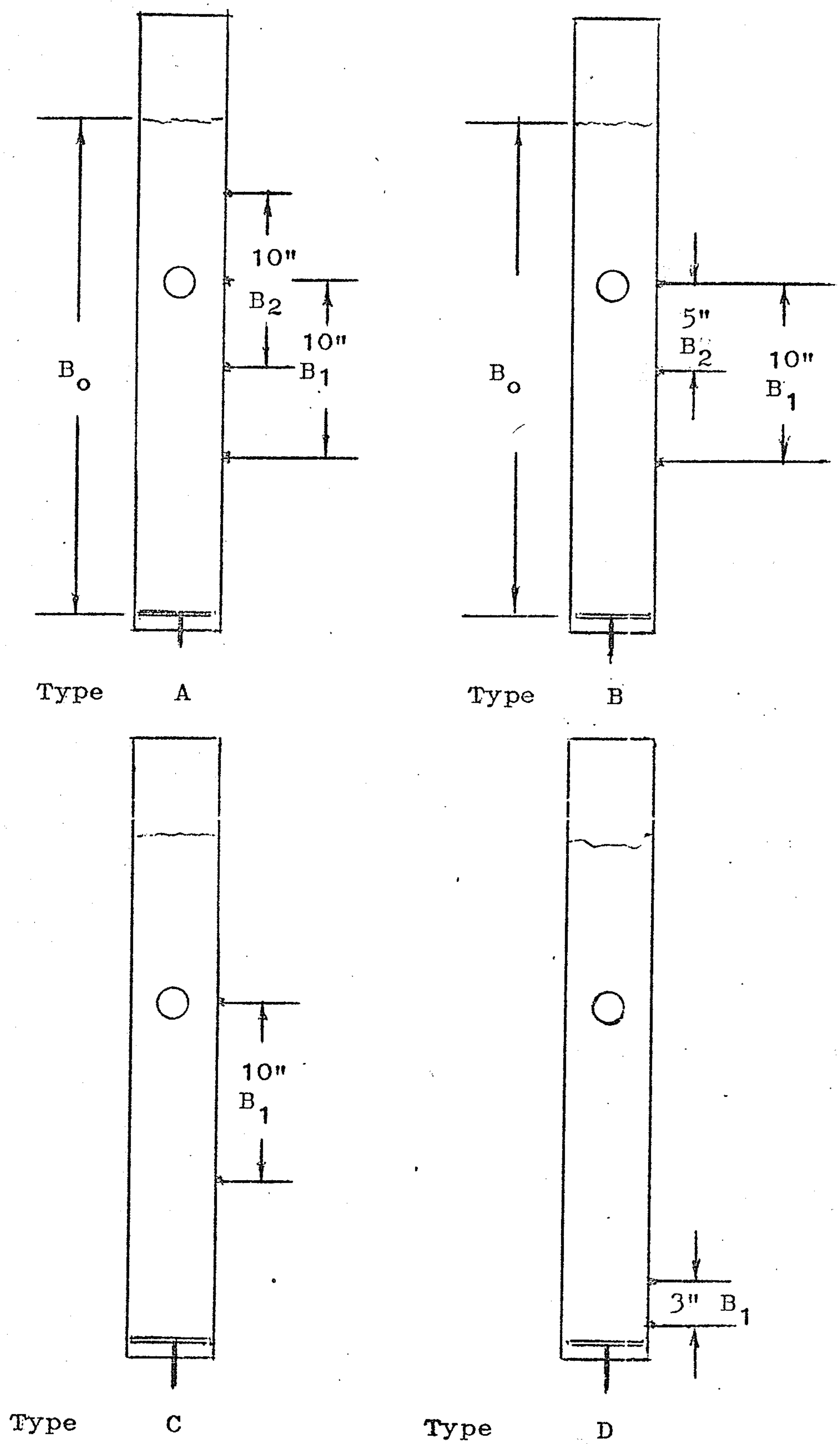

Fig. 5. 1 Type of tap arrangement

Fig. 5.1

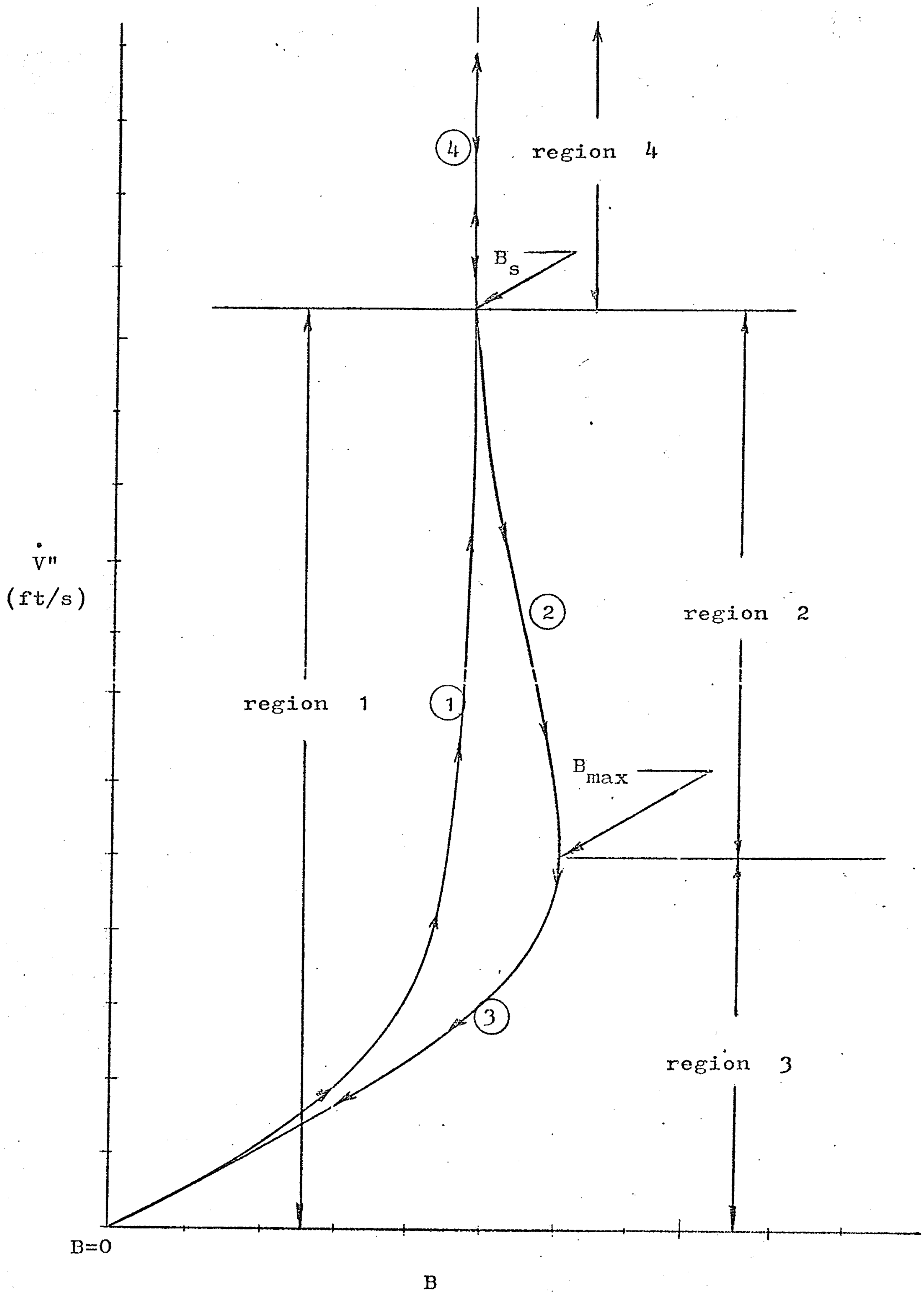

Fig. 5.2 Sketch of four flow regions

Fig. 5.2

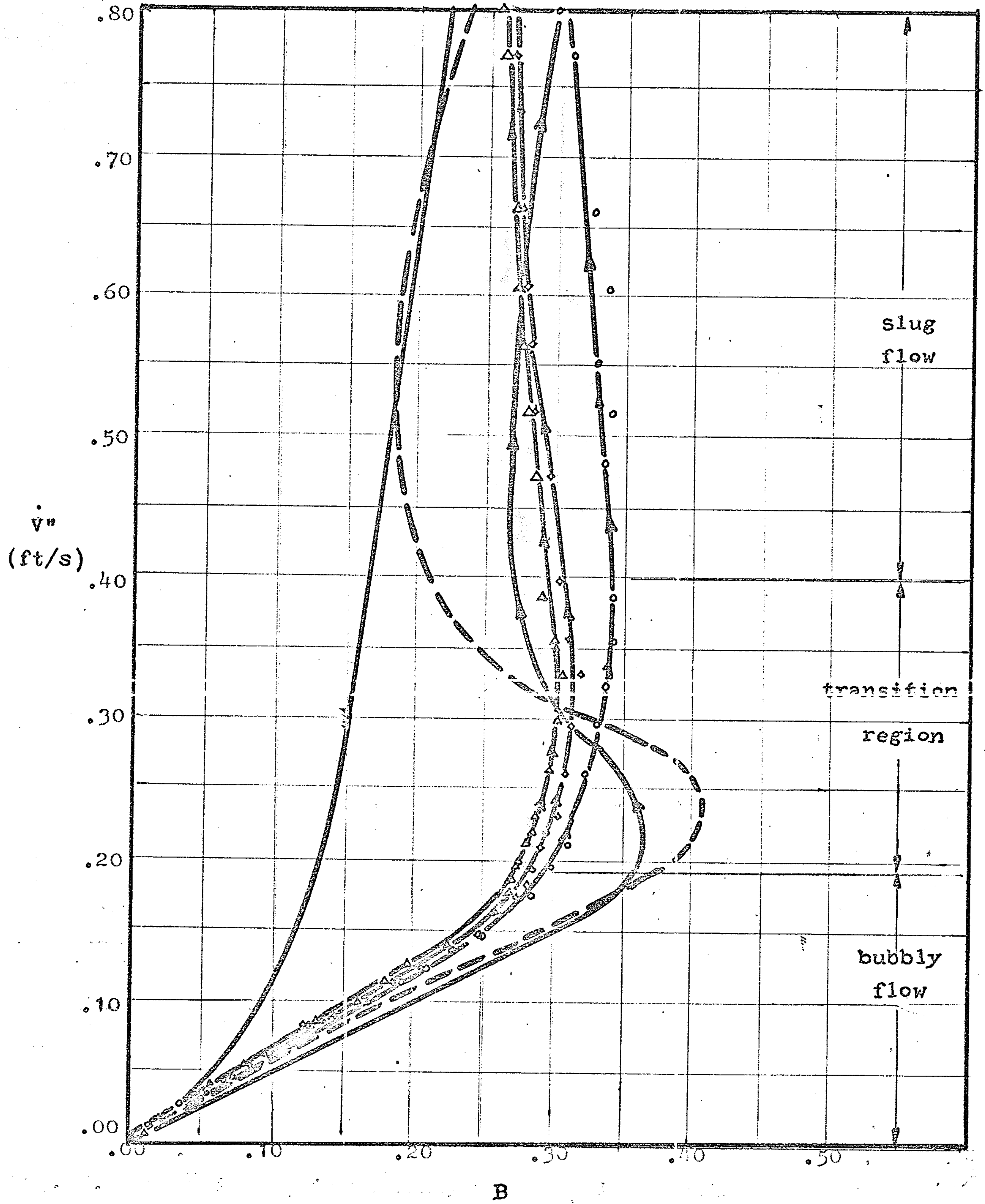

Fig. 5.3 Superficial air velocity versus void fraction(No.160)

Remarks: D.W.(Wallis) T.W.(Wallis)
T.W.(Card) O B_o △ B_1 ◇ B_2 D.W.*(present work)
*The distilled water used 5 times

Fig. 5.3

Fig. 5.4

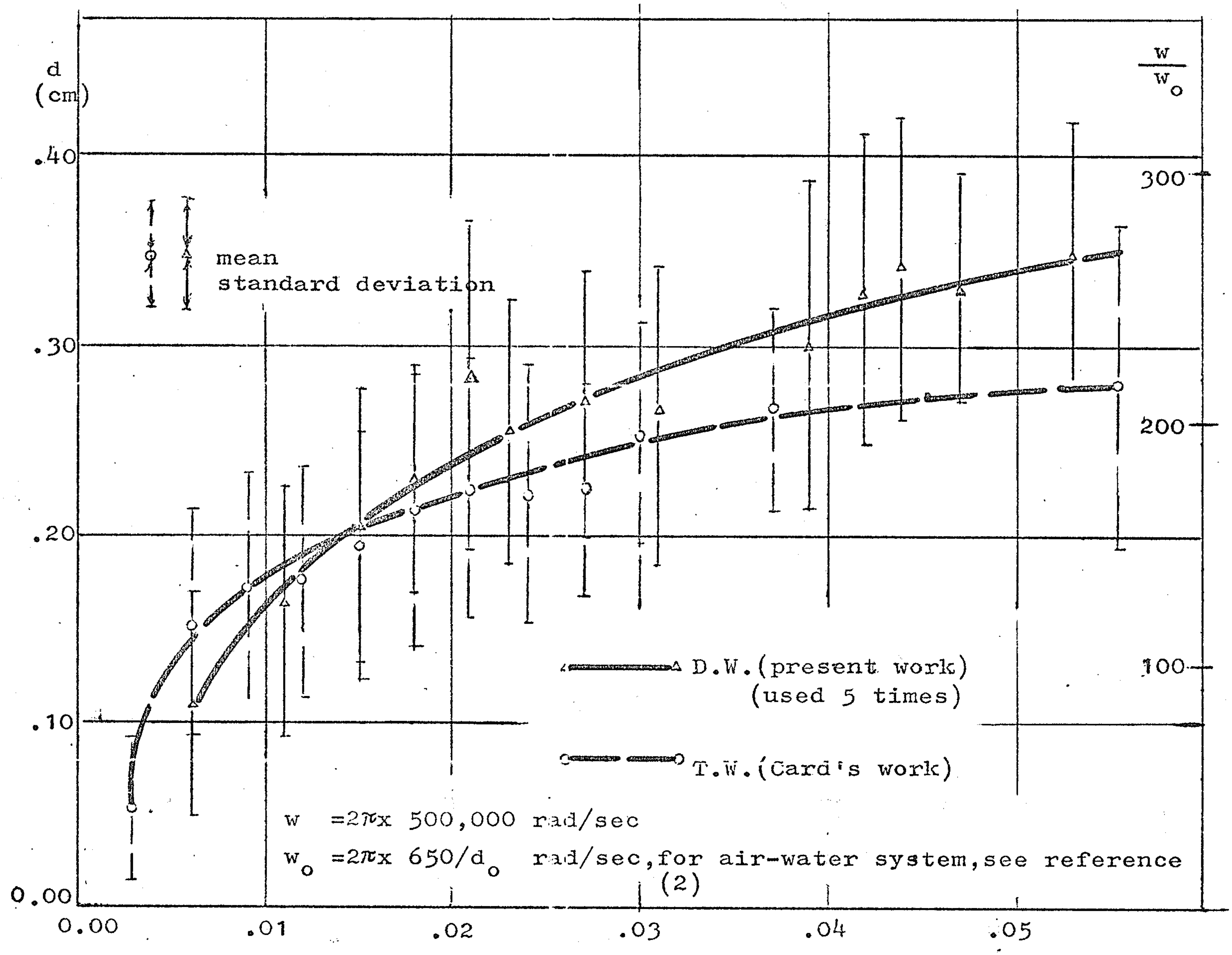

Fig. 5.4 Mean bubble diameter and frequency ratio versus void fraction (No.160)

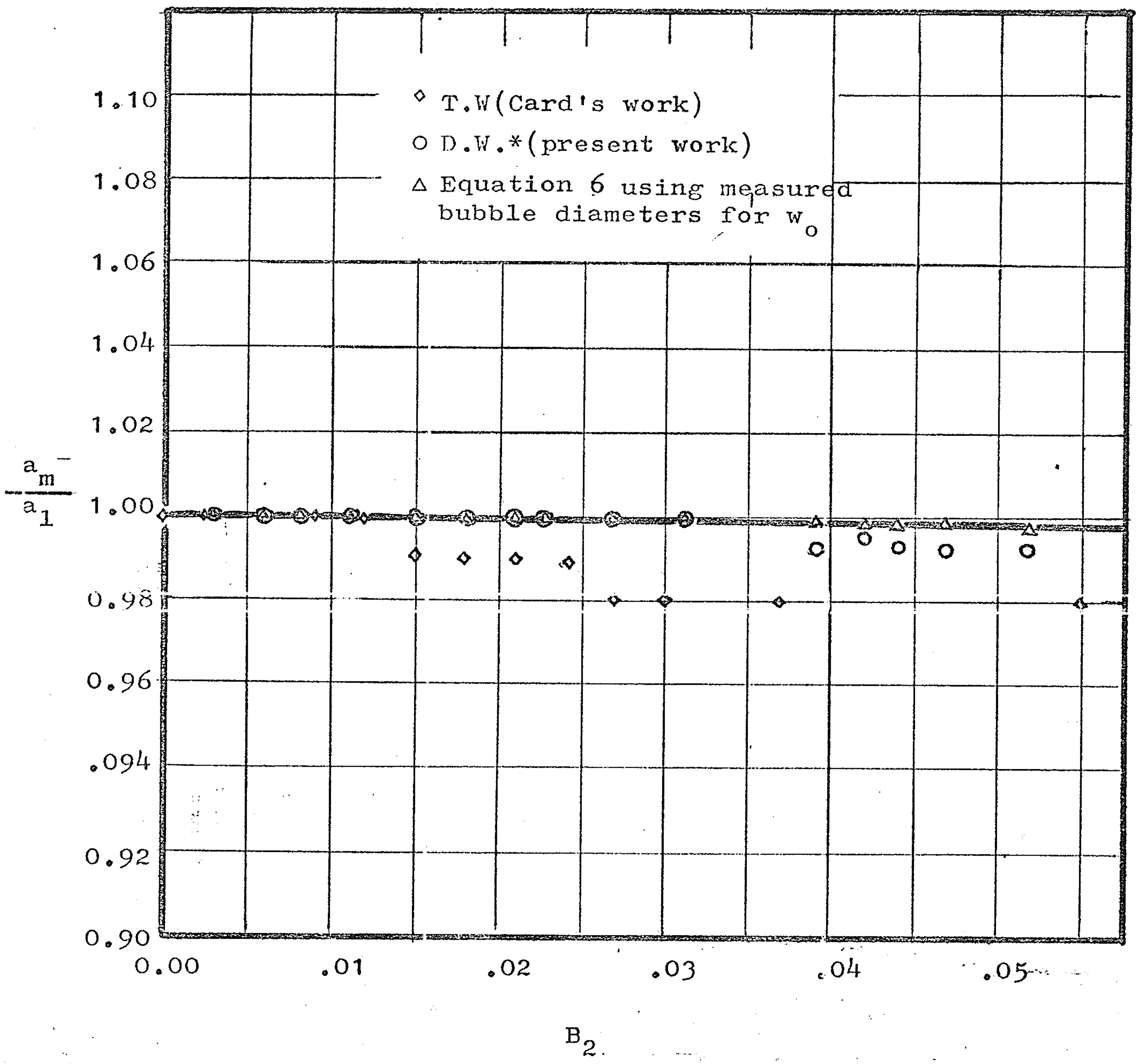

Fig. 5.5 Ultrasonic measurement of acoustic velocity versus void fraction for air-water mixture in the low void fraction range (No.160)

Remark: *The distilled water used 5 times.

Fig. 5.5

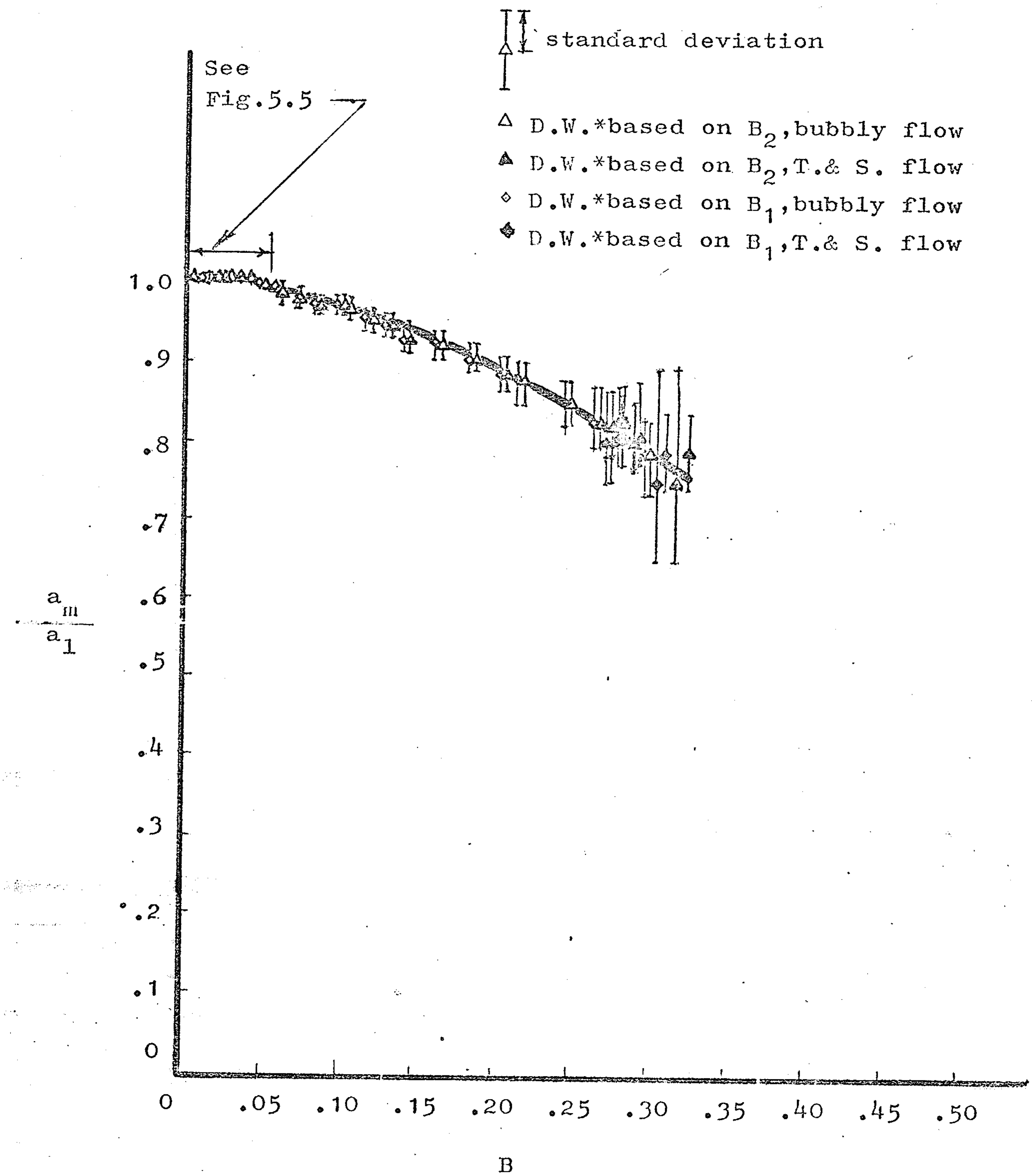

Fig. 5.6 Ultrasonic measurement of acoustic velocity versus void fracions (B_1 and B_2) for air-distilled water mixture(No.160)

Remark:* The distilled water used 5 times

Fig.5.6

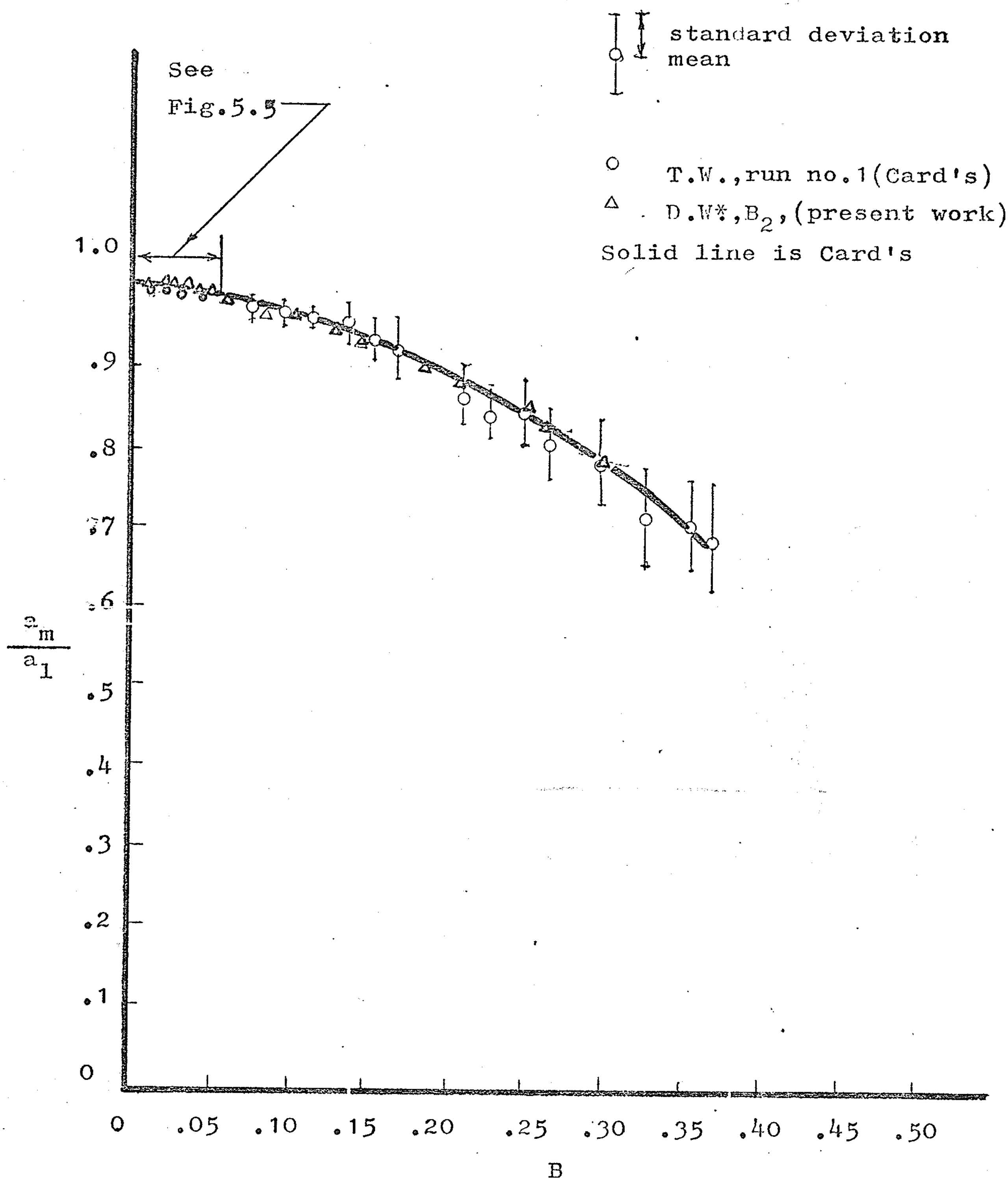

Fig. 5.7 Ultrasonic measurement of acoustic velocity versus void fraction for air-water mixture in bubbly flow (No.160)

Remark:*The distilled water used 5 times

Fig. 5.7

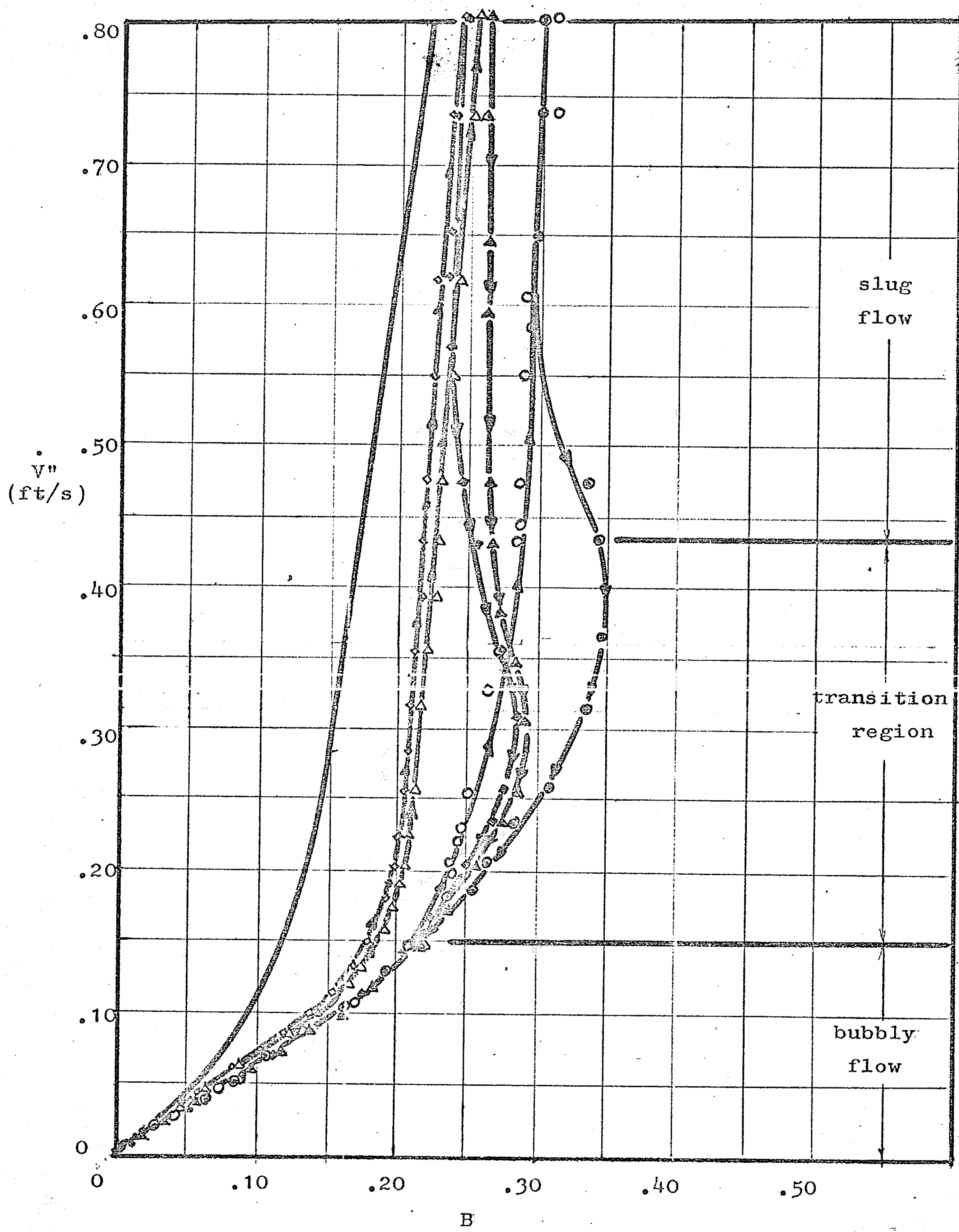

Fig. 5.8 Superficial air velocity versus void fraction(No.401)

Remarks: D.W.(Wallis)

△ B_1 ◇ B_2 ○ B_0 deionized D.W.(present work)

Fig. 5.8

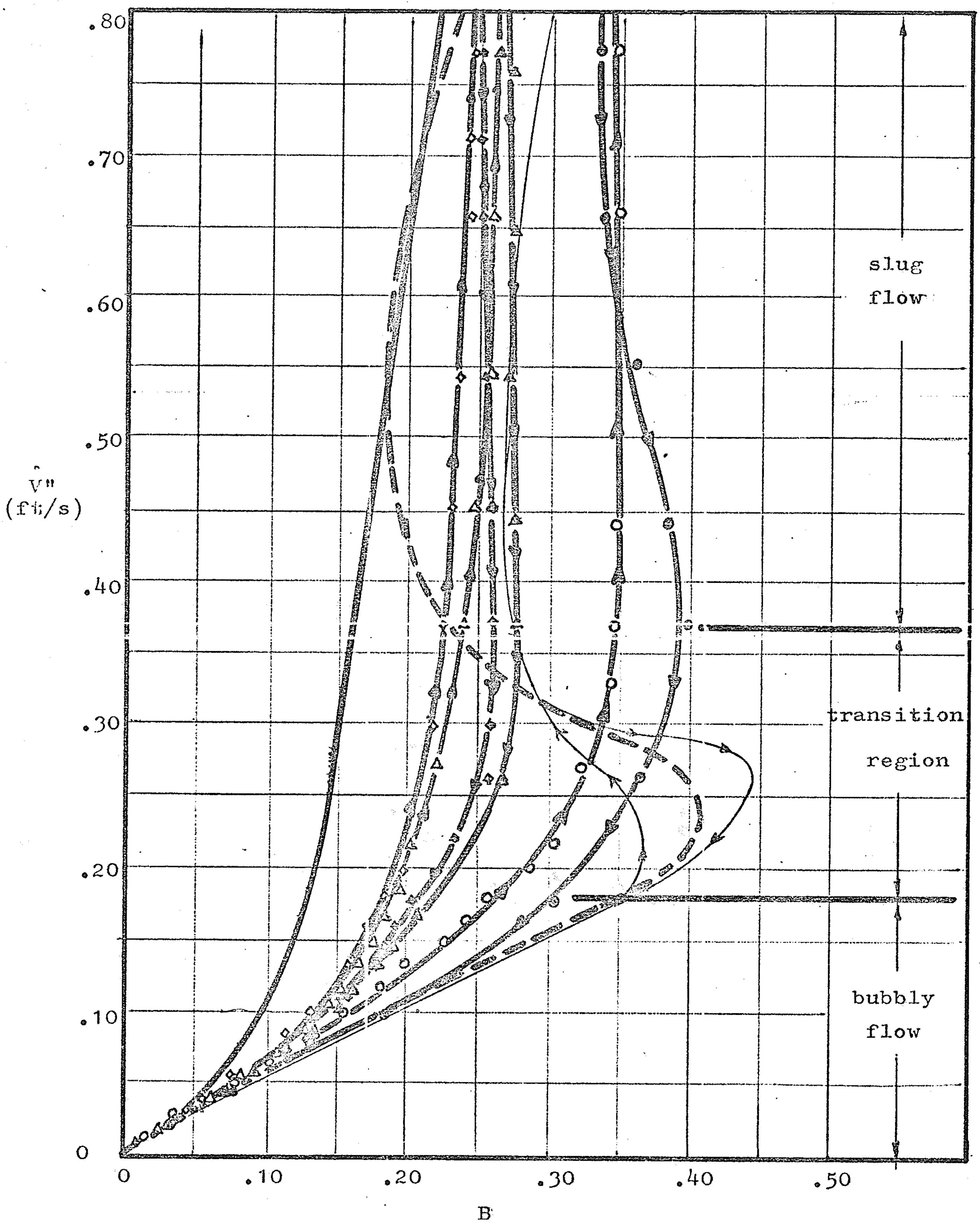

Fig. 5.9 Superficial air velocity versus void fraction (No.601)
Remarks: ——— D.W.(Wallis) — — — T.W.(Wallis)
——> T.W.(Card) o B_0 △ B_1 ◇ B_2 T.W.(present work)

Fig. 5.9

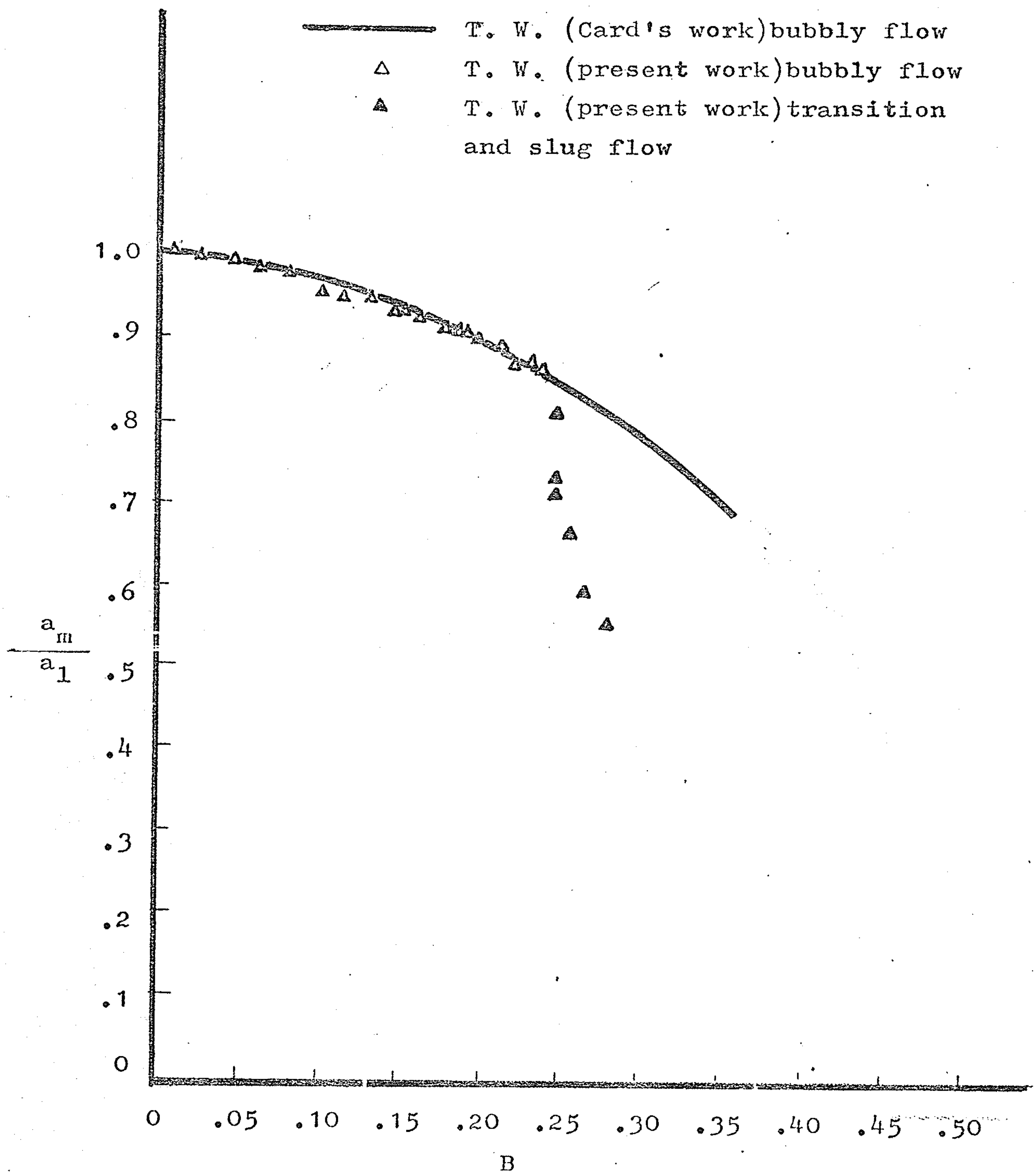

Fig. 5.10 Ultrasonic measurement of acoustic velocity versus void fraction(B_1) for air-water mixture (No.601)

Fig. 5.10

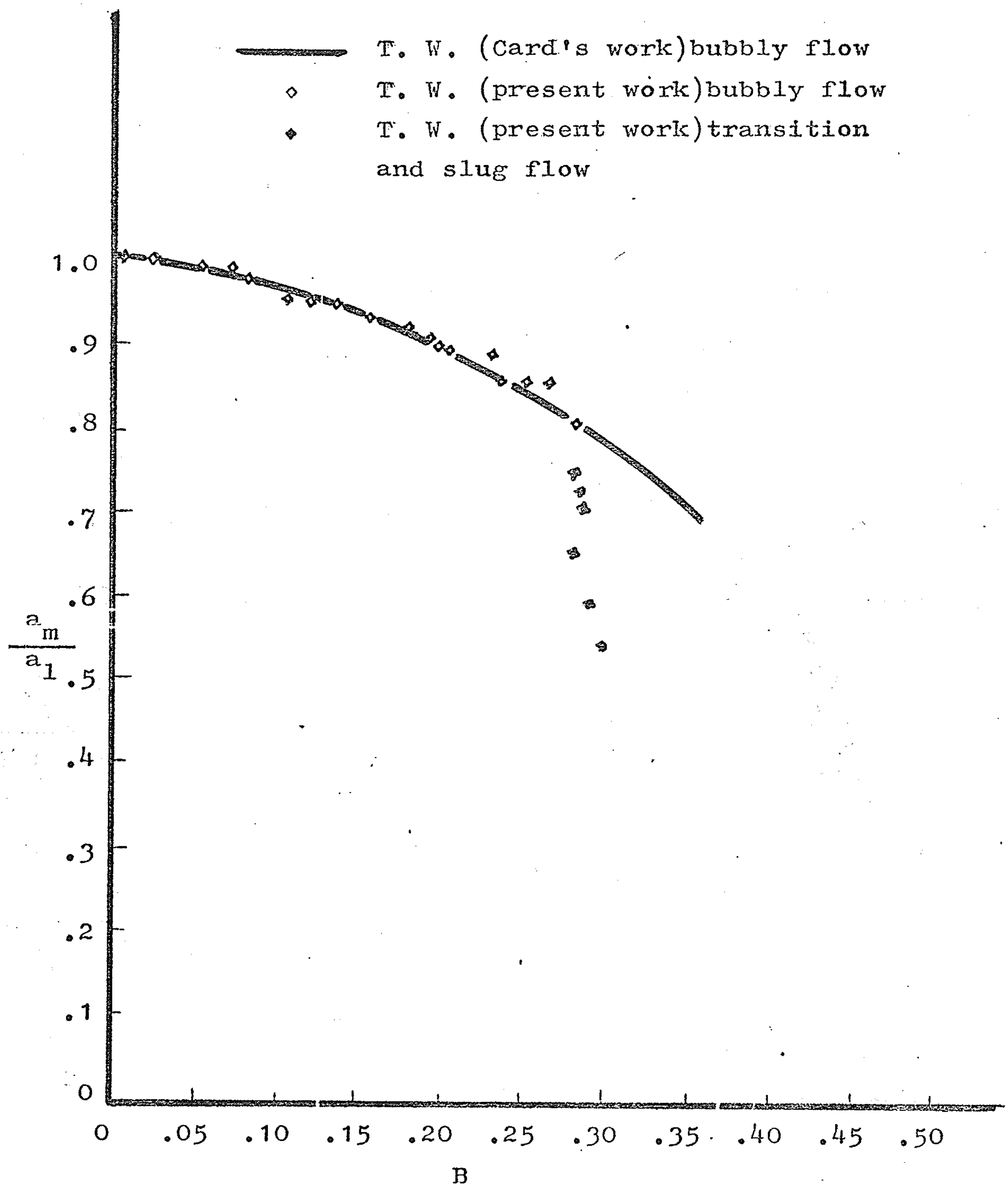

Fig. 5.11 Ultrasonic measurement of acoustic velocity versus void fraction(B_2) for air-water mixture (No.601)

Fig. 5.11

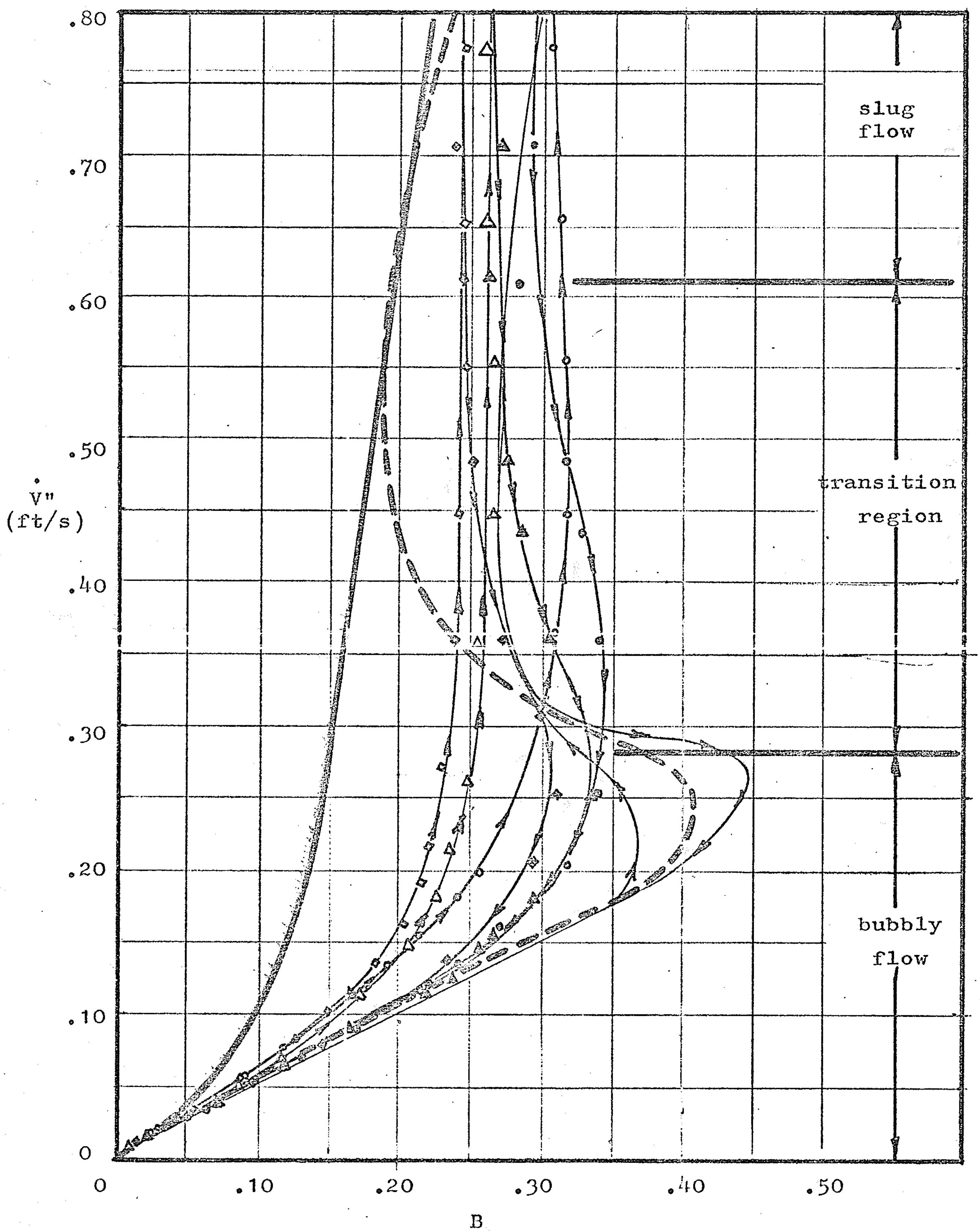

Fig. 5.12 Superficial air velocity versus void fraction (No.1101)
Remarks: ——— D.W.(Wallis) — — — T.W.(Wallis)
——— T.W.(Card)
$\triangle B_1 \diamond B_2 \circ B_o$ T.W.+KCl (present work)

Fig. 5.12

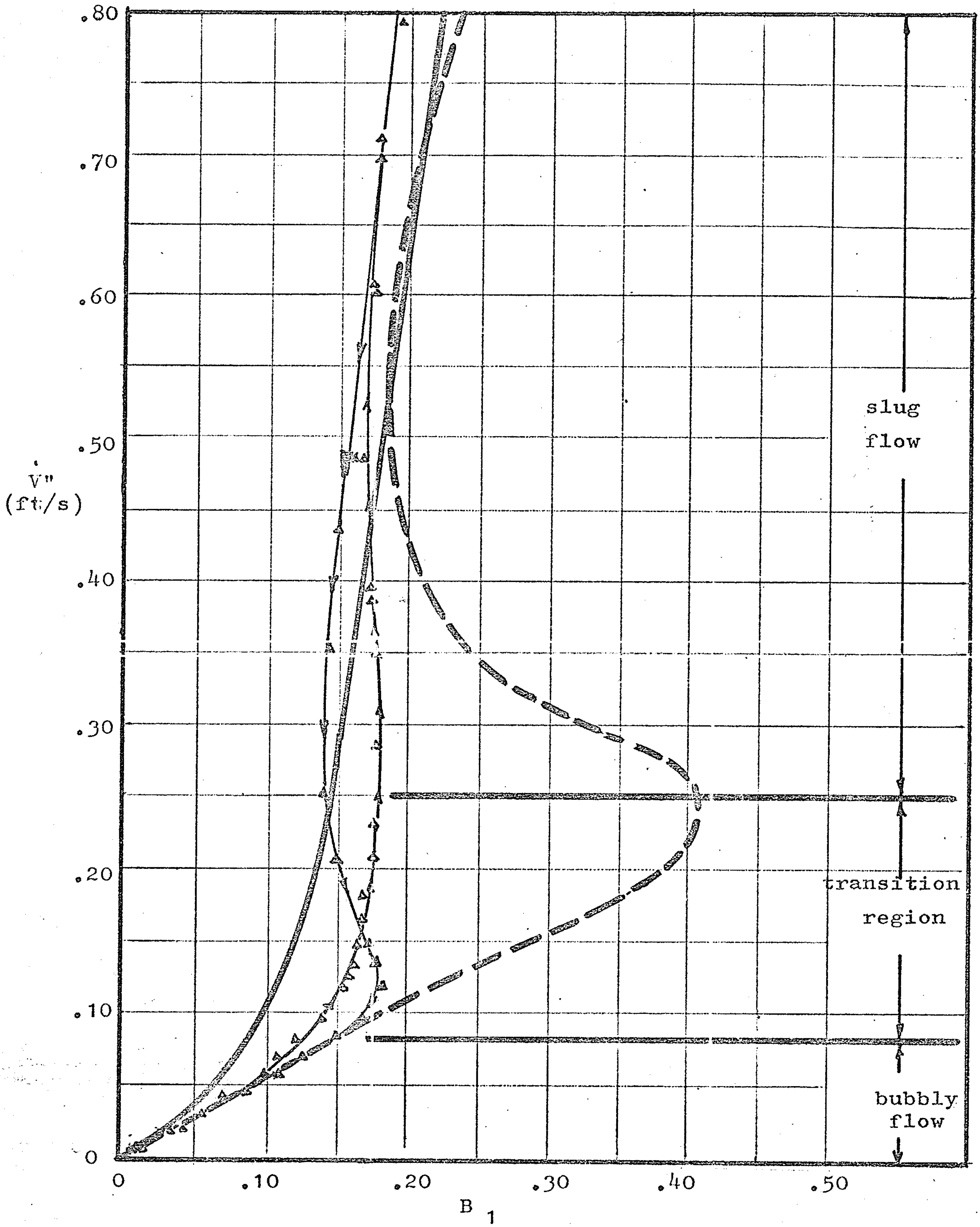

Fig. 5.13 Superficial air velocity versus void fraction(No.1220)
Remarks: ——— D.W.(Wallis) — — — T.W.(Wallis)
△ T.W.+soap solution (present work) Fig. 5.13

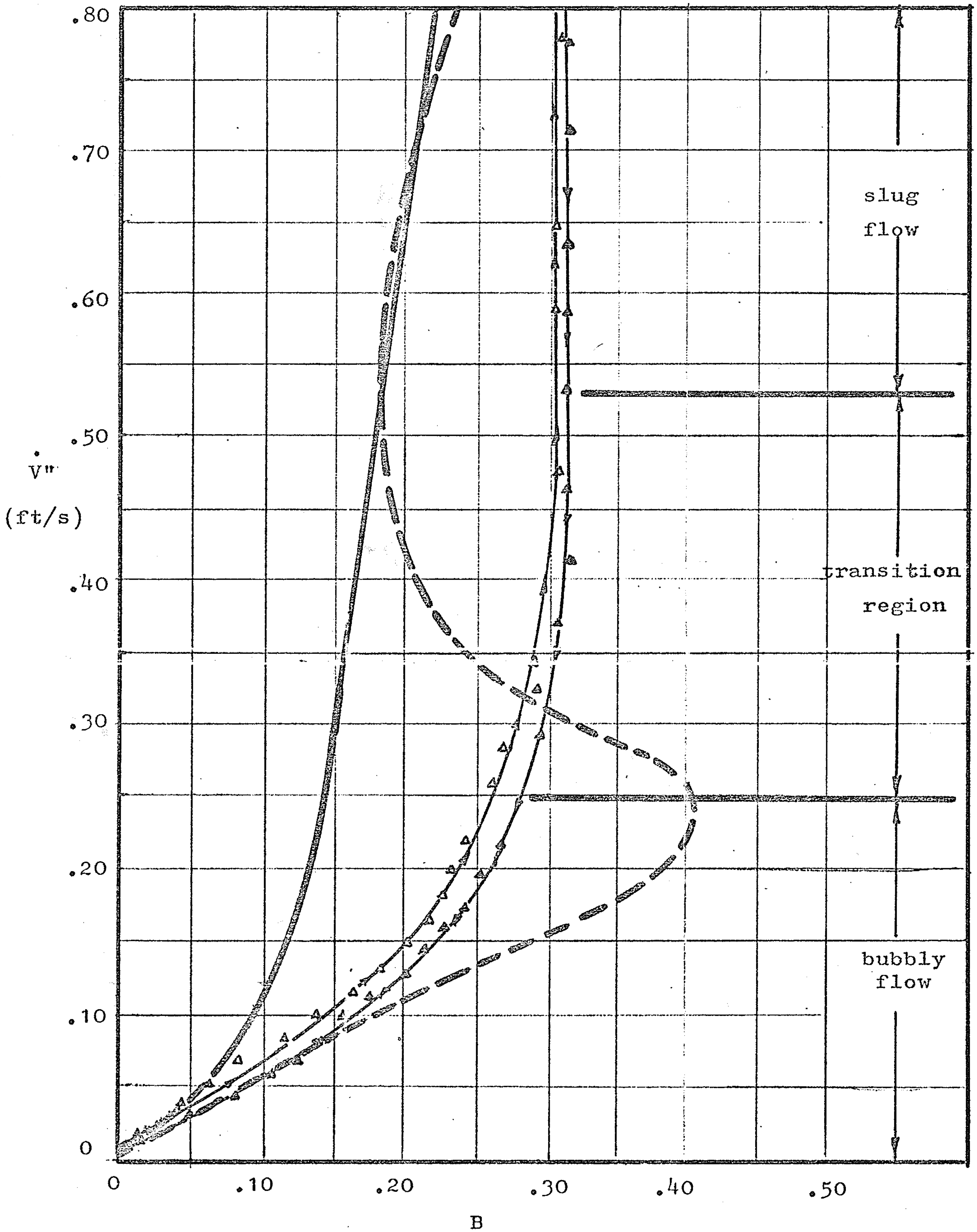

Fig. 5.14 Superficial air velocity versus void fraction (1301)

Remarks: D.W.(Wallis) T.W.(Wallis)

△ T.W.+detergent(present work) Fig. 5.14

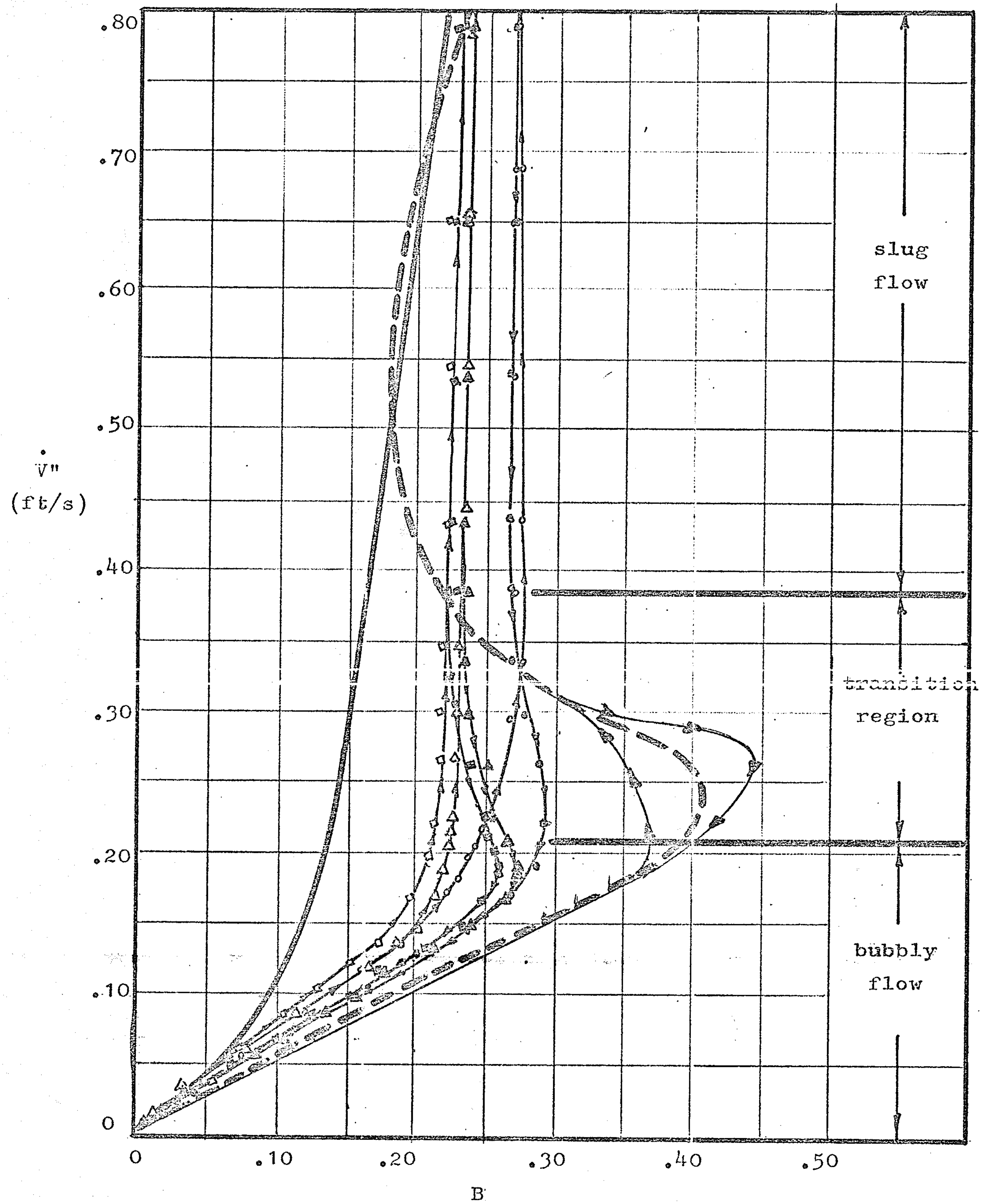

Fig. 5.15 Superficial air velocity versus void fraction(No.1401)

Remarks: ——— D.W.(Wallis) — — — T.W.(Wallis)

——— T.W.(Card)

△ B_1 ◇ B_2 ○ B_o D.W.(present work)

Fig. 5.15

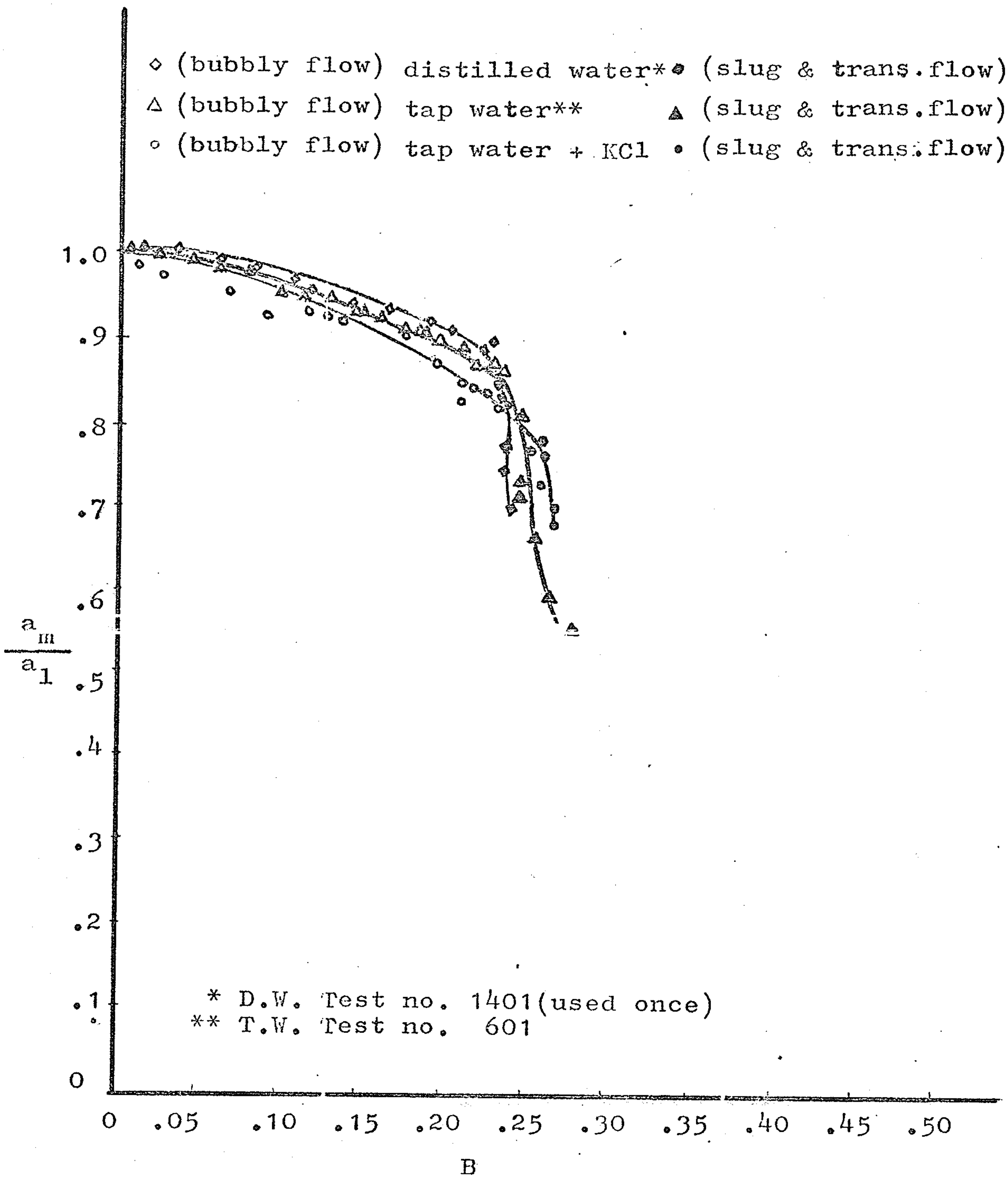

Fig. 5.16 Ultrasonic measurement of acoustic velocity versus void fraction for air-T.W., D.W. and T.W. plus KCl.

Fig. 5.16

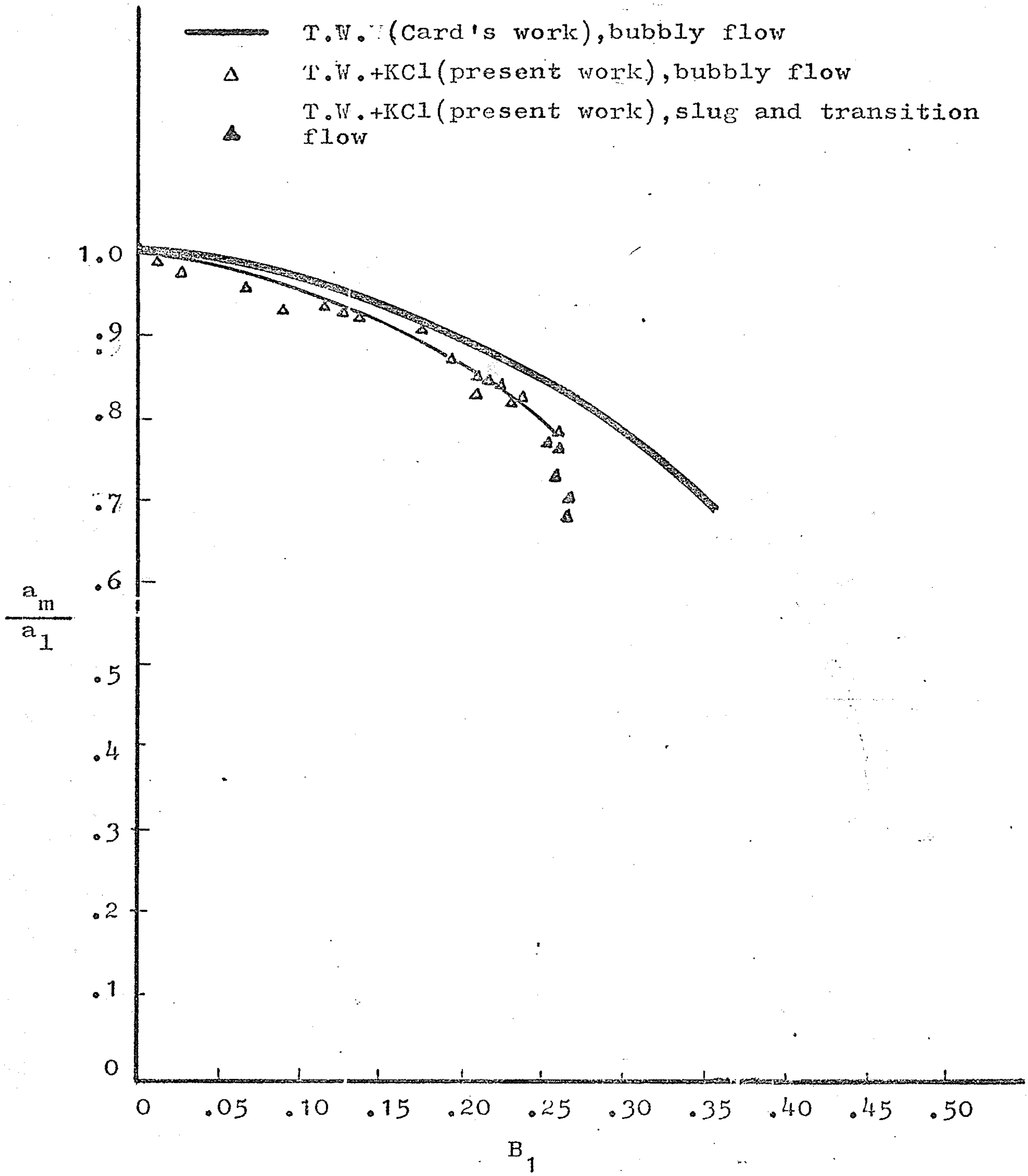

Fig. 5.17 Ultrasonic measurement of acoustic velocity versus void fraction for air-T.W. and air-T.W.+KCl (Test no. 1101)

Fig. 5.17

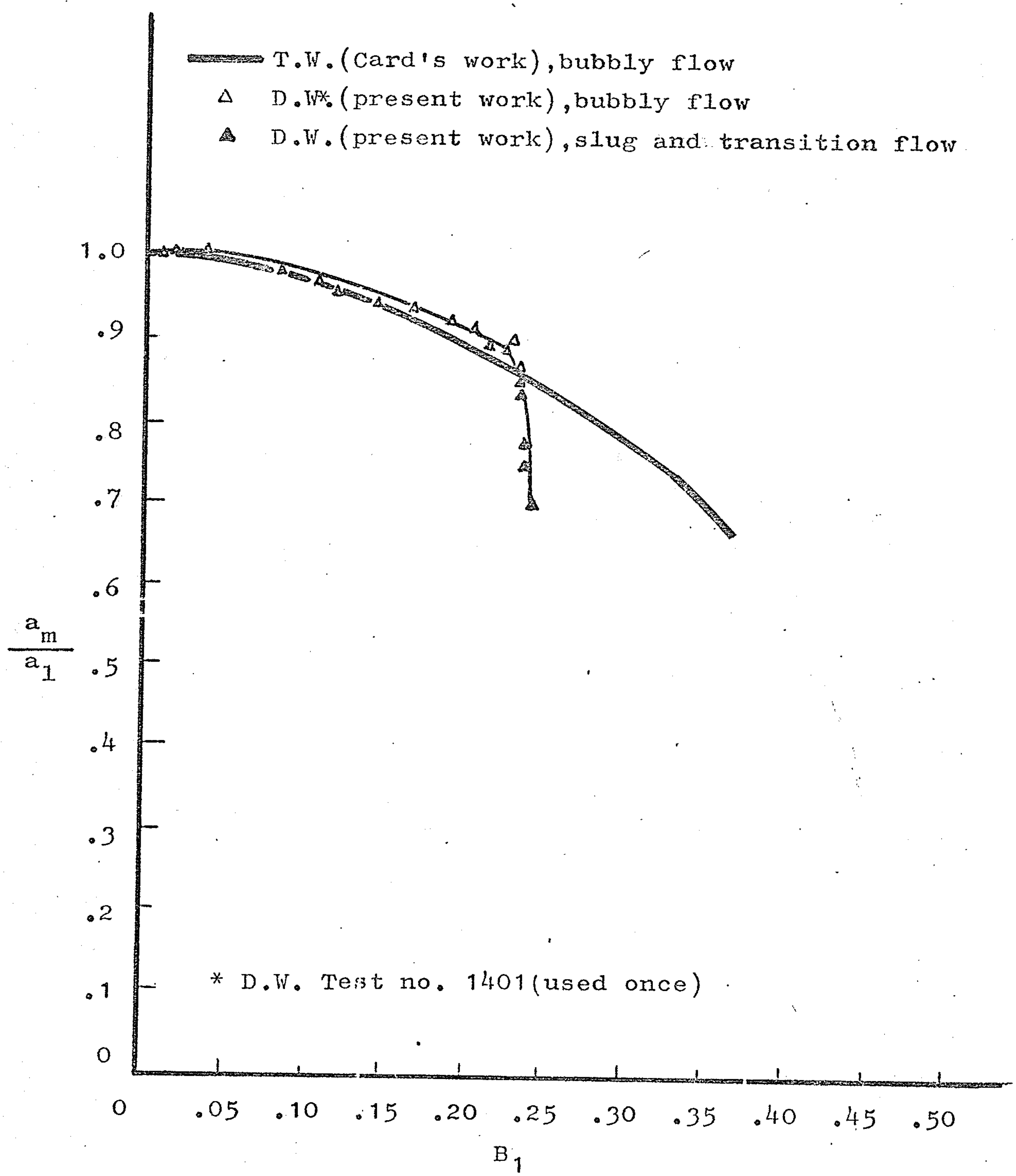

Fig. 5.18 Ultrasonic measurement of acoustic velocity versus void fraction for air-T.W. and air-D.W.

Fig. 5.18

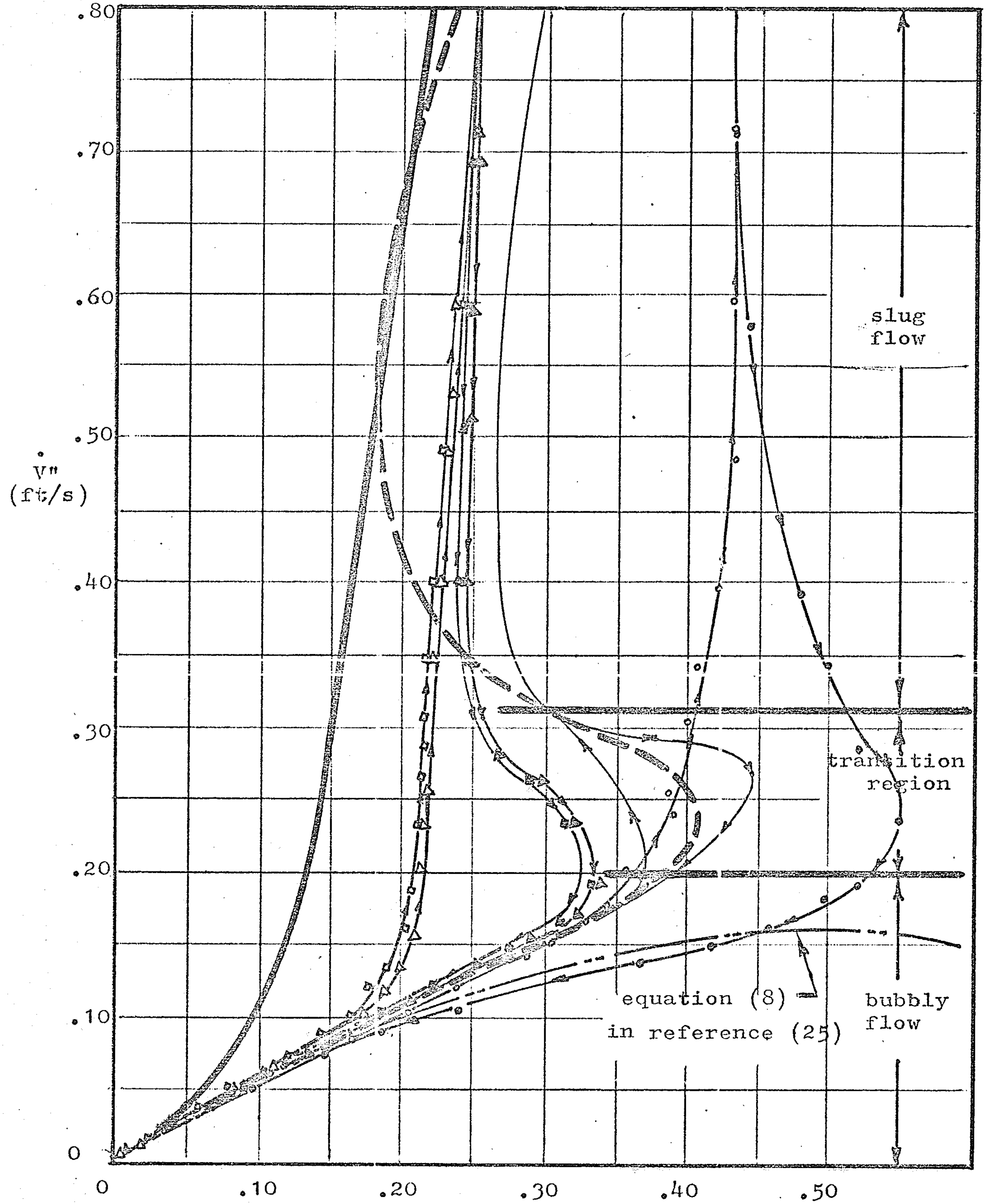

Fig. 5.19 Superficial air velocity versus void fraction (No. 1601)
Remarks: D.W. (Wallis) T.W. (Wallis)
T.W. (Card) $\Delta B_1 \diamond B_2 \circ B_0$ T.W. was blown with air for 30 hrs. (present work)

Fig. 5.19

		Test No.							
		160	401	601	1101	1220	1301	1401	1601
Fig. No.		5.3	5.8	5.9	5.12	5.13	5.14	5.15	5.19
Liquid used		(2) D.W.	(3) D.D.W.	(4) T.W.	T.W. +KCl	T.W. +soap	T.W. +detgt.	D.W.	(7) T.W.
Max. difference of B bet. 1 and 2 * formed by loop:	B_1		.07	.042	.085	.040	.020	.050	.120
	B_2		.07	.042	.080			.050	.120
	B_o		.07	.045	.060			.050	.120
Max. difference between B_o and B_1 **			.06	.075	.050			.050	.18
*** Length of region: (ft/s)	1		.90	.90	.80	.70	.53	.43	.83
	2		.60	.57	.55	.585	.00	.245	.63
	3		.30	.33	.25	.115	.53	.185	.20
Max. B of	B_1	.30	.29	.275	.335	.180	.310	.272	.34
	B_o	.345	.35	.395	.340			.292	.55

Remarks:

* The maximum difference of void fraction between the traces of increasing flow rate and the decreasing air flow rate is the distance from B_{max} to B of 1 (Fig. 5.2).

** The distance between B_s from loop B_o to B_s from loop B_1 was measured as maximum difference in void fraction from B_o to B_1.

*** The length of regions were measured on B_1.

The numbers (2), (3), (4) and (7) refer to notes of those same numbers on Table 1.

Table 4 Summary of present work on relationship of superficial gas velocity and void fraction.

CHAPTER 6

CONCLUSIONS

The conclusions drawn from the present work may be summarized as follows:

1. The previous work of Card [2], one of the most important results of which was the reporting of the a_m/a_1 versus B relationship for high frequency sound waves in tap water, has been verified (see Figs. 5.10 and 5.11).

2. There is a dramatic decrease in the curve of a_m/a_1 versus B when transition and slug flow develops; this was true for tap water, tap water and KCl additive and distilled water (see Figs. 5.10,11,16,17 and 18).

3. As with the previous work of Card et al [3], for the low B region, the theoretical equation for the group velocity for the constant-density case and the measured signal velocity agree closely (see Fig. 5.5); it is understood that for the present high frequencies the signal velocity and the group velocity are virtually identical.

4. There appears to be a tendency for lower a_m/a_1 with increasing surface tension in curves of a_m/a_1 versus B, although this conclusion is somewhat tentative (see Fig. 5.16).

5. In many tests at least two measurements of B (B_1 and B_2) were taken simultaneously (B_o is not considered because of the large errors due to foaming). The differences between B_1 and B_2 were extremely small (see Figs. 5.3,8,9,12,15 and 19) and make no difference at all to curves of a_m/a_1 versus B (see Fig. 5.6, 5.10 and 5.11).

6. A new method of categorizing flow regions has been proposed based only on measurements of $\dot{V}''$ versus B; it has the advantage of being based on quantitative measurements and not on the somewhat subjective visual observation of flow in the transparent tube.

REFERENCES

[1] Campbell, I.J. and Pitcher, A.S., "Shock Wave in a Liquid Containing Gas Bubbles", Proc. Roy. Soc. 243 (Series A) 1235, 534-5, 1958.

[2] Card, D.C. "Determination of Void Fraction in a Gas-Liquid Mixture by an Ultrasonic Technique", thesis presented to the Faculty of Graduate Studies of The University of Manitoba, May 1969.

[3] Card, D.C., Sims, G.E. and Chant, R.E. "Determination of Void Fraction in a Bubbly Gas-Liquid Mixture by an Ultrasonic Technique", to be submitted for publication.

[4] Cartensen, E.L. and Foldy, L.L., "Propagation of Sound Through a Liquid Containing Bubbles" J. Acoustical Soc. Am. 19, No. 3, 481-501, 1947.

[5] Davids, N. and Thurston, E.G., "The Acoustical Impedance of a Bubbly Mixture and Its Size Distribution Function", J. Acoustical Soc. Am. 19, No. 1, 20-23, 1950.

[6] Devin, C. Jr., "Survey of Thermal, Radiation and Viscous Damping of Pulsating Air Bubbles in Water", David Taylor Model Basin Report 1329, August 1959.

[7] Evans, R.G., Gouse, S.W. Jr. and Bergles, A.E., "Pressure Wave Propagation in Adiabatic Two-Phase Flow", Report No. DSR 74629-2, Contract No. 3963(15), M.I.T. May 1968.

[8] Fox, F.E. Curley, S.R. and Larson, G.S., Phase Velocity and Absorption Measurements in Water Containing Air Bubbles", J. Acoustical Soc. Am., 27, No. 3, 534-539, 1955.

[9] Gouse, S.W. Jr. and Brown, G.A., "A Survey of the Velocity of Sound in Two-Phase Mixtures", ASME Paper 64-WA/FE-35.

[10] Henry, R.E., Golmes, M.A. and Fauske, H.K., "Propagation Velocity of Pressure Wave in Gas-Liquid Mixtures", International Symposium on Research in Cocurrent Gas-Liquid Flow", Sept. 18-19, 1968, Waterloo, Ontario, Canada.

[11] Hsieh, D.Y. and Plesset, M.S., "On the Propagation of Sound in a Liquid Containing Gas Bubbles", Phys. of Fluid, 4, No. 8, 970-975, 1961.

[12] Karplus, H.B., "The Velocity of Sound in a Liquid Containing Gas Bubbles", Coo-248, June, 1958.

[13] Karplus, H.B., "Propagation of Pressure Waves in a Mixture of Water and Steam", ARF 4123-12, January, 1961.

[14] Laird, D.T. and Kendig, P.M., "Attenuation of Sound in Water Containing Air Bubbles", J. Acoustical Soc. Am., 24, No. 1, 29-32, 1952.

[15] Meyer, E. and Skudrzyk, E., "Uber die Akustischen Eigenschaften von Gasblasenschleiern in Wasser", Acustica, 3, 434-440, 1953.

[16] Pfriem, H., "Zur Thermischen Dampfung in Kugelsymmetrisch Schwingenden Gasblasen", Akust, Z. 5, 202-12, 1940.

[17] Semenov, N.I. and Kosterin, S.I., "Results of Studying the Speed of Sound in Moving Gas-Liquid Systems", Teploenergetika 11, No. 8, 33-36, 1964.

[18] Silberman, E., "Sound Velocity and Attenuation in Bubbly Mixtures Measured in Standing Wave Tubes", J. Acoustical Soc. Am. 29, No. 8, 925-933, 1957.

[19] Skudrzyk, E., "Die Grundlagen der Akustik", Springer-Verlag, Vienna, 862-868, 1954.

[20] Stewart, G.W. and Lindsay, R.B., "Acoustics" D. Van Nostrand Co., Inc., New York, 328, 1930.

[21] Straub, L.G., Ripken, S.F. and Olson, R.M., "A Study of the Influence of Gas Nuclei on Cavitation Scale Effects in Water Tunnel Test (with an Appendix, A Sonic Method of Measuring the Concentration of Undissolved Gas Nuclei in Water)", St. Anthony Falls Hydraulic Laboratory, University of Minnesota, Project Report No. 58, February, 1958.

[22] Strasberg, M., "Undissolved Air Cavitation Nuclei", Symposium on Cavitation in Hydrodynamics Teddington, England: National Physical Laboratory, 1955.

[23] Tangren, R.F., Dodge, C.H. and Seifer, H.S. "Compressibility Effects in Two Phase Flow" J. App. Phys. 20, No. 7, 637-45, 1949.

[24] Walle, F.V.D., Verheugen, A.J., Haagy, V.J.M. and Bogaardt, M., "A Study of Application of Acoustical Methods for Determining Void Fraction in Boiling Water System" EUR 233e., 1966.

[25] Wallis, G.B., "Some Hydrodynamic Aspects of Two-Phase Flow and Boiling", Part 1, International Developments in Heat Transfer, 1961-62.

[26] Wood, A.B., "A Textbook of Sound", B. Bell and Sons Ltd., London, 1960, pp. 360-363.

[27] Braddick, "Vibrations, Waves and Diffraction", p. 134, McGraw-Hill Publishing Co. Ltd., 1965.

[28] Brillouin, L., "Wave Propagation and Group Theory", Academic Press, New York, 1960.

[29] Towne, "Wave Phenomena", Addison-Wesely Publishing Co., Inc., 1967.

[30] Charles D. Hodgman, "Handbook of Chemistry and Physics" The Chemical Rubber Publishing Co., 42nd Edition, 1960, pp. 2176-2182.

APPENDIX A

ESTIMATING THE ERROR IN THE MEASURED SUPERFICIAL GAS VELOCITY

Two rotameters were used in this investigation. Consider first the smaller of the two. This rotameter, R-6-15-B, was checked by a wet gas flow meter which had been checked by the Greater Winnipeg Gas Company with a 20 ft^3 measuring tank. The maximum deviation of flow rates calculated from the tank and from the wet flow meter was 3%. This would suggest an error in the wet flow meter of certainly not more than 3%, and probably more like 2 1/2%. The calibration curve for the smaller rotameter is shown in Fig. A.1; the difference between the manufacturer's curve and the present calibration curve is shown for interest. Considering the accuracy of the wet meter, a reasonable estimate of the error in using the rotameter readings corrected by the present calibration appears to be approximately 3%. This would give an error of 3.2% in the superficial velocity $\dot{V}''$ when the error in measuring the perspex tube cross-sectional area is estimated at 1% and the errors are negligibly small in correcting the flow rate for slightly different temperature and pressure conditions on the top of the porous sparger. The above estimates would not apply below a superficial velocity of 0.025 ft/s (7 SCFH) where the discrimination error (0.5 mm in the reading on the rotameter tube) becomes very significant (2%) compared with the accuracy of the calibrating device. For interest, this error in scale reading is shown in Fig. A.2. The small rotameter generally covered bubbly flow and approximately one-half of the transition flow regime.

There was no device available for conveniently calibrating the large rotameter. However, there was a range of flow rates where the two rotameters did overlap; in this overlap range the small rotameter was used to check the manufacturer's curve of the large rotameter. Indications were that the relative position of the calibration curve and the manufacturer's curve would look very similar to that shown for the smaller rotameter (Fig. A.1) except, of course, that the values marked on the abscissa would be greater. This curve was then used to obtain corrected flow rates. An error of 4% is suggested for the range of flow rates where the large rotameter was used (in the overlap range the small rotameter was used). The large rotameter covered flow rates corresponding to slug flow and approximately one-half of the transition flow regime.

The use of the word "error" above would correspond to "uncertainty interval" in Kline and McClintock (Mechanical Engineering, vol. 37, p.6, 1953) with "odds" of approximately 20 to 1.

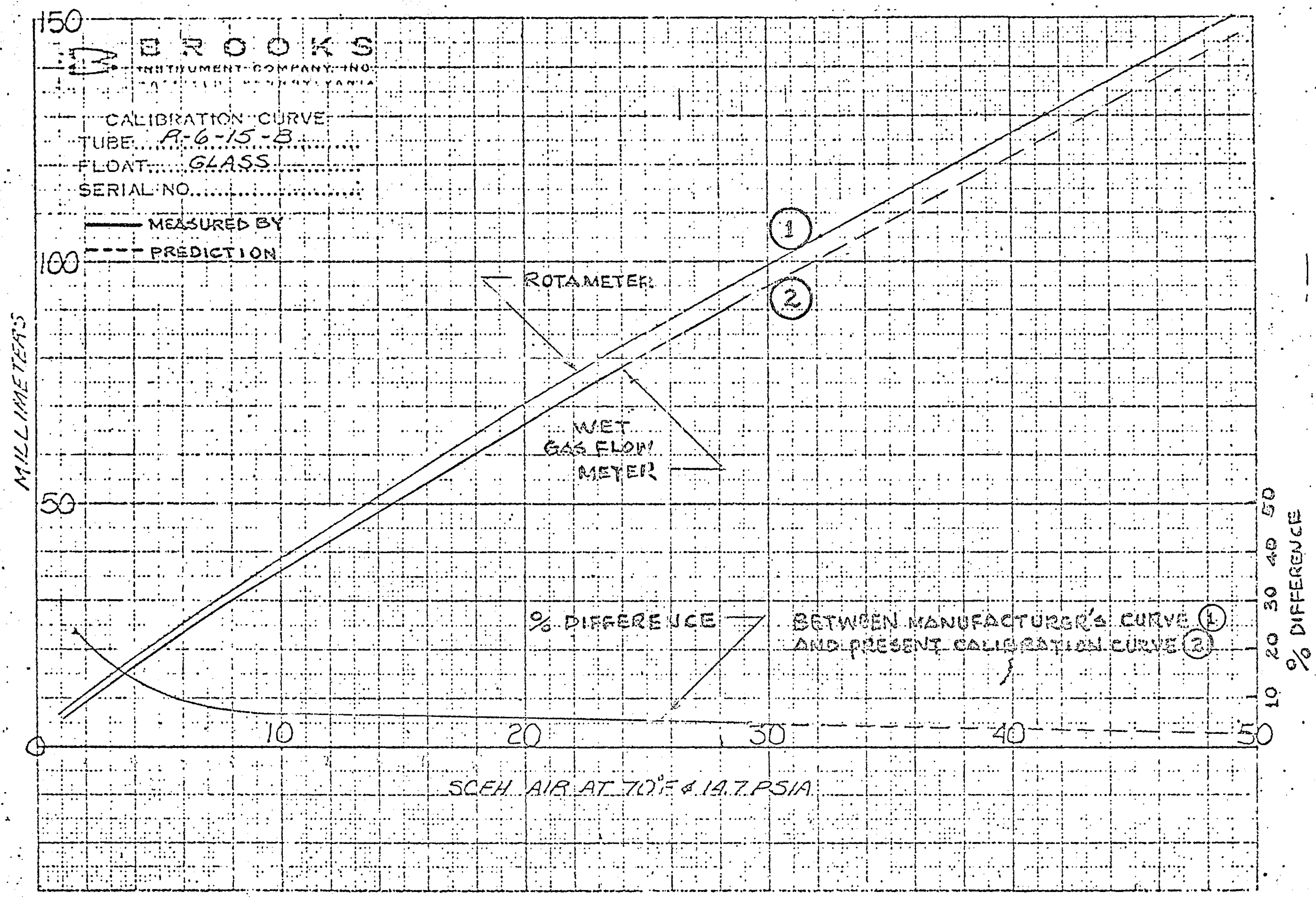

Fig. A.1

Fig. A.1 Calibration of rotameter

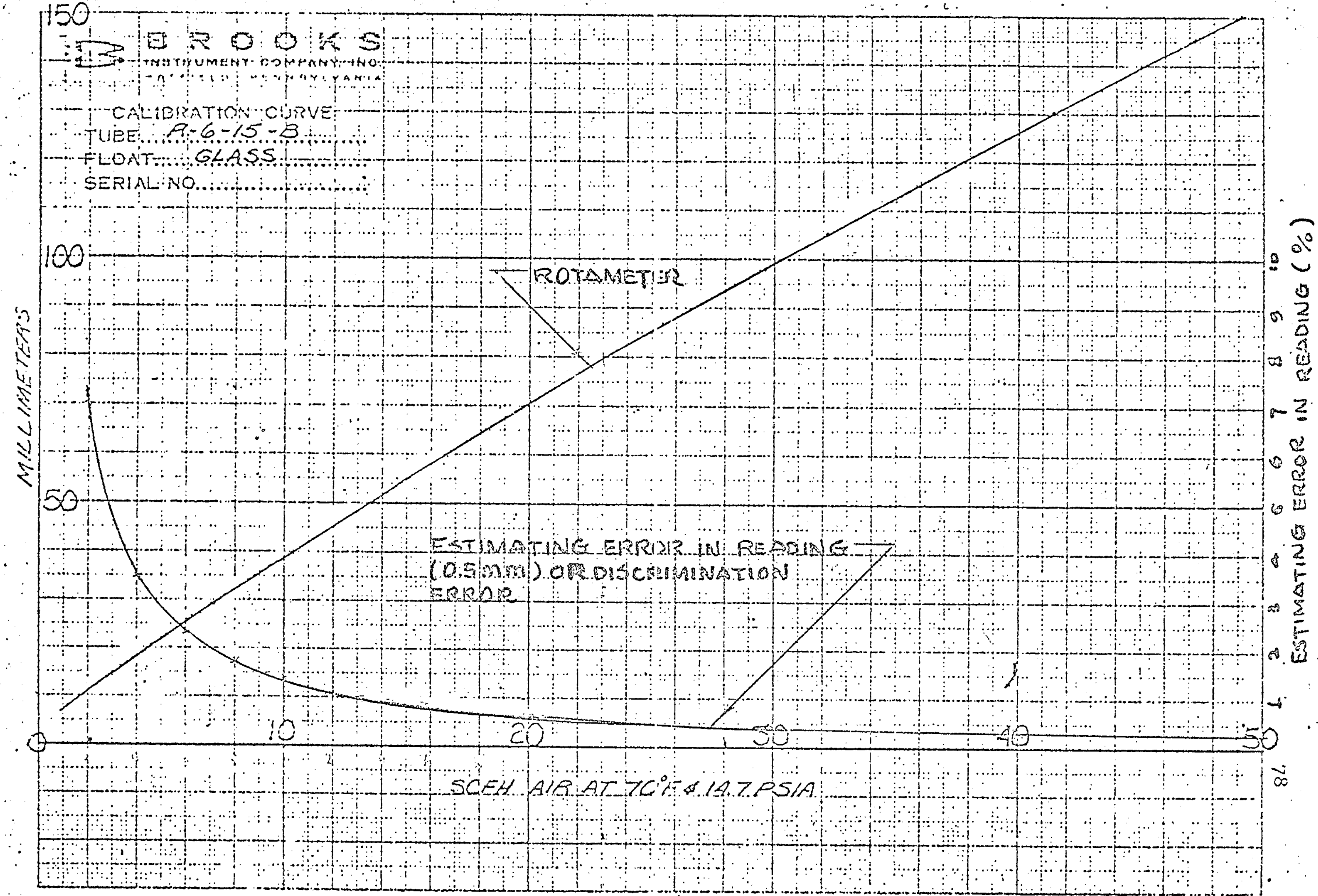

Fig. A.2

Fig. A.2 Scale-reading error on rotameter

APPENDIX B

VOID FRACTION MEASUREMENT ANALYSIS

B.1 Nomenclature

B = void fraction

ρ = density (lb_m/ft^3)

h = height (ft)

H = height (ft)

V = volume (ft^3)

W = mass (lb_m)

Subscripts

a = level at position a

b = level at position b

R = marian oil*

w = water

m = air-liquid mixture

air = air bubbles

θ = sloping at angle θ

liquid = liquid

B.2 Derivation of Basic Equations

For following the presentation below, reference should be made to Fig. B.1.

$$P_a = P_2 + h_2\rho_w$$

---

* Specific gravity of marian oil is 0.827

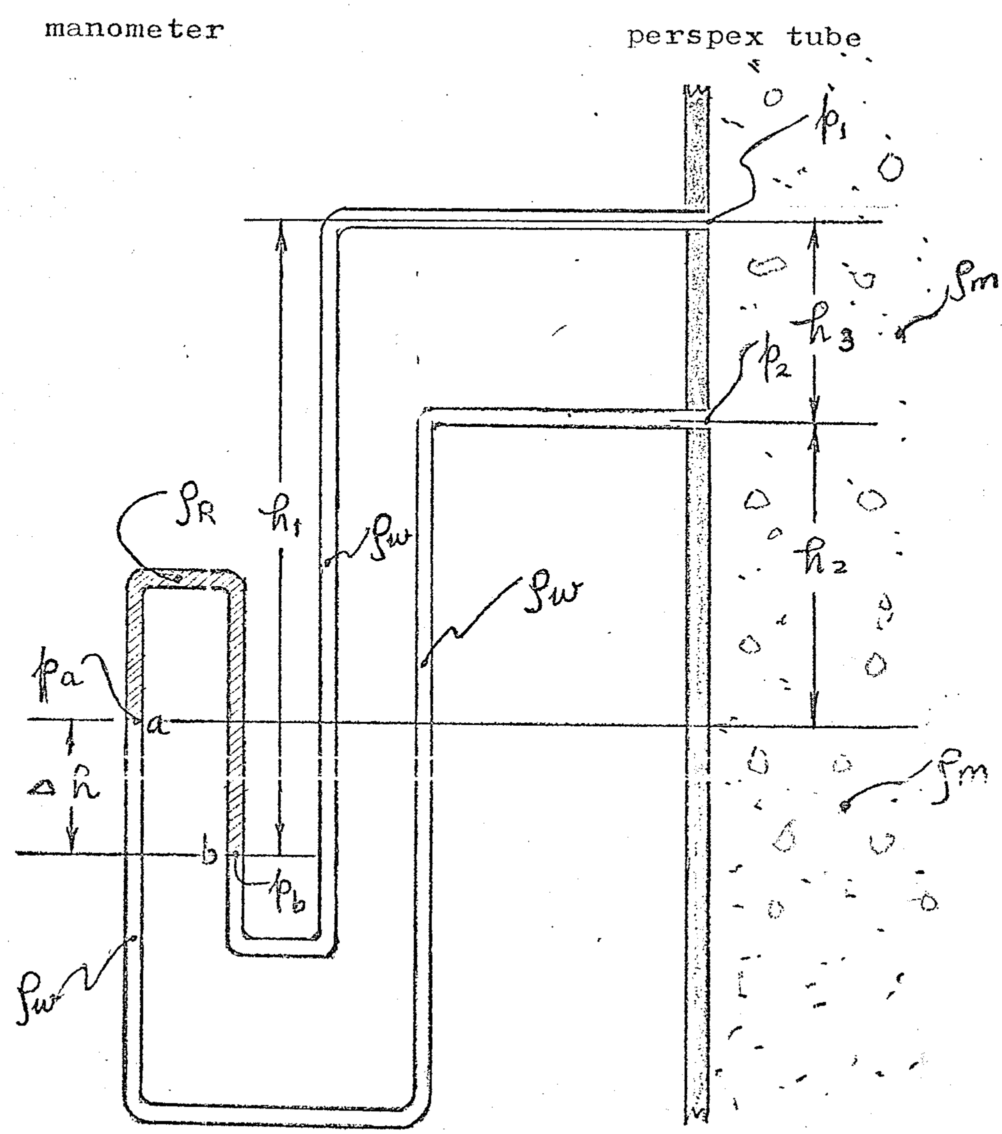

Fig. B.1 Sketch of inverted U tube manometer

Therefore

$$P_2 = P_a - h_2\rho_w \tag{B1}$$

Further

$$P_a = P_1 + h_1\rho_w - \Delta h\rho_R$$

which may be rearranged as

$$P_1 = P_a - h_1\rho_w + \Delta h\rho_R \tag{B2}$$

subtracting (B2) from (B1) yields

$$P_2 - P_1 = (h_1 - h_2)\rho_w - \Delta h\rho_R$$

Also

$$P_1 + \rho_m h_3 = P_2$$

or

$$P_2 - P_1 = \rho_m h_3 = (h_1 - h_2)\rho_w - \Delta h\rho_R \tag{B3}$$

From Fig. B.1 it may be seen that

$$h_1 = h_2 + h_3 + \Delta h \quad \text{or} \quad h_1 - h_2 = h_3 + \Delta h \tag{B4}$$

If $\Delta h = 0$, then

$$h_1 - h_2 = h_3 \tag{B5}$$

and from (B3)

$$\rho_m = \rho_w$$

This means there are no bubbles in the perspex tube, i.e. with water only in perspex tube. This is the principle used for checking the manometer; that is, the level should be even in manometer when there are no bubbles in perspex tube.

Using (B4), then (B3) can be written as

$$\rho_m h_3 = (h_3 + \Delta h)\rho_w - h\rho_R$$

or

$$\rho_m = (1 + \frac{\Delta h}{h_3})\rho_w - \frac{\Delta h}{h_3}\rho_R \qquad \text{(B6)}$$

From the void fraction relationship

$$B = \frac{V_{air}}{V_m} = \frac{V_{air}}{V_{air} + V_w}$$

and

$$\rho_m = \frac{W_m}{V_m} = \frac{W_{air} + W_w}{V_m}$$

$$= \frac{V_{air}}{V_m}\frac{W_{air}}{V_{air}} + \frac{V_w}{V_m}\frac{W_w}{V_w}$$

one can obtain

$$\rho_m = B\rho_{air} + (1 - B)\rho_w$$

$$= \rho_w - B(\rho_w - \rho_{air})$$

Since ρ_{air} is very small compared with ρ_w, it can be neglected in the above formula, which then can be written as

$$\rho_m = \rho_w(1 - B) \qquad \text{(B7)}$$

From (B6) and (B7)

$$\rho_w(1 - B) = (1 + \frac{\Delta h}{h_3})\rho_w - \frac{\Delta h}{h_3}\rho_R$$

$$-B = -\frac{\Delta h}{h_3}(\frac{\rho_R}{\rho_w} - 1)$$

$$B = \frac{\Delta h}{h_3}(\frac{\rho_R}{\rho_w} - 1)$$

For an inclined manometer

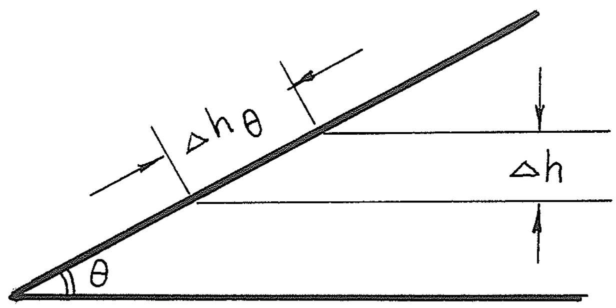

$$\Delta h = \Delta h_\theta \sin\theta$$

then $$B = \frac{\Delta h_\theta \sin\theta}{h_3}\left(\frac{\rho_R}{\rho_W} - 1\right)$$

In this investigation θ was 30° and sin θ = 0.5.

The Δh_θ was measured on a scale with 10 major divisions per foot; then 1 division = 1.2 inches.

When $h_3 = 10$ inches and $\frac{\rho_R}{\rho_W} = 0.827$,

$$B = \frac{1.2\Delta h_\theta\ 0.5}{10.0}(0.827 - 1)$$

($B = -0.12*0.173*\Delta h_\theta*0.5$ was used in computer program.)

When $h_3 = 5$ inches,

then $$B = \frac{1.2\Delta h_\theta\ 0.5}{5}(0.827 - 1)$$

($B = -0.24*0.173*\Delta h_\theta*0.5$ was used in the computer program.)

B.3 <u>Error estimate</u>

1. Estimating the error in measured manometer angle as 0.5 degree, this gives a percentage error of $\frac{0.508 - 0.500}{0.500} = 1.6\%$.

2. Estimating the error in reading the scale on the manometer for Δh_θ as half of the smallest scale division ($= 0.5 \times \frac{1}{10} \times 1.2$ inch $= 0.06$ inch), then the percentage error in Δh_θ is a function of Δh_θ itself and can be estimated as:

Δh_θ -	1 in.	5 in.	10 in.	15 in.	20 in.	28 in.
error	6%	1.2%	0.6%	0.6%	0.3%	0.24%

3. Estimating the error in measuring h_3 as 2/100 in., then the percentage error in measured h_3 for measuring B can be estimated as 0.05% based on $h_3 = 5$ in. and 0.02% based on $h_3 = 10$ in.; these are very small and can be neglected.

4. The error in the density ratio ρ_R/ρ_w is negligibly small. Therefore the estimat error (or "uncertainty interval" in Kline and McClintock at "odds" of approximately 20 to 1) can be obtained using equation 7 of Kline and McClintock (Mechanical Engineering vol. 37, 1953) as shown below:

Δh_θ	1 in.	5 in.	10 in.	15 in.	20 in.	25 in.
B(h_3 = 10")	0.009	0.043	0.09	0.13	0.17	0.22
B(h_3 = 5")	0.018	0.086	0.18	0.26	0.34	0.44
Error (%) in B	6.2	2.0	1.7	1.6	1.6	1.6

5. Conclusion

When B based on $h_3 = 10$ inches is greater than 0.043* or when B based on $h_3 = 5$ inches is greater than 0.086, then the estimated error is within 2.0%. For other conditions, see above but note that for the low void fractions where the errors would be >2%, these errors can be tolerated as the acoustic velocity is insensitive to the void fraction.

* (by far the most common situation)

The foregoing estimate of errors was based on static conditions (i.e. no movement of the interface in the manometer). However, at high void fractions in transition and slug flow, considerable fluctuations in the void fraction may occur, these fluctuations often being much greater than the error discussed above. In the majority of cases, though, in bubbly flow, one would not need to allow more than about 1% to account for errors due to the movement of the manometer level. One can therefore estimate about a 3% error in bubbly flow for void fractions greater than 0.043.

B.4 Calculation of void fraction B using column height measurements

The void fraction may be calculated using column heights as follows:

$$B = \frac{V_{air}}{V_m} = \frac{V_{air}}{V_{air} + V_{liquid}}$$

$$= \frac{\Delta H}{\Delta H + H_{liquid}}$$

where H_{liquid} is the height of the liquid column with no air bubbles present and ΔH is the increase in height of the column when air is present in the column.

Because under many conditions there is a foam at the top of the column, erroneous readings of the height of the air-liquid mixture ensue, which leads to erroneous readings of the void fraction. The magnitude of this foam effect is difficult to assess, but can be large, and is most certainly much larger than errors in void fraction measurement using a manometer. For this reason void fractions obtained using a manometer are of prime interest and were used in the body of this thesis for graphs of acoustic velocity versus void fraction.

APPENDIX C

SAMPLE OF COMPUTER PROGRAM AND TABULATED DATA

This appendix gives a sample of the computer program and the tabulated data for superficial velocity, void fraction and acoustic velocity.

The tables for the various test runs are arranged as follows:

Test Run No.	Table
160	C.1
401	C.2
601	C.3
1101	C.4
1220	C.5
1301	C.6
1401	C.7
1601	C.8
160	C.9
601	C.10
1101	C.11
1401	C.12

The inclusion of table C.9,10,11 and 12 is to illustrate quantitatively the extremely small differences which arise when using "time-mean" or "velocity-mean" acoustic velocity means (see body of thesis 4.2).

In the tables the various symbols have meanings described below.

AL = acoustic velocity of the bubble-free liquid (m/s)

AM = mean acoustic velocity of gas-liquid mixture based on mean of time measurements (m/s)

AMN = mean acoustic velocity of gas-liquid mixture based on mean of velocities (each individual time measurement gives a corresponding individual velocity)(m/s)

B0,B1,B2 = void fractions given the symbols B_0,B_1 and B_2 and described in the body of the thesis

N = number of readings of transit time for one nominal void fraction setting

RD = difference of acoustic velocity ratio between the two different methods of calculating the mean acoustic velocity

SDT = corresponding standard deviation of acoustic velocity based on standard deviation of measured times

SDTV = standard deviation of acoustic velocity based on standard deviation of velocity (see description of AMN above)(m/s)

V = superficial velocity (ft/s)

```
$JOB
C
C
C
C
C                    Sample of Computer Program
C
C                       of Test Run No. 160
C
C                 (Out-put print shown on Table C.1)
C
C      X       =DISTANCE BT. TWO CRYSTALS(M)
C      H3      =HEIGH DISTANCE BT. TWO TAPS ON THE TUBE(IN)
C      WLO     =LIQUID LEVEL IN TUBE WHEN THERE ARE NO BUBBLES FLOW(IN)
C      TL      =TIME OF SOUND THROUGH THE LIQUID BT. TWO CRYSTALS(SEC)
C      AL      =VEL. OF SOUND IN LIQUID WHEN THERE ARE NO BUBBLES FLOW(M/S)
C      M       = TESTING NO
C      WL1     =LIQUID LEVEL WHEN THERE ARE BUBBLES FLOW ( IN )
C      DL1     =READING ON MANOMETER FOR TAP NO. 1 ON TUBE(FT/10)
C      DL2     =READING ON MANOMETER FOR TAP NO. 2 ON TUBE(FT/10)
C      HGL1    =READING ON HG. PRESSURE GAGE (LH)FOR GAS FLOW VOLUME METER(IN)
C      HGL2    =READING ON HG. PRESSURE GAGE (RH)FOR GAS FLOW VOLUME METER(IN)
C      ROVO    =GAS FLOW RATE ( CU FT/MIN ) BY ROTAMETER
C      N       = NO. OF READING IN TIME DATA
C      BATATS  =VOID FRACTION COUNTED WITH COLUNM HEIGHT ( IN. )------B0
C      BATA1   =VOID FRACTION COUNTED WITH MANOMETER /N POSITION 1 ---B1
C      BATA2   =VOID FRACTION COUNTED WITH MANOMETER /N POSITION 2 ---B2
C      VOLPS   =SUPERFICIAL GAS VEL(FT/S)     -------------------------V
C      VOLFM   =GAS FLOW RATE MEASURED BY WET FLOW METER (CU FT / MIN )
C      AM      = ACOUSTIC VELOCITY MEAN OF GAS LIQUID MIXTURE BASED ON TIME MEAN
C                (M/S)
C      AMN     = ACOUSTIC VELOCITY MEAN OF GAS LIQUID MIXTURE BASED ON VEL. MEAN
C               (M/S)
C      SDT     =STANDARD DEVIATION BASE ON TIME BASE OF ACOUSTIC VELOCITY OF MIX.
C               (S)
C      SDTV    =STANDARD DEVIATION BASE ON VLOCITY OF ACOUSTIC VELOCITY OF MIX.
C               (M/S)
C      RD=DIFFERENCE OF ACOUSTIC VELOCITY RATIO BT. DIFFERENT BASE
C
C
       DIMENSION T(90),A(90),D(90)
       X=3.241*2.54/100.
       H3=10.
       TL=.000063
       WLO=21.75
       AL=X/TL
       WRITE(6,88)
    88 FORMAT('1')
       WRITE(6,2200)
  2200 FORMAT(/////)
       WRITE(6,1000)
  1000 FORMAT(/////7X'TEST NO'4X'V   '4X'B1'4X'B2'5X'AM'5X'AM/AL'4X'SDTV'8
      1X'SDT     N')
     1 READ(5,100)M,WL1,DL1,DL2,DL3,DL4,HGL1,HGL2,VOLFM,DFOM,N,CC
   100 FORMAT(I5,7F5.2,2F10.2,I5,F7.4)
       IF(M.EQ.0) GO TO 30
       WL1=WL1+30.-WLO
       BATATS=ABS(WL1)/(WL1+WLO)
       BATA1=.12*.173*ABS(DL1-DL2)*.5
       BATA2=.12*.173*ABS(DL3-DL4)*.5
```

```
      HG=ABS(HGL1-HGL2)
      V=(1.+HG/29.921)*VOLFM
      VOLPS=V*144./(60.*1.00*.7854*3.75**2)
    2 READ(5,200)(D(I),I=1,N)
  200 FORMAT(10F7.2)
      ST=0.0
      DO 11 I=1,N
      T(I)=D(I)*0.00001
   11 ST=ST+T(I)
      SN=N
   12 TM=ST/SN
   13 AM=X/TM
      SDTM=0.0
      DO 14 I=1,N
   14 SDTM=SDTM+(T(I)-TM)**2
      SDT=SQRT(SDTM/SN)
      AMU=X/(TM-SDT)
      AML=X/(TM+SDT)
      DO 15 I=1,N
   15 A(I)=X/T(I)
      SAMN=0.0
      DO 16 I=1,N
   16 SAMN=SAMN+A(I)
      AMN=SAMN/SN
      DO 17 I=1,N
      SDTVM=0.0
   17 SDTVM=SDTVM+(A(I)-AMN)**2
      SDTV=SQRT(SDTVM/SN)
      AMNU=AMN+SDTV
      AMNL=AMN-SDTV
      AMALR=AM/AL
      ARU=AMU/AL
      ARL=AML/AL
      ARNU=AMNU/AL
      ARNL=AMNL/AL
   20 WRITE(6,500)M,VOLPS,BATA1,BATA2,AMN,AMALR,SDTV,SDT,N
  500 FORMAT(  5X,I8,3F7.3,2X,F7.1,F7.4,2E12.4,I3)
   22 GO TO  1
   30 CALL EXIT
      END

$ENTRY
```

Table C.1

Data of Test Run No. 160 and Figs.5.3,4,5,6 and 7.

TEST NO	V	B1	B2	AM	AM/AL	SDTV	SDT	N
160	0.001	0.003	0.002	1306.7	1.0000	0.1544E-03	0.1601E-09	10
161	0.001	0.006	0.006	1306.7	1.0000	0.1544E-03	0.1601E-09	10
162	0.004	0.008	0.007	1306.7	1.0000	0.1544E-03	0.1601E-09	10
163	0.007	0.011	0.012	1306.7	1.0000	0.1544E-03	0.1601E-09	10
164	0.012	0.015	0.019	1306.7	1.0000	0.1544E-03	0.1601E-09	10
165	0.013	0.018	0.019	1306.7	1.0000	0.1544E-03	0.1601E-09	10
166	0.015	0.021	0.021	1306.7	1.0000	0.1544E-03	0.1601E-09	10
167	0.016	0.023	0.023	1306.7	1.0000	0.1544E-03	0.1601E-09	10
168	0.042	0.027	0.027	1306.7	1.0000	0.1544E-03	0.1601E-09	10
169	0.055	0.031	0.031	1306.7	1.0000	0.1544E-03	0.1601E-09	10
170	0.027	0.039	0.036	1288.3	0.9859	0.6381E 00	0.1000E-06	10
171	0.029	0.042	0.039	1290.7	0.9878	0.1154E 01	0.1400E-06	10
172	0.031	0.044	0.042	1289.1	0.9865	0.3822E 00	0.1231E-06	10
173	0.031	0.047	0.046	1288.3	0.9859	0.6365E 00	0.1612E-06	10
174	0.036	0.052	0.048	1288.3	0.9859	0.6365E 00	0.1612E-06	10
175	0.040	0.060	0.054	1278.5	0.9783	0.2682E 01	0.7918E-06	20
176	0.047	0.071	0.071	1275.5	0.9760	0.2025E 01	0.8646E-06	20
177	0.055	0.085	0.079	1265.6	0.9685	0.1951E 00	0.5895E-06	20
178	0.060	0.100	0.093	1267.6	0.9700	0.2541E 00	0.7399E-06	20
179	0.068	0.108	0.100	1258.0	0.9626	0.1699E 01	0.8646E-06	20
180	0.086	0.122	0.116	1239.4	0.9483	0.1963E 01	0.9894E-06	30
181	0.083	0.135	0.129	1231.5	0.9422	0.5070E 00	0.1087E-05	30
182	0.089	0.145	0.141	1214.0	0.9287	0.2679E 01	0.1267E-05	30
183	0.100	0.166	0.037	1204.5	0.9215	0.1110E 01	0.1278E-05	30
184	0.112	0.187	0.183	1186.9	0.9078	0.4332E 01	0.1685E-05	30
185	0.123	0.208	0.203	1154.0	0.8824	0.8613E 00	0.2200E-05	40
186	0.137	0.228	0.224	1137.9	0.8696	0.8725E 01	0.2819E-05	40
187	0.148	0.249	0.245	1109.8	0.8485	0.1047E 02	0.2353E-05	40
188	0.162	0.264	0.259	1092.5	0.8344	0.1475E 01	0.3428E-05	40
189	0.174	0.276	0.270	1079.3	0.8238	0.3778E 01	0.3879E-05	40
190	0.183	0.282	0.274	1089.0	0.8314	0.9156E 00	0.3684E-05	40
191	0.192	0.284	0.274	1050.1	0.7997	0.8313E 00	0.5579E-05	40
192	0.200	0.286	0.278	1065.6	0.8132	0.1229E 02	0.4225E-05	40
193	0.210	0.291	0.230	1055.9	0.8059	0.6265E 01	0.4195E-05	40
194	0.219	0.295	0.284	1088.6	0.8300	0.1120E 02	0.4732E-05	40
195	0.232	0.305	0.302	1025.6	0.7812	0.4710E 01	0.5677E-05	40
196	0.261	0.307	0.299	1023.7	0.7809	0.1396E 02	0.4596E-05	40
197	0.299	0.313	0.301	1138.9	0.7577	0.6531E 01	0.1385E-04	40
198	0.323	0.322	0.307	1038.4	0.7920	0.1412E 02	0.4717E-05	40
199	0.359	0.307	0.301	1050.0	0.8000	0.9881E 01	0.5356E-05	40
200	0.386	0.301	0.291	1056.4	0.8028	0.4326E 01	0.6738E-05	40
201	0.395	0.307	0.297	1042.2	0.7952	0.6479E 01	0.4339E-05	40
202	0.471	0.295	0.286	1049.4	0.7997	0.1802E 02	0.5126E-05	40
203	0.515	0.282	0.278	1052.2	0.8018	0.1845E 02	0.5152E-05	40
204	0.565	0.280	0.276	1075.0	0.8154	0.1248E 02	0.7650E-05	30
205	0.606	0.276	0.274	1092.8	0.8319	0.6819E 01	0.5744E-05	30
206	0.661	0.274	0.270	1083.0	0.8227	0.2017E 02	0.6953E-05	40

Table C.1(Cont. on next page)

207	0.722	0.268	0.259	1112.8	0.8516	0.7286E 00	0.4876E-05	40
208	0.804	0.262	0.259	1104.5	0.8453	0.1508E 02	0.6103E-05	30
209	0.876	0.259	0.264	1042.0	0.7975	0.2214E 02	0.9037E-05	30
210	0.958	0.257	0.264	989.0	0.7569	0.3336E 02	0.1132E-04	30
211	1.030	0.259	0.259	1018.0	0.7791	0.2558E 02	0.1128E-04	30
212	1.113	0.270	0.274	1018.0	0.7791	0.2558E 02	0.1128E-04	30

Table C.1 (Cont.)

Table C.2

Data of Test Run No. 401 and Fig. 5.8.

TEST NO	V	B1	B2	B0
401	0.004	0.002	0.002	0.002
402	0.007	0.010	0.010	0.011
403	0.013	0.017	0.017	0.025
404	0.019	0.031	0.027	0.029
405	0.025	0.035	0.035	0.042
406	0.031	0.046	0.042	0.054
407	0.037	0.056	0.050	0.067
408	0.044	0.066	0.058	0.074
409	0.052	0.081	0.073	0.086
410	0.062	0.087	0.085	0.098
411	0.071	0.108	0.102	0.119
412	0.079	0.118	0.112	0.130
413	0.085	0.125	0.120	0.140
414	0.100	0.145	0.141	0.163
415	0.114	0.162	0.156	0.179
416	0.131	0.174	0.170	0.200
418	0.149	0.187	0.183	0.209
419	1.478	0.197	0.191	0.223
420	0.182	0.199	0.193	0.234
421	0.200	0.206	0.199	0.245
422	0.219	0.203	0.195	0.245
423	0.141	0.170	0.168	0.179
424	0.228	0.208	0.203	0.237
425	0.269	0.208	0.203	0.245
426	0.286	0.216	0.203	0.250
427	0.352	0.216	0.208	0.263
428	0.394	0.220	0.210	0.270
429	0.434	0.228	0.218	0.275
430	0.480	0.228	0.218	0.280
431	0.504	0.237	0.218	0.287
432	0.526	0.237	0.220	0.287
433	0.611	0.239	0.222	0.287
434	0.687	0.243	0.226	0.298
435	0.736	0.247	0.228	0.298
436	0.817	0.251	0.237	0.310
437	0.897	0.255	0.245	0.310
438	0.984	0.255	0.245	0.310
439	1.063	0.259	0.253	0.314
440	1.154	0.262	0.262	0.316
441	0.941	0.270	0.270	0.320
442	1.287	0.270	0.270	0.322
443	1.243	0.270	0.274	0.320
444	1.154	0.270	0.262	0.316
445	1.063	0.058	0.262	0.314
446	0.984	0.262	0.249	0.303

Table C.2 (Cont. on next page)

447	0.897	0.262	0.245	0.298
448	0.817	0.262	0.237	0.298
449	0.732	0.262	0.237	0.299
450	0.648	0.257	0.239	0.287
451	0.526	0.266	0.249	0.331
451	0.480	0.266	0.257	0.341
453	0.394	0.282	0.272	0.341
454	0.286	0.289	0.278	0.310
455	0.264	0.274	0.266	0.280
456	0.228	0.257	0.249	0.263
457	0.184	0.199	0.199	0.203
458	0.141	0.156	0.156	0.147
461	0.219	0.237	0.210	0.250
462	0.198	0.220	0.209	0.237
463	0.181	0.224	0.214	0.237
464	0.164	0.224	0.218	0.223
465	0.146	0.220	0.216	0.220
466	0.129	0.201	0.201	0.206
467	0.114	0.187	0.181	0.188
468	0.099	0.168	0.162	0.163
467	0.083	0.143	0.139	0.130
470	0.070	0.120	0.116	0.112
471	0.057	0.100	0.091	0.086
472	0.030	0.042	0.037	0.046

Table C.2 (Cont.)

Table C.3

Data of Test Run No. 601 and Figs.5.9,10 and 11.

TEST NO	V	B1	B2	AM	AM/AL	SDTV	SDT	N
601	0.007	0.006	0.006	1419.3	1.0000	0.4632E-03	0.1455E-10	10
602	0.019	0.025	0.029	1407.2	0.9915	0.7720E-03	0.8731E-10	10
603	0.031	0.054	0.042	1407.2	0.9915	0.7720E-03	0.8731E-10	10
604	0.044	0.071	0.058	1403.4	0.9887	0.1195E 01	0.3878E-06	10
605	0.058	0.081	0.075	1387.1	0.9773	0.2521E 01	0.8078E-06	10
606	0.071	0.104	0.095	1351.4	0.9521	0.3651E 01	0.1342E-05	30
607	0.085	0.120	0.116	1344.0	0.9469	0.3056E 01	0.1160E-05	30
608	0.100	0.137	0.131	1339.1	0.9435	0.5061E 01	0.1612E-05	40
609	0.116	0.154	0.149	1320.0	0.9300	0.1323E 01	0.1278E-05	30
610	0.131	0.168	0.160	1306.7	0.9206	0.3664E 01	0.1770E-05	30
611	0.148	0.181	0.174	1291.0	0.9096	0.1050E 02	0.1820E-05	30
612	0.165	0.189	0.181	1289.0	0.9081	0.7830E 00	0.2291E-05	30
613	0.182	0.197	0.187	1269.7	0.8946	0.2754E 01	0.2207E-05	30
614	0.200	0.199	0.193	1277.6	0.9002	0.5054E 01	0.2140E-05	30
615	0.218	0.201	0.195	1267.1	0.8928	0.3427E 00	0.2057E-05	30
616	0.199	0.206	0.195					
617	0.181	0.201	0.195					
618	0.164	0.203	0.191					
619	0.147	0.187	0.185					
620	0.130	0.181	0.174					
621	0.114	0.162	0.162					
622	0.099	0.152	0.149					
623	0.083	0.133	0.129					
624	0.070	0.108	0.108					
625	0.057	0.087	0.079					
626	0.043	0.073	0.062					
627	0.033	0.050	0.046					
628	0.019	0.033	0.029					
629	0.007	0.008	0.008					
630	0.193	0.149	0.145	1316.4	0.9275	0.1963E 01	0.1310E-05	30
631	0.180	0.197	0.187	1287.6	0.9072	0.4720E 00	0.1999E-05	30
632	0.271	0.220	0.208	1264.5	0.8909	0.3571E 01	0.2725E-05	30
633	0.360	0.237	0.222	1226.8	0.8644	0.3598E 01	0.3618E-05	30
634	0.453	0.241	0.228	1223.8	0.8622	0.3166E 01	0.3958E-05	30
635	0.542	0.255	0.233	1222.0	0.8610	0.2857E 01	0.3987E-05	30
636	0.660	0.259	0.245	1146.5	0.8078	0.1737E 02	0.4269E-05	30
637	0.772	0.259	0.245	1068.6	0.7529	0.8982E 01	0.7355E-05	30
638	0.892	0.262	0.245	1033.3	0.7280	0.2429E 02	0.7739E-05	30
639	1.018	0.264	0.249	1007.2	0.7096	0.1866E 02	0.7793E-05	30
640	1.134	0.259	0.255	935.5	0.6591	0.6282E 01	0.1013E-04	30
641	1.297	0.270	0.266	840.0	0.5918	0.3922E 01	0.7024E-05	30
642	1.440	0.278	0.270	779.1	0.5489	0.1907E 02	0.1174E-04	30
645	1.194	0.270	0.270					
646	1.028	0.266	0.259					
647	0.904	0.266	0.255					
648	0.798	0.253	0.251					
649	0.690	0.266	0.249					
650	0.537	0.266	0.251					
651	0.491	0.266	0.253					

Table C.3(Cont. on next page)

652	0.402	0.274	0.259
653	0.319	0.272	0.259
654	0.237	0.266	0.257
655	0.160	0.266	0.257
656	0.091	0.156	0.156

Table C.3(Cont.)

Table C.4

Data of Test Run No. 1101 and Figs. 5.12,16 and 17.

TEST NO	V	B1	B2	AM	AM/AL	SDTV	SDT	N
1101	0.007	0.010	0.010	1395.3	0.9831	0.0000E 00	0.0000E 00	10
1102	0.019	0.025	0.017	1383.6	0.9748	0.3860E-03	0.7276E-10	10
1104	0.031	0.066	0.062	1356.2	0.9555	0.2151E 01	0.6000E-06	10
1105	0.058	0.087	0.083	1318.6	0.9290	0.2339E 01	0.1687E-05	30
1106	0.071	0.112	0.104	1332.8	0.9390	0.2903E 01	0.1585E-05	30
1107	0.084	0.125	0.125	1315.0	0.9265	0.1026E 02	0.1519E-05	30
1108	0.099	0.135	0.133	1306.0	0.9202	0.3819E 01	0.1622E-05	30
1109	0.115	0.172	0.162	1298.4	0.9148	0.6050E 01	0.1908E-05	30
1110	0.131	0.191	0.183	1247.3	0.8788	0.2699E 00	0.2309E-05	30
1111	0.147	0.208	0.191	1216.0	0.8567	0.1320E 01	0.2673E-05	30
1112	0.163	0.214	0.203	1196.5	0.8430	0.4296E 01	0.3478E-05	30
1113	0.181	0.224	0.208	1201.8	0.8467	0.1748E 02	0.4985E-05	30
1114	0.198	0.228	0.212	1171.0	0.8250	0.1678E 02	0.4236E-05	30
1115	0.216	0.233	0.216	1182.8	0.8333	0.1344E 02	0.3693E-05	30
1116	0.197	0.264	0.241					
1117	0.180	0.264	0.241					
1118	0.164	0.262	0.241					
1119	0.148	0.253	0.237					
1220	0.133	0.237	0.233					
1122	0.118	0.216	0.224					
1123	0.089	0.166	0.166					
1124	0.076	0.145	0.145					
1126	0.063	0.118	0.112					
1126	0.052	0.095	0.100					
1127	0.039	0.073	0.071					
1128	0.028	0.056	0.050					
1129	0.017	0.027	0.033					
1151	0.103	0.206	0.195	1187.9	0.8369	0.1013E 02	0.3985E-05	30
1152	0.179	0.239	0.224	1182.8	0.8333	0.4433E 01	0.3826E-05	30
1153	0.270	0.249	0.220	1116.0	0.7863	0.1704E 02	0.5596E-05	30
1154	0.349	0.255	0.233	1042.9	0.7348	0.2496E 02	0.7023E-05	30
1155	0.450	0.264	0.237	971.9	0.6848	0.9603E 01	0.5622E-05	30
1156	0.556	0.266	0.241	998.2	0.7033	0.3341E 02	0.1339E-04	30
1157	0.664	0.259	0.241	1128.2	0.7949	0.4159E 02	0.8448E-05	30
1158	0.776	0.256	1.690	1103.5	0.7775	0.1063E 02	0.9065E-05	30
1159	0.894	0.259	0.228	1085.1	0.7645	0.1408E 02	0.8842E-05	30
1160	1.027	0.264	0.241	1006.0	0.7088	0.2358E 02	0.9173E-05	30
1161	1.122	0.259	0.241	991.8	0.6988	0.1724E 02	0.1038E-04	30
1162	1.295	0.259	0.257	997.8	0.7030	0.3022E 01	0.9287E-05	30
1170	1.019	0.262	0.241					
1171	0.916	0.262	0.233					
1172	0.808	0.259	0.228					
1173	0.707	0.270	0.233					
1174	0.611	0.259	0.241					
1175	0.486	0.276	0.249					
1176	0.436	0.286	0.249					
1177	0.351	0.303	0.270					
1178	0.254	0.332	0.307					
1179	0.201	0.266	0.257					

Table C.4(Cont. on next page)

1180	0.123	0.162	0.154
1181	0.201	0.276	0.270
1182	0.254	0.332	0.299
1183	0.353	0.306	0.278
1184	0.432	0.295	0.262
118	0.481	0.272	0.673
1186	0.608	0.274	0.249
1187	0.690	0.266	0.241
1188	0.812	0.259	0.228
1189	0.916	0.266	0.233
1190	1.031	0.259	0.241
1191	1.152	0.270	0.257
1192	1.287	0.266	0.249
1193	1.152	0.259	0.241
1194	1.035	0.000	0.241
1195	0.912	0.274	0.274
1196	0.804	0.257	0.241
1197	0.700	0.259	0.228
1198	0.604	0.274	0.249
1199	0.483	0.280	0.249
1200	0.434	0.295	0.262
1201	0.353	0.311	0.278
1202	0.255	0.328	0.307
1203	0.202	0.257	0.249
1204	0.124	0.135	0.137

Table C.4(Cont.)

Table C.5

Data of Test Run No. 1220 and Fig.5.13.

TEST NO	V	B1	B2	B0
1220	0.007	0.015	0.015	0.002
1221	0.019	0.035	0.033	0.029
1222	0.031	0.056	0.054	0.050
1223	0.043	0.077	0.071	0.067
1224	0.058	0.098	0.091	0.090
1225	0.070	0.108	0.108	0.105
1226	0.084	0.120	0.125	0.120
1227	0.099	0.141	0.141	0.141
1228	0.115	0.156	0.154	0.161
1229	0.130	0.162	0.158	0.167
1230	0.147	0.166	0.158	0.174
1231	0.163	0.166	0.162	0.180
1232	0.180	0.166	0.162	0.174
1233	0.198	0.166	0.162	0.167
1234	0.216	0.168	0.162	0.167
1235	0.197	0.166	0.158	0.167
1236	0.180	0.164	0.154	0.161
1237	0.163	0.168	0.166	0.158
1238	0.147	0.170	0.170	0.151
1239	0.130	0.176	0.174	0.183
1240	0.114	0.183	0.183	0.192
1241	0.099	0.170	0.174	0.198
1242	0.083	0.149	0.158	0.141
1243	0.070	0.129	0.133	0.123
1244	0.057	0.108	0.116	0.098
1245	0.043	0.087	0.091	0.075
1246	0.030	0.058	0.066	0.050
1247	0.019	0.042	0.033	0.033
1248	0.007	0.015	0.017	0.011
1261	0.140	0.156	0.158	0.161
1262	0.229	0.176	0.174	0.210
1263	0.286	0.176	0.174	0.198
1264	0.396	0.174	0.158	0.198
1265	0.487	0.166	0.149	0.198
1266	0.540	0.168	0.170	0.198
1267	0.678	0.176	0.170	0.213
1268	0.782	0.179	0.183	0.213
1269	0.893	0.197	0.187	0.240
1270	0.060	0.199	0.000	0.240
1271	1.140	0.212	0.216	0.253
1272	1.264	0.220	0.199	0.278
1274	1.424	0.233	0.228	0.278
1274	1.253	0.218	0.224	0.278
1275	1.128	0.208	0.216	0.290
1236	1.570	0.241	0.237	0.302

Table C.5(Cont. on next page)

1287	1.406	0.228	0.228	0.290
1276	0.999	0.199	0.191	0.253
1277	0.885	0.187	0.191	0.240
1278	0.770	0.179	0.183	0.198
1279	0.670	0.174	0.174	0.213
1280	0.534	0.158	0.158	0.183
1281	0.482	0.149	0.145	0.167
1282	0.390	0.141	0.133	0.151
1283	0.282	0.137	0.129	0.134
1284	0.224	0.145	0.137	0.134
1235	0.137	0.141	0.141	0.134
1170	1.145	0.262	0.241	0.313
1171	1.018	0.262	0.233	0.302

Table C.5(Cont.)

Table C.6

Data of Test Run No. 1301 and Fig. 5.14.

TEST NO	V	B1	B2	B0
1301	0.007		0.007	
1302	0.018		0.014	
1303	0.030		0.028	
1304	0.043		0.048	
1305	0.057		0.062	
1306	0.070		0.083	
1307	0.083		0.118	
1308	0.099		0.138	
1309	0.114		0.166	
1310	0.130		0.187	
1311	0.147		0.208	
1312	0.165		0.221	
1313	0.182		0.228	
1314	0.200		0.235	
1315	0.220		0.242	
1316	0.259		0.249	
1317	0.278		0.256	
1318	0.337		0.291	
1319	0.381		0.311	
1321	0.429		0.298	
1322	0.477		0.304	
1323	0.531		0.311	
1324	0.590		0.304	
1325	0.648		0.304	
1326	0.705		0.010	
1327	0.770		0.311	
1328	0.874		0.311	
1329	1.035		0.311	
1330	0.893		0.311	
1331	0.777		0.311	
1332	0.713		0.311	
1333	0.633		0.311	
1334	0.576		0.311	
1335	0.523		0.311	
1336	0.468		0.311	
1337	0.416		0.311	
1338	0.371		0.291	
1339	0.326		0.291	
1340	0.283		0.277	
1341	0.216		0.270	
1342	0.197		0.256	
1343	0.178		0.242	
1344	0.161		0.228	
1345	0.144		0.215	
1346	0.127		0.201	

Table C.6(Cont. on next page)

1347	0.112	0.180
1348	0.096	0.163
1349	0.082	0.149
1350	0.068	0.138
1351	0.056	0.121
1352	0.042	0.097
1353	0.030	0.066
1354	0.018	0.028

Table C.6(Cont.)

Table C.7

Data of Test Run No. 1401 and Figs. 5.15,16 and 18.

TEST NO	V	B1	B2	AM	AM/AL	SDTV	SDT	N
1401	0.007	0.002	0.008	1419.3	1.0000	0.4632E-03	0.1455E-10	10
1402	0.019	0.015	0.017	1431.7	1.0087	0.0000E 00	0.8731E-10	10
1403	0.031	0.033	0.033	1431.7	1.0087	0.0000E 00	0.8731E-10	10
1404	0.045	0.062	0.058	1414.1	0.9963	0.9065E 00	0.8821E-06	30
1405	0.059	0.081	0.075	1402.0	0.9878	0.5536E 01	0.9100E-06	30
1406	0.072	0.104	0.095	1379.7	0.9721	0.1457E 01	0.9068E-06	30
1407	0.086	0.116	0.108	1359.2	0.9576	0.5839E 01	0.1230E-05	30
1408	0.102	0.143	0.129	1344.4	0.9472	0.8658E 00	0.1055E-05	30
1409	0.118	0.166	0.154	1339.3	0.9436	0.9764E 01	0.1147E-05	30
1410	0.134	0.189	0.174	1312.9	0.9250	0.6507E 01	0.1696E-05	30
1411	0.152	0.203	0.195	1303.9	0.9187	0.1732E 02	0.2217E-05	30
1412	0.169	0.214	0.199	1277.0	0.8997	0.2088E 01	0.1765E-05	30
1413	0.188	0.222	0.208	1268.4	0.8937	0.6623E 01	0.2534E-05	30
1414	0.195	0.226	0.208	1289.0	0.9081	0.1481E 02	0.2500E-05	30
1415	0.207	0.224	0.216	1275.6	0.8988	0.2026E 01	0.2539E-05	30
1416	0.216	0.224	0.212	1201.8	0.8467	0.2828E 02	0.5795E-05	30
1417	0.226	0.228	0.216	1280.9	0.9025	0.6468E 01	0.2394E-05	30
1418	0.267	0.228	0.216	1292.3	0.9105	0.8446E 01	0.1969E-05	30
1419	0.300	0.226	0.216	1236.1	0.8709	0.2373E 02	0.4848E-05	30
1420	0.346	0.228	0.220	1208.8	0.8517	0.9363E 01	0.4969E-05	30
1421	0.392	0.233	0.229	1194.2	0.8414	0.5328E 02	0.7155E-05	30
1422	0.440	0.233	0.228	1241.0	0.8744	0.3150E 02	0.4650E-05	30
1423	0.545	0.233	0.220	1191.3	0.8394	0.1882E 02	0.6128E-05	30
1424	0.657	0.233	0.216	1105.5	0.7789	0.3020E 02	0.8895E-05	30
1425	0.784	0.235	0.233	1058.1	0.7455	0.8687E 01	0.1041E-04	30
1426	0.916	0.235	0.224	1062.7	0.7487	0.3126E 02	0.1125E-04	30
1427	1.072	0.239	0.237	991.0	0.6982	0.1756E 02	0.1087E-04	30
1428	0.912	0.237	0.228					
1429	0.780	0.235	0.224					
1430	0.648	0.230	0.224					
1431	0.535	0.235	0.224					
1432	0.433	0.233	0.224					
1433	0.386	0.237	0.228					
1434	0.339	0.235	0.233					
1435	0.293	0.243	0.237					
1436	0.260	0.251	0.241					
1437	0.221	0.253	0.249					
1438	0.209	0.266	0.253					
1439	0.202	0.268	0.257					
1440	0.188	0.274	0.262					
1441	0.184	0.272	0.262					
1442	0.166	0.257	0.249					
1443	0.149	0.241	0.233					
1444	0.131	0.212	0.208					
1445	0.115	0.179	0.174					
1446	0.099	0.158	0.158					
1447	0.084	0.131	0.125					

Table C.7(Cont. on next page)

1448	0.070	0.104	0.104
1449	0.057	0.077	0.075
1450	0.043	0.058	0.054
1451	0.030	0.037	0.033
1452	0.018	0.025	0.025
1455	0.007	0.008	0.008

Table C.7 (Cont.)

Table C.8

Data of Test Run No. 1601 and Fig.5.19.

TEST NO	V	B1	B2	B0
1601	0.006	0.004	0.004	0.003
1602	0.017	0.021	0.021	0.020
1603	0.028	0.042	0.042	0.042
1604	0.039	0.062	0.058	0.063
1605	0.052	0.079	0.075	0.093
1606	0.064	0.112	0.104	0.117
1607	0.076	0.131	0.120	0.139
1608	0.090	0.000	0.145	0.168
1609	0.105	0.176	0.166	0.207
1610	0.119	0.189	0.179	0.242
1611	1.348	0.199	0.191	0.290
1612	0.150	0.203	0.199	0.304
1613	0.167	0.208	0.208	0.331
1614	0.174	0.203	0.199	0.344
1615	0.183	0.201	0.191	0.344
1616	0.191	0.203	0.195	0.344
1617	0.201	0.212	0.199	0.357
1618	0.238	0.212	0.199	0.391
1619	0.266	0.218	0.212	0.391
1620	0.307	0.222	0.216	0.402
1621	0.349	0.222	0.220	0.402
1622	0.393	0.228	0.224	0.422
1623	0.487	0.235	0.237	0.432
1624	0.591	0.243	0.241	0.432
1625	0.712	0.249	0.245	0.432
1626	0.821	0.259	0.264	0.432
1627	0.950	0.270	0.266	0.432
1634	0.814	0.259	0.257	0.432
1635	0.693	0.251	0.245	0.432
1636	0.578	0.249	0.245	0.441
1637	0.402	0.245	0.241	0.450
1638	0.348	0.253	0.249	0.483
1639	0.344	0.255	0.253	0.499
1640	0.277	0.270	0.267	0.526
1641	0.262	0.297	0.291	0.551
1642	0.235	0.316	0.311	0.551
1643	0.199	0.336	0.336	0.551
1644	0.190	0.338	0.336	0.526
1645	0.181	0.332	0.328	0.499
1646	0.172	0.328	0.320	0.467
1647	0.165	0.322	0.311	0.459
1648	0.149	0.289	0.282	0.412
1648	0.133	0.257	0.249	0.369
1650	0.118	0.224	0.224	0.304
1651	0.103	0.189	0.187	0.242

Table C.8(Cont. on next page)

1652	0.089	0.162	0.154	0.188
1653	0.075	0.129	0.129	0.147
1654	0.063	0.108	0.108	0.103
1655	0.051	0.083	0.083	0.078
1656	0.039	0.062	0.058	0.053
1657	0.027	0.042	0.037	0.026
1658	0.017	0.021	0.021	0.014
1659	0.006	0.004	0.004	0.003

Table C.8(Cont. on next page)

Table C.9

Differences in acoustic velocity using different calculating bases (Test run no 160)

TEST NO	V	B1	AM	AMN	AM/AL	AMN/AL	RD	N
160	0.001	0.003	1306.7	1306.7	0.9206	0.9206	-0.0000	10
161	0.001	0.006	1306.7	1306.7	0.9206	0.9206	-0.0000	10
162	0.004	0.008	1306.7	1306.7	0.9206	0.9206	-0.0000	10
163	0.007	0.011	1306.7	1306.7	0.9206	0.9206	-0.0000	10
164	0.012	0.015	1306.7	1306.7	0.9206	0.9206	-0.0000	10
165	0.013	0.018	1306.7	1306.7	0.9206	0.9206	-0.0000	10
166	0.015	0.021	1306.7	1306.7	0.9206	0.9206	-0.0000	10
167	0.016	0.023	1306.7	1306.7	0.9206	0.9206	-0.0000	10
168	0.042	0.027	1306.7	1306.7	0.9206	0.9206	-0.0000	10
169	0.055	0.031	1306.7	1306.7	0.9206	0.9206	-0.0000	10
170	0.027	0.039	1288.3	1288.3	0.9077	0.9077	-0.0000	10
171	0.028	0.042	1290.7	1290.7	0.9094	0.9094	0.0000	10
172	0.031	0.044	1289.1	1289.1	0.9082	0.9082	0.0000	10
173	0.031	0.047	1288.3	1288.3	0.9077	0.9077	0.0000	10
174	0.036	0.052	1283.3	1288.3	0.9077	0.9077	0.0000	10
175	0.040	0.060	1278.3	1278.5	0.9006	0.9008	0.0001	20
176	0.047	0.071	1275.3	1275.5	0.8985	0.8987	0.0002	20
177	0.055	0.085	1265.5	1265.6	0.8916	0.8917	0.0001	20
178	0.060	0.100	1267.5	1267.6	0.8930	0.8931	0.0001	20
179	0.068	0.108	1257.8	1258.0	0.8862	0.8863	0.0002	20
180	0.086	0.122	1239.2	1239.4	0.8731	0.8732	0.0002	30
181	0.083	0.135	1231.1	1231.5	0.8674	0.8676	0.0002	30
182	0.089	0.145	1213.6	1214.0	0.8550	0.8553	0.0003	30
183	0.100	0.166	1204.1	1204.5	0.8484	0.8487	0.0003	30
184	0.112	0.187	1186.2	1186.9	0.8357	0.8362	0.0005	30
185	0.123	0.208	1153.0	1154.0	0.8123	0.8131	0.0007	40
186	0.137	0.228	1136.3	1137.9	0.8006	0.8017	0.0011	40
187	0.148	0.249	1108.7	1109.8	0.7811	0.7819	0.0008	40
188	0.162	0.264	1090.4	1092.5	0.7682	0.7697	0.0015	40
189	0.174	0.276	1076.4	1079.3	0.7584	0.7604	0.0020	40
190	0.183	0.282	1086.4	1089.0	0.7654	0.7672	0.0018	40
* 191	0.192	0.284	1045.0	1050.1	0.7363	0.7399	0.0036 **	40
192	0.200	0.286	1062.6	1065.6	0.7486	0.7508	0.0021	40
193	0.210	0.291	1053.0	1055.9	0.7419	0.7440	0.0020	40
194	0.219	0.295	1084.6	1088.6	0.7642	0.7670	0.0028	40
195	0.232	0.305	1020.7	1025.6	0.7192	0.7226	0.0034	40
196	0.261	0.307	1020.4	1023.7	0.7189	0.7213	0.0023	40
197	0.299	0.313	990.0	1138.9	0.6975	0.8024	0.1049	40
198	0.323	0.322	1034.8	1038.4	0.7291	0.7316	0.0025	40
199	0.358	0.307	1045.4	1050.0	0.7365	0.7398	0.0032	40
200	0.386	0.301	1049.0	1056.4	0.7391	0.7443	0.0052	40
201	0.395	0.307	1039.1	1042.2	0.7321	0.7343	0.0022	40
202	0.471	0.295	1045.0	1049.4	0.7363	0.7394	0.0031	40
203	0.515	0.282	1047.7	1052.2	0.7381	0.7413	0.0032	40
204	0.565	0.280	1065.4	1075.0	0.7506	0.7574	0.0068	30
205	0.606	0.276	1087.0	1092.8	0.7658	0.7699	0.0041	30
206	0.661	0.274	1075.0	1083.0	0.7574	0.7631	0.0056	40

Table C.9(Cont. on next page)

207	0.722	0.268	1112.8	1117.1	0.7841	0.7870	0.0030	40
208	0.804	0.262	1104.5	1111.6	0.7782	0.7832	0.0050	30
209	0.876	0.259	1042.0	1054.7	0.7342	0.7431	0.0089	30
210	0.958	0.257	989.0	1005.9	0.6968	0.7087	0.0119	30
211	1.030	0.259	1018.0	1035.9	0.7172	0.7299	0.0126	30
212	1.113	0.270	1018.0	1035.9	0.7172	0.7299	0.0126	30

*The data above the line belong to the bubbly flow region.

**This is the maximum difference in the bubbly flow region in RD.

Table C.9(Cont.)

Table C.10

Differences in acoustic velocity using different calculating bases (Test run no. 601)

TEST NO	V	B1	AM	AMN	AM/AL	AMN/AL	RD	N
601	0.007	0.006	1419.3	1419.3	1.0000	1.0000	-0.0000	10
602	0.019	0.025	1407.2	1407.2	0.9915	0.9915	-0.0000	10
603	0.031	0.054	1407.2	1407.2	0.9915	0.9915	-0.0000	10
604	0.044	0.071	1403.4	1403.4	0.9887	0.9888	0.0000	10
605	0.058	0.081	1387.1	1387.3	0.9773	0.9774	0.0002	10
606	0.071	0.104	1351.4	1352.0	0.9521	0.9526	0.0005	10
607	0.085	0.120	1344.0	1344.5	0.9469	0.9473	0.0003	30
608	0.100	0.137	1339.1	1340.0	0.9435	0.9441	0.0006	30
609	0.116	0.154	1320.0	1320.5	0.9300	0.9304	0.0004	40
610	0.131	0.168	1306.7	1307.7	0.9206	0.9213	0.0007	30
611	0.148	0.181	1291.0	1292.0	0.9096	0.9103	0.0007	30
612	0.165	0.189	1289.0	1290.6	0.9081	0.9093	0.0011 **	30
613	0.182	0.197	1269.7	1271.2	0.8946	0.8956	0.0010	30
614	0.200	0.199	1277.6	1279.0	0.9002	0.9011	0.0010	30
615	0.219	0.201	1267.1	1268.4	0.8928	0.8936	0.0009	30
630	0.103	0.149	1316.4	1317.0	0.9275	0.9279	0.0004	30
* 631	0.180	0.197	1287.6	1288.9	0.9072	0.9081	0.0009	30
632	0.271	0.220	1264.5	1266.7	0.8909	0.8925	0.0015	30
633	0.360	0.237	1226.8	1230.3	0.8644	0.8668	0.0024	30
634	0.452	0.241	1223.8	1227.9	0.8622	0.8652	0.0029	30
635	0.542	0.255	1222.0	1226.3	0.8610	0.8640	0.0030	30
636	0.660	0.259	1146.5	1150.5	0.8078	0.8106	0.0028	30
637	0.772	0.259	1068.6	1078.2	0.7529	0.7597	0.0067	30
638	0.892	0.262	1033.3	1043.0	0.7280	0.7349	0.0068	30
639	1.018	0.264	1007.2	1016.9	0.7096	0.7164	0.0068	30
640	1.136	0.259	935.5	949.1	0.6591	0.6687	0.0096	30
641	1.297	0.270	840.0	844.7	0.5918	0.5951	0.0033	30
642	1.440	0.278	779.1	790.5	0.5489	0.5569	0.0080	30

*The data above the line belong to the bubbly flow region.

**This is the maximum difference in the bubbly flow region in RD.

Table C.11

Differences in acoustic velocity using different calculating bases (Test run no. 1101)

TEST NO	V	B1	AM	AMN	AM/AL	AMN/AL	RD		N
1101	0.007	0.010	1395.3	1395.3	0.9831	0.9831	0.0000		10
1102	0.019	0.025	1383.6	1383.6	0.9748	0.9748	-0.0000		10
1104	0.031	0.066	1356.2	1356.3	0.9555	0.9556	0.0001		10
1105	0.058	0.087	1318.6	1319.5	0.9290	0.9297	0.0007		30
1106	0.071	0.112	1332.8	1333.6	0.9390	0.9396	0.0006		30
1107	0.084	0.125	1315.0	1315.8	0.9265	0.9271	0.0005		30
1108	0.099	0.135	1306.0	1306.8	0.9202	0.9207	0.0006		30
1109	0.115	0.172	1298.4	1299.6	0.9148	0.9157	0.0008		30
1110	0.131	0.191	1247.3	1248.8	0.8788	0.8798	0.0010		30
1111	0.147	0.208	1216.0	1217.8	0.8567	0.8580	0.0013		30
1112	0.163	0.214	1196.5	1199.6	0.8430	0.8452	0.0021		30
1113	0.181	0.224	1201.8	1208.2	0.8467	0.8513	0.0045	**	30
1114	0.198	0.228	1171.0	1175.1	0.8250	0.8279	0.0029		30
1115	0.216	0.233	1182.8	1186.1	0.8333	0.8357	0.0023		30
1151	0.103	0.206	1187.9	1191.8	0.8369	0.8397	0.0028		30
1152	0.179	0.239	1182.8	1186.3	0.8333	0.8358	0.0025		30
* 1153	0.270	0.249	1116.0	1122.4	0.7863	0.7908	0.0045		30
1154	0.349	0.255	1042.9	1051.4	0.7348	0.7408	0.0060		30
1155	0.450	0.264	971.9	976.4	0.6848	0.6879	0.0032		30
1156	0.556	0.266	998.2	1023.0	0.7033	0.7208	0.0174		30
1157	0.664	0.259	1128.2	1142.5	0.7949	0.8049	0.0100		30
1158	0.776	0.256	1103.5	1117.8	0.7775	0.7875	0.0101		30
1159	0.894	0.259	1085.1	1098.9	0.7645	0.7742	0.0097		30
1160	1.027	0.264	1006.0	1019.5	0.7088	0.7183	0.0095		30
1161	1.122	0.259	991.8	1009.1	0.6988	0.7110	0.0122		30
1162	1.295	0.259	997.8	1012.5	0.7030	0.7133	0.0103		30

*The data above the line belong to the bubbly flow region.

**This is the maximum difference in the bubbly flow region in RD.

Table C.12

Differences in acoustic velocity using different calculating bases (Test run no.1401)

TEST NO	V	B1	AM	AMN	AM/AL	AMN/AL	RD		N
1401	0.007	0.002	1419.3	1419.3	1.0000	1.0000	-0.0000		10
1402	0.019	0.015	1431.7	1431.7	1.0087	1.0087	-0.0000		10
1403	0.031	0.033	1431.7	1431.7	1.0087	1.0087	-0.0000		10
1404	0.045	0.062	1414.1	1414.4	0.9963	0.9965	0.0002		30
1405	0.059	0.081	1402.0	1402.3	0.9878	0.9880	0.0002		30
1406	0.072	0.104	1379.7	1380.0	0.9721	0.9723	0.0002		30
1407	0.086	0.116	1359.2	1359.7	0.9576	0.9580	0.0004		30
1408	0.102	0.143	1344.4	1344.8	0.9472	0.9475	0.0003		30
1409	0.118	0.166	1339.3	1339.7	0.9436	0.9439	0.0003		30
1410	0.134	0.189	1312.9	1313.9	0.9250	0.9257	0.0007		30
1411	0.152	0.203	1303.9	1305.5	0.9187	0.9198	0.0011		30
1412	0.169	0.214	1277.0	1277.9	0.8997	0.9004	0.0007		30
1413	0.188	0.222	1268.4	1270.4	0.8937	0.8951	0.0014	**	30
* 1414	0.195	0.226	1289.0	1290.9	0.9081	0.9095	0.0014		30
1415	0.207	0.224	1275.6	1277.6	0.8988	0.9001	0.0014		30
1416	0.216	0.224	1201.8	1210.3	0.8467	0.8527	0.0060		30
1417	0.226	0.228	1280.9	1282.7	0.9025	0.9037	0.0013		30
1418	0.267	0.228	1292.3	1293.6	0.9105	0.9114	0.0009		30
1419	0.300	0.226	1236.1	1242.4	0.8709	0.8753	0.0045		30
1420	0.346	0.228	1208.8	1215.2	0.8517	0.8562	0.0045		30
1421	0.392	0.233	1194.2	1206.5	0.8414	0.8501	0.0087		30
1422	0.440	0.233	1241.0	1246.8	0.8744	0.8785	0.0041		30
1423	0.545	0.233	1191.3	1200.7	0.8394	0.8460	0.0066		30
1424	0.657	0.233	1105.5	1120.9	0.7789	0.7897	0.0108		30
1425	0.784	0.235	1058.1	1077.7	0.7455	0.7593	0.0138		30
1426	0.916	0.235	1062.7	1085.9	0.7487	0.7651	0.0164		30
1427	1.072	0.239	991.0	1010.9	0.6982	0.7122	0.0140		30

*The data above the line belong to the bubbly flow region.

**This is the maximum difference in the bubbly flow region in RD.

Table C.12

APPENDIX D

COMPUTER PROGRAM AND OUTPUT FOR CONVERSION OF AN ELLIPSOIDAL BUBBLE INTO AN EQUIVALENT SPHERE

This appendix gives the computer program used for converting an ellipsoidal bubble into an equivalent sphere. The data are for Test Run No. 160 in which photographs were taken of the flow conditions between the crystals. Details of the measurements are described in section 4.2 of the body of the thesis. The output is also given in which the meaning of the important symbols is given below.

NO = Datum point number

BATA = void fraction

N = number of bubbles

A = major axis (in.)

B = minor axis (in.)

D = equivalent diameter of equivolume sphere (mm)

```
FORTRAN IV G LEVEL 1, MOD 3                MAIN                DATE = 70006               14/50/18

                 C
                 C      INTERMS A ELLIPSOID INTO AN EQUIVALENT SPHERE WITH A DIA=D
                 C      N        = NO. OF BUBBLES IN SAMPLE
                 C      BATA    =VID FRACTION
                 C      E, OR F=SEMIAXIS OF ELLIPSOID
                 C
                        DIMENSION E(900),F(900),D(900),G(900),H(900)
                      1 READ(5,10)N,BATA,NO
                     10 FORMAT(I5,F7.3,I5)
                        READ(5,20)(E(I),I=1,N),(F(I),I=1,N)
                     20 FORMAT(20F4.2)
                        DO 11 I=1,N
                        G(I)=.333*E(I)
                        H(I)=.333*F(I)
                     11 D(I)=50.8*(.125*G(I)**2*H(I))**.333
                        WRITE(6,21)NO,BATA,N
                     21 FORMAT(///5X'NO='I5//5X'BATA='F7.2,5X'N='I5)
                        WRITE(6,22)(E(I),I=1,N)
                     22 FORMAT(/5X'A='20F6.2)
                        WRITE(6,23)(F(I),I=1,N)
                     23 FORMAT(/5X'B='20F6.2)
                        WRITE(6,24)(D(I),I=1,N)
                     24 FORMAT(/5X'D='20F6.2)
                     44 WRITE(7,55)BATA,NO,N
                     55 FORMAT('BUBBLES DISTRIBUTION BATA='F5.3,'NO='I3,3X,I5,'T        0.0
                      1      0.5           TT      ')
                     42 WRITE(7,43)(D(I),I=1,N)
                     43 FORMAT(20F4.1)
                        GO TO 1
                     33 CALL EXIT
                        END
```

BATA= 0.01 N= 13

A= 0.30 0.30 0.08 0.05 0.03 0.12 0.12 0.12 0.04 0.16 0.15 0.17 0.16

B= 0.18 0.22 0.08 0.05 0.03 0.10 0.10 0.11 0.04 0.12 0.11 0.12 0.12

D= 2.15 2.30 0.68 0.42 0.26 0.96 0.96 0.99 0.34 1.23 1.15 1.28 1.23

NO= 162

BATA= 0.01 N= 21

A= 0.04 0.06 0.05 0.05 0.03 0.15 0.10 0.25 0.04 0.06 0.04 0.09 0.05 0.04 0.28 0.18 0.16 0.11 0.18 0.30

A= 0.18

B= 0.04 0.06 0.05 0.05 0.03 0.13 0.08 0.22 0.04 0.06 0.04 0.09 0.05 0.04 0.12 0.12 0.12 0.10 0.12 0.18

B= 0.12

D= 0.34 0.51 0.42 0.42 0.26 1.21 0.79 2.03 0.34 0.51 0.34 0.76 0.42 0.34 1.79 1.33 1.23 0.90 1.33 2.15

D= 1.33

NO= 163

BATA= 0.01 N= 22

A= 0.58 0.11 0.12 0.30 0.32 0.18 0.30 0.11 0.15 0.10 0.38 0.20 0.28 0.20 0.20 0.30 0.20 0.20 0.32 0.20

A= 0.10 0.10

B= 0.31 0.10 0.15 0.12 0.12 0.20 0.12 0.22 0.10 0.12 0.10 0.22 0.32 0.20 0.15 0.18 0.12 0.12 0.16 0.12

B= 0.10 0.10

D= 3.99 0.90 1.10 1.88 1.96 1.58 1.88 1.18 1.11 0.90 2.07 1.75 2.48 1.70 1.54 2.15 1.43 1.43 2.16 1.43

D= 0.85 0.85

NO= 164

BATA= 0.01 N= 25

A= 0.32 0.40 0.22 0.22 0.60 0.30 0.30 0.40 0.22 0.30 0.48 0.20 0.16 0.20 0.28 0.28 0.28 0.10 0.11 0.32

A= 0.30 0.12 0.40 0.22 0.30

B= 0.22 0.20 0.20 0.14 0.32 0.18 0.16 0.20 0.16 0.20 0.30 0.15 0.11 0.13 0.16 0.16 0.18 0.10 0.10 0.30

B= 0.15 0.11 0.25 0.15 0.12

D= 2.40 2.69 1.51 1.51 4.13 2.15 2.06 2.69 1.68 2.22 3.48 1.54 1.20 1.47 1.97 1.97 2.05 0.85 0.90 2.66

D= 2.02 0.99 2.70 1.68 1.33

C

NO= 165

BATA= 0.02 N= 36

A= 0.30 0.30 0.30 0.28 0.16 0.22 0.28 0.30 0.50 0.25 0.48 0.20 0.22 0.38 0.32 0.40 0.30 0.22 0.30 0.32

A= 0.21 0.22 0.28 0.40 0.32 0.50 0.42 0.50 0.20 0.38 0.30 0.50 0.30 0.30 0.40 0.20

B= 0.30 0.30 0.20 0.22 0.14 0.16 0.18 0.25 0.28 0.20 0.30 0.18 0.22 0.20 0.28 0.28 0.22 0.15 0.20 0.28

B= 0.16 0.20 0.18 0.25 0.15 0.20 0.15 0.30 0.12 0.22 0.16 0.20 0.10 0.15 0.18 0.14

D= 2.55 2.55 2.22 2.19 1.30 1.65 2.05 2.40 3.50 1.93 3.48 1.64 1.87 2.60 2.60 3.01 2.30 1.64 2.22 2.60

D= 1.63 1.81 2.05 2.90 2.11 3.12 2.53 3.58 1.43 2.55 2.06 3.12 1.77 2.02 2.60 1.51

NO= 166

BATA= 0.02 N= 28

A= 0.60 0.30 0.40 0.38 0.25 0.12 0.20 0.50 0.38 0.36 0.30 0.75 0.20 0.50 0.30 0.36 0.40 0.43 0.30 0.60

A= 0.50 0.40 0.50 0.50 0.30 0.40 0.40 0.50

B= 0.35 0.20 0.35 0.28 0.22 0.10 0.18 0.20 0.22 0.28 0.12 0.60 0.18 0.22 0.22 0.22 0.22 0.20 0.20 0.25

B= 0.18 0.20 0.22 0.40 0.18 0.30 0.18 0.25

D= 4.25 2.22 3.24 2.91 2.03 0.96 2.15 3.12 2.69 2.31 1.38 5.90 1.64 3.23 2.30 2.59 2.78 3.04 2.22 3.80

D= 3.02 2.69 3.23 3.94 2.15 3.08 2.60 3.37

NO= 167

BATA= 0.23 N= 25

A= 0.58 0.35 0.30 0.32 0.30 0.30 0.23 0.50 0.30 0.35 0.40 0.40 0.50 0.32 0.32 0.40 0.20 0.30 0.32 0.50

A= 0.40 0.30 0.40 0.20 0.18

B= 0.35 0.20 0.20 0.20 0.18 0.18 0.18 0.26 0.20 0.28 0.20 0.25 0.16 0.20 0.20 0.28 0.16 0.25 0.20 0.20

B= 0.25 0.20 0.22 0.12 0.12

D= 4.16 2.46 2.22 2.32 2.15 2.15 1.80 3.41 2.22 2.76 2.69 2.90 2.90 2.32 2.32 3.01 1.58 4.60 2.32 3.12

D= 2.90 2.22 2.76 1.43 1.33

NO= 168

BATA= 0.03 N= 28

A= 0.50 0.50 0.20 0.30 0.50 0.35 0.42 0.38 0.22 0.56 0.50 0.18 0.35 0.30 0.50 0.28 0.40 0.20 0.32 0.25

A= 0.36 0.38 0.40 0.40 0.48 0.30 0.50 0.50

B= 0.[illegible]0 0.32 0.14 0.15 0.25 0.20 0.30 0.22 0.20 0.[illegible]0 0.[illegible]0 0.15 0.20 0.20 0.35 0.35 0.30 0.13 0.28 0.22

B= 0.28 0.20 0.16 0.28 0.22 0.20 0.20 0.20

D= 3.58 3.65 1.64 2.02 3.50 2.46 3.18 2.69 1.81 3.76 3.58 1.47 2.46 2.22 3.76 2.56 3.08 1.64 2.60 2.03

D= 2.81 2.60 2.50 3.01 3.14 2.22 3.17 3.12

NO= 169

BATA= 0.03 N= 30

A= 0.40 0.42 0.35 0.38 0.50 0.30 0.35 0.30 0.40 0.22 0.32 0.30 0.50 0.30 0.38 0.58 0.40 0.30 0.55 0.30

A= 0.50 0.40 0.50 0.35 0.18 0.22 0.40 0.12 0.60 0.55

B= 0.30 0.32 0.25 0.26 0.18 0.10 0.20 0.20 0.22 0.20 0.22 0.12 0.30 0.20 0.15 0.27 0.12 0.15 0.30 0.20

B= 0.35 0.30 0.40 0.18 0.12 0.15 0.30 0.12 0.30 0.23

D= 3.08 3.25 2.65 2.91 3.02 1.77 2.46 2.22 2.78 1.31 2.40 1.88 3.58 2.22 2.36 3.81 2.27 2.02 3.81 2.22

D= 3.76 3.08 3.44 2.33 1.33 1.75 3.08 1.02 4.04 2.35

NO= 170

BATA= 0.04 N= 33

A= 0.40 0.40 0.30 0.30 0.70 0.40 0.23 0.40 0.32 0.30 0.30 0.42 0.50 0.20 0.50 0.58 0.30 0.65 0.60 0.52

A= 0.55 0.40 0.25 0.40 0.67 0.40 0.60 0.25 0.50 0.30 0.50 0.32 0.30

B= 0.30 0.25 0.18 0.12 0.32 0.25 0.20 0.25 0.22 0.20 0.20 0.30 0.30 0.18 0.30 0.30 0.22 0.45 0.30 0.30

B= 0.30 0.25 0.15 0.25 0.25 0.25 0.30 0.18 0.32 0.20 0.30 0.20 0.12

D= 3.05 2.90 2.15 1.88 4.57 2.90 2.12 2.90 2.40 2.22 2.22 3.18 3.58 1.64 3.58 3.95 2.30 4.85 4.04 3.67

D= 3.81 2.90 1.79 2.90 4.09 2.90 4.04 1.90 3.65 2.22 3.58 2.32 1.58

NO= 171

BATA= 0.04 N= 27

A= 0.80 0.50 0.40 0.40 0.30 0.40 0.70 0.60 0.50 0.[illegible] 0.50 0.22 0.40 0.45 0.60 0.42 0.70 0.70 0.30 0.50

A= 0.60 0.40 0.50 0.40 0.40 0.40 0.40

B= 0.30 0.28 0.25 0.30 0.25 0.15 0.40 0.40 0.30 0.[illegible] 0.30 0.20 0.15 0.32 0.30 0.35 0.26 0.30 0.25 0.40

B= 0.45 0.25 0.20 0.18 0.20 0.25 0.12

D= 4.89 3.50 2.90 3.08 2.40 2.45 4.92 4.44 3.58 3.[illegible] 3.58 1.31 2.45 3.41 4.04 3.35 4.27 4.47 2.40 3.94

D= 4.62 2.90 3.12 2.60 2.69 2.90 2.27

NO= 172

```
BATA=   0.04      N=    29
A=  0.50  0.55  0.30  0.30  0.35  0.45  0.38  0.40  0.80  0.55  0.70  0.40  0.65  0.60  0.55  0.40  0.40  0.60  0.22  0.42
A=  0.50  0.30  0.40  0.50  0.40  0.70  0.22  0.50
B=  0.35  0.45  0.35  0.28  0.25  0.30  0.22  0.30  0.30  0.30  0.40  0.32  0.40  0.32  0.40  0.42  0.35  0.22  0.20  0.18
B=  0.18  0.30  0.35  0.30  0.30  0.30  0.22  0.45
D=  3.76  4.36  3.76  2.49  2.65  3.33  2.69  3.08  4.89  3.31  4.92  3.15  4.69  4.13  4.19  3.45  3.24  3.64  1.81  2.69
D=  3.02  2.55  3.24  3.58  3.08  4.47  1.87  4.09

NO=  173
BATA=   0.05      N=    30
A=  0.55  0.38  0.50  0.50  0.40  0.50  0.50  0.40  0.30  0.30  0.40  0.30  0.30  0.30  0.40  0.60  0.60  0.60  0.50  0.40
A=  0.40  0.30  0.40  0.40  0.40  0.60  0.30  0.30  0.40  0.50
B=  0.40  0.22  0.30  0.35  0.20  0.30  0.35  0.25  0.25  0.22  0.22  0.30  0.22  0.22  0.30  0.32  0.32  0.30  0.40  0.40
B=  0.30  0.20  0.30  0.20  0.30  0.25  0.20  0.25  0.25  0.30
D=  4.19  2.69  3.58  3.76  2.69  3.58  3.76  2.90  2.40  2.30  2.78  2.55  2.30  2.30  3.08  4.13  4.13  4.04  3.94  3.39
D=  3.08  2.22  3.08  2.69  3.08  3.80  2.22  2.40  2.90  3.58

NO=  174
BATA=   0.05      N=    29
A=  0.50  0.50  0.52  0.32  0.70  0.50  0.50  0.50  0.40  0.70  0.40  0.55  0.40  0.50  0.50  0.40  0.40  0.32  0.50  0.40
A=  0.55  0.85  0.40  0.50  0.22  0.70  0.50  0.50  0.50
B=  0.30  0.35  0.30  0.30  0.45  0.30  0.30  0.40  0.30  0.30  0.40  0.35  0.30  0.20  0.40  0.30  0.30  0.22  0.30  0.22
B=  0.25  0.40  0.30  0.30  0.20  0.30  0.25  0.30  0.20
D=  3.53  3.76  3.57  2.66  5.12  3.58  3.58  3.94  3.08  4.47  3.39  4.01  3.08  3.12  3.94  3.08  3.08  2.40  3.58  2.78
D=  3.59  5.60  3.08  3.58  1.81  4.47  3.37  3.58  3.12
IHC217I
TRACEBACK FOLLOWS-   ROUTINE    ISN   REG. 14    REG. 15    REG. 0     REG. 1
                     IBCOM            0004393C   00043090   0000001E   00043838
                     MAIN             0000AC2A   0103F038   FD000006   000447F8
ENTRY POINT=  0103F038
```

117

APPENDIX E

BUBBLE SIZE DISTRIBUTIONS

During Test Run No. 160, photographs were taken of flow conditions in the perspex tube between the crystals. The photographs were analyzed in the manner described in section 4.2 of this thesis. From the measurements on the photographs, it was possible to calculate the diameter of an equivolume sphere (appendix D) for the ellipsoidal bubbles observed. These diameters were used as input into the standard University of Manitoba Basic Statistics Program from which mean diameters, standard deviations and frequency distribution information were obtained. These are shown in table E.1.

The bubble diameter distributions are plotted in Figs. E.1 to E.14. The symbol F is the frequency density (frequency divided by class width) and B is the void fraction.

Table E.1

Tabulated Data for Bubble Distributions. (Test Run No. 160)

Test No.	B void fraction	Identi-fication on photo	No. of bubbles	Arith. Mean Dia. (mm)	Std. Devia-tion (mm)	Skewness	Class (mm)	Freq.	Fig. No.
161	0.006	161	13	1.0692	0.6088	0.5238	0.0-0.5	3	E.1
							0.5-1.0	4	
							1.0-1.5	4	
							1.5-2.0	0	
							2.0-2.5	2	
162	0.008		21	0.8762	0.5915	0.3973	0.0-0.5	10	E.2
							0.5-1.0	3	
							1.0-1.5	5	
							1.5-2.0	2	
							2.0-2.5	1	
163	0.011		22	1.6500	0.7176	0.8323	0.0-0.5	0	E.3
							0.5-1.0	4	
							1.0-1.5	7	
							1.5-2.0	6	
							2.0-2.5	4	
							2.5-3.0	0	
							3.0-3.5	0	
							3.5-4.0	1	
164	0.015	164	25	2.0440	0.7719	0.4987	0.0-0.5	0	E.4
							0.5-1.6	3	
							1.0-1.5	3	
							1.5-2.0	8	
							2.0-2.5	5	
							2.5-3.0	4	
							3.0-3.5	1	
							3.5-4.0	0	
							4.0-4.5	1	
165	0.018		36	2.3111	0.6013	0.2178	0.0-0.5	0	E.5
							0.5-1.0	0	
							1.0-1.5	3	
							1.5-2.0	9	
							2.0-2.5	12	
							2.5-3.0	7	
							3.0-3.5	4	
							3.5-4.0	1	

Table E.1 (cont.)

Test No.	B void fraction	Identi-fication on photo	No. of bubbles	Arith. Mean Dia. (mm)	Std. Devia-tion (mm)	Skewness	Class (mm)	Freq.	Fig. No.
166	0.021		28	2.8429	0.9291	0.6733	0.0-0.5 0.5-1.0 1.0-1.5 1.5-2.0 2.0-2.5 2.5-3.0 3.0-3.5 3.5-4.0 4.0-4.5 4.5-5.0 5.0-5.5 5.5-6.0	0 1 0 3 5 9 6 2 1 0 0 1	E.6
167	0.023		25	2.5560	0.7649	0.9254	0.0-0.5 0.5-1.0 1.0-1.5 1.5-2.0 2.0-2.5 2.5-3.0 3.0-3.5 3.5-4.0 4.0-4.5 4.5-5.0	0 0 2 2 10 7 2 0 1 1	E.7
168	0.027		28	2.7286	0.9686	0.2395	0.0-0.5 0.5-1.0 1.0-1.5 1.5-2.0 2.0-2.5 2.5-3.0 3.0-3.5 3.5-4.0	0 0 1 5 5 6 6 5	E.8
169	0.031	169	30	2.6967	0.8265	0.3837	0.0-0.5 0.5-1.0 1.0-1.5 1.5-2.0 2.0-2.5 2.5-3.0 3.0-3.5 3.5-4.0	0 1 1 5 8 4 4 7	E.9

Table E.1 (cont.)

Test No.	B void fraction	Identi-fication on photo	No. of bubbles	Arith. Mean Dia. (mm)	Std. Devia-tion (mm)	Skewness	Class (mm)	Freq.	Fig. No.
170	0.039		33	2.9727	0.8819	0.2366	0.0-0.5	0	E.10
							0.5-1.0	0	
							1.0-1.5	0	
							1.5-2.0	5	
							2.0-2.5	8	
							2.5-3.0	6	
							3.0-3.5	2	
							3.5-4.0	9	
							4.0-4.5	1	
							4.5-5.0	2	
171	0.042		27	3.3333	0.8651	0.0110	0.0-0.5	0	E.11
							0.5-1.0	0	
							1.0-1.5	0	
							1.5-2.0	1	
							2.0-2.5	5	
							2.5-3.0	5	
							3.0-3.5	6	
							3.5-4.0	4	
							4.0-4.5	3	
							4.5-5.0	3	
172	0.044	172	28	3.4500	0.8373	0.3299	0.0-0.5	0	E.12
							0.5-1.0	0	
							1.0-1.5	0	
							1.5-2.0	2	
							2.0-2.5	2	
							2.5-3.0	4	
							3.0-3.5	7	
							3.5-4.0	5	
							4.0-4.5	5	
							4.5-5.0	3	
173	0.047		30	3.1200	0.6562	0.0906	0.0-0.5	0	E.13
							0.5-1.0	0	
							1.0-1.5	0	
							1.5-2.0	0	
							2.0-2.5	8	
							2.5-3.0	6	
							3.0-3.5	5	
							3.5-4.0	8	
							4.0-4.5	3	

Table E.1 (cont.)

Test No.	B void fraction	Identi-fication on photo	No. of bubbles	Arith. Mean Dia. (mm)	Std. Devia-tion (mm)	Skewness	Class (mm)	Freq.	Fig. No.
174	0.053	174	29	3.5310	0.7579	0.6314	0.0-0.5	0	E.14
							0.5-1.0	0	
							1.0-1.5	0	
							1.5-2.0	1	
							2.0-2.5	1	
							2.5-3.0	2	
							3.0-3.5	9	
							3.5-4.0	12	
							4.0-4.5	2	
							4.5-5.0	0	
							5.0-5.5	1	
							5.5-6.0	1	

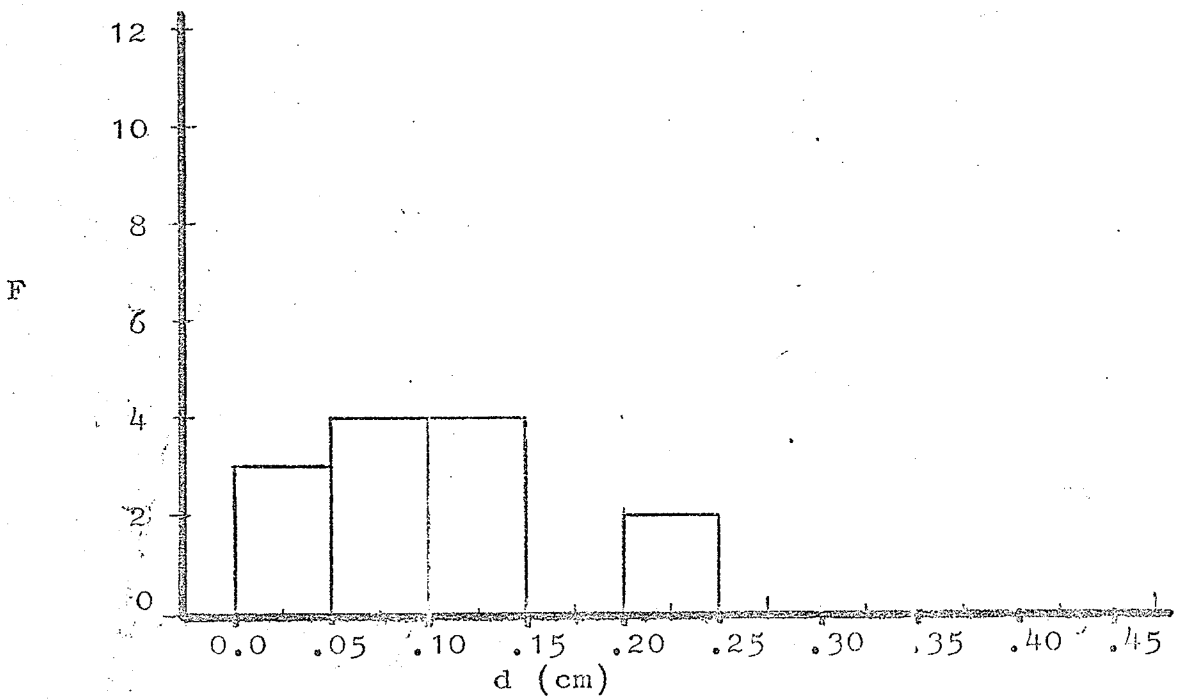

Fig. E.1 Bubble distribution, B=0.006

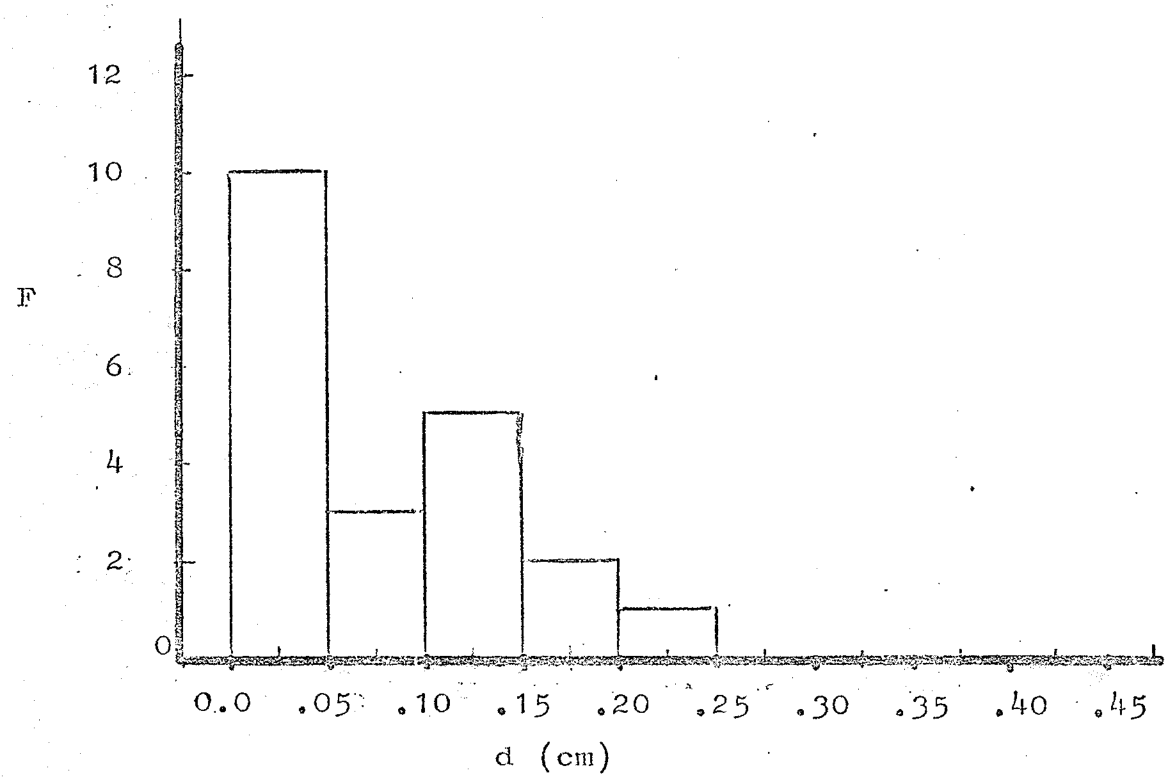

Fig. E.2 Bubble distribution, B=0.008

Fig. E.1,2

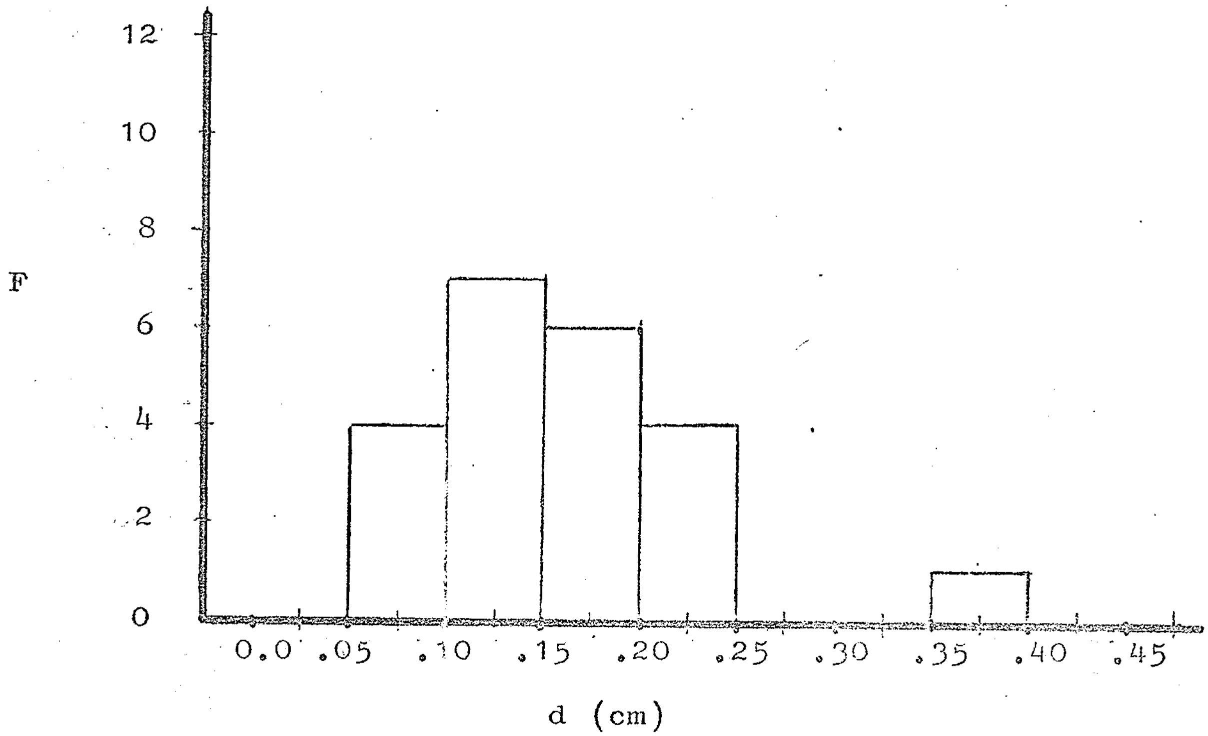

Fig. E.3 Bubble distribution, B=0.011

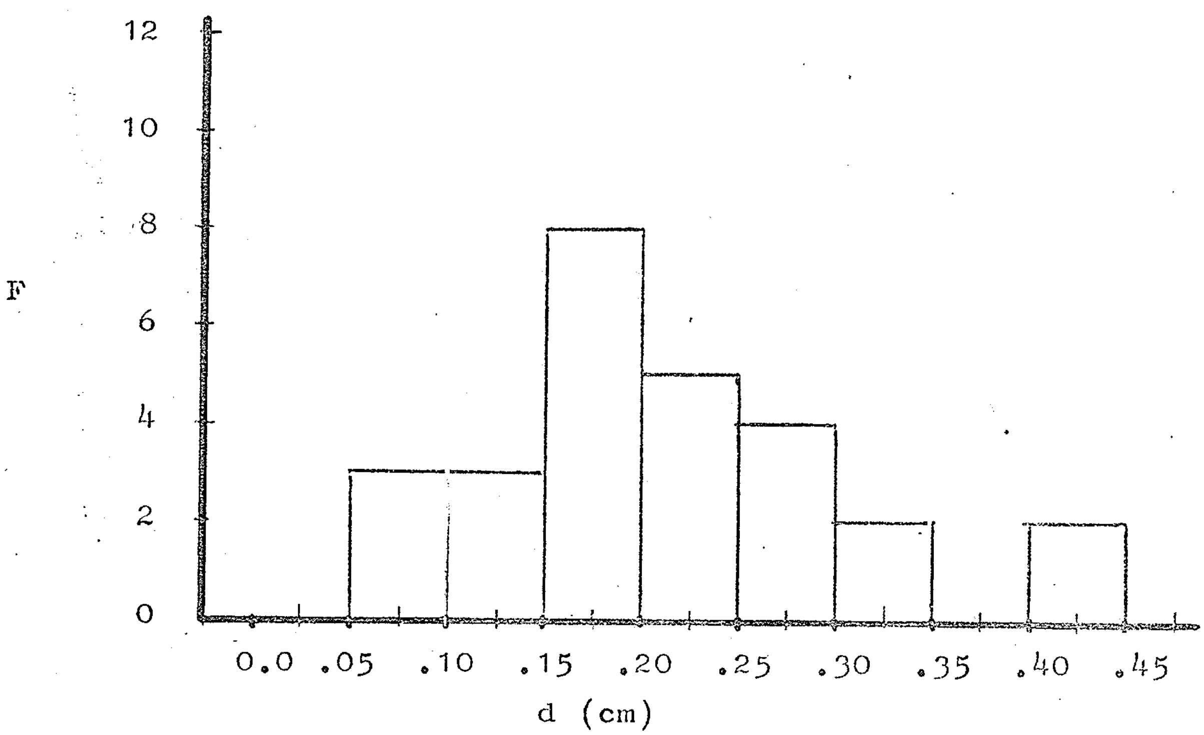

Fig. E.4 Bubble distribution, B=0.015

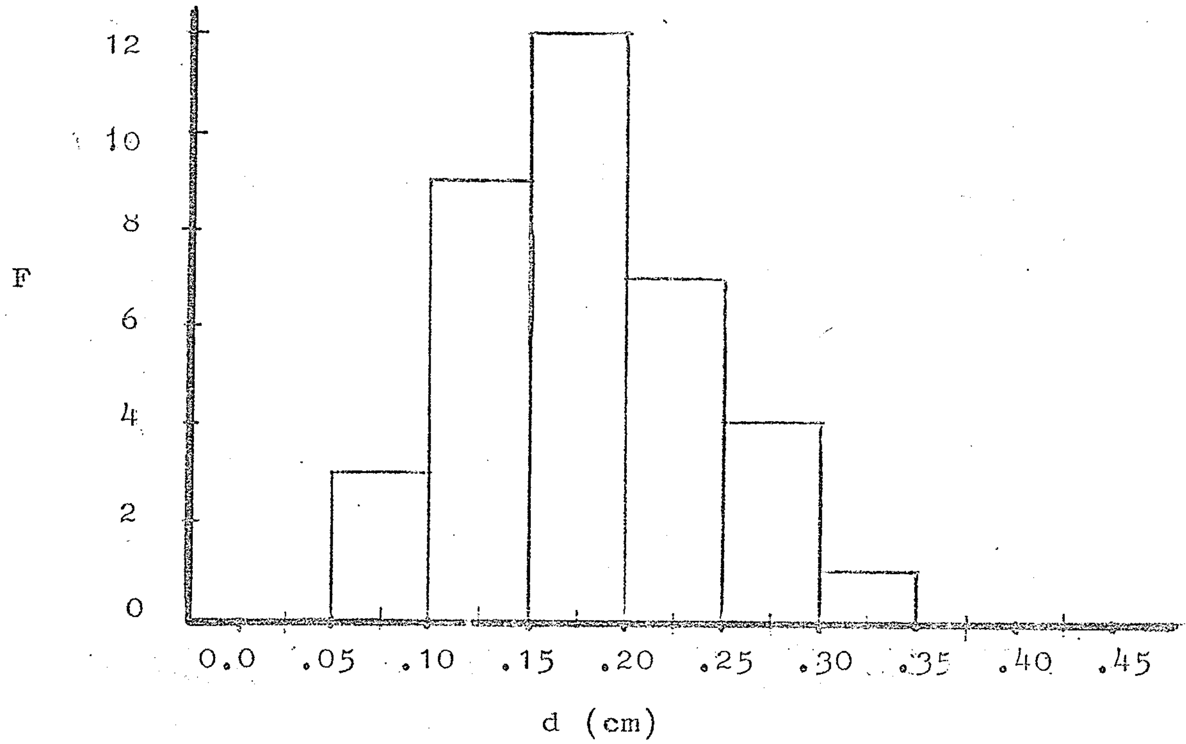

Fig. E.5 Bubble distribution, B=0.018

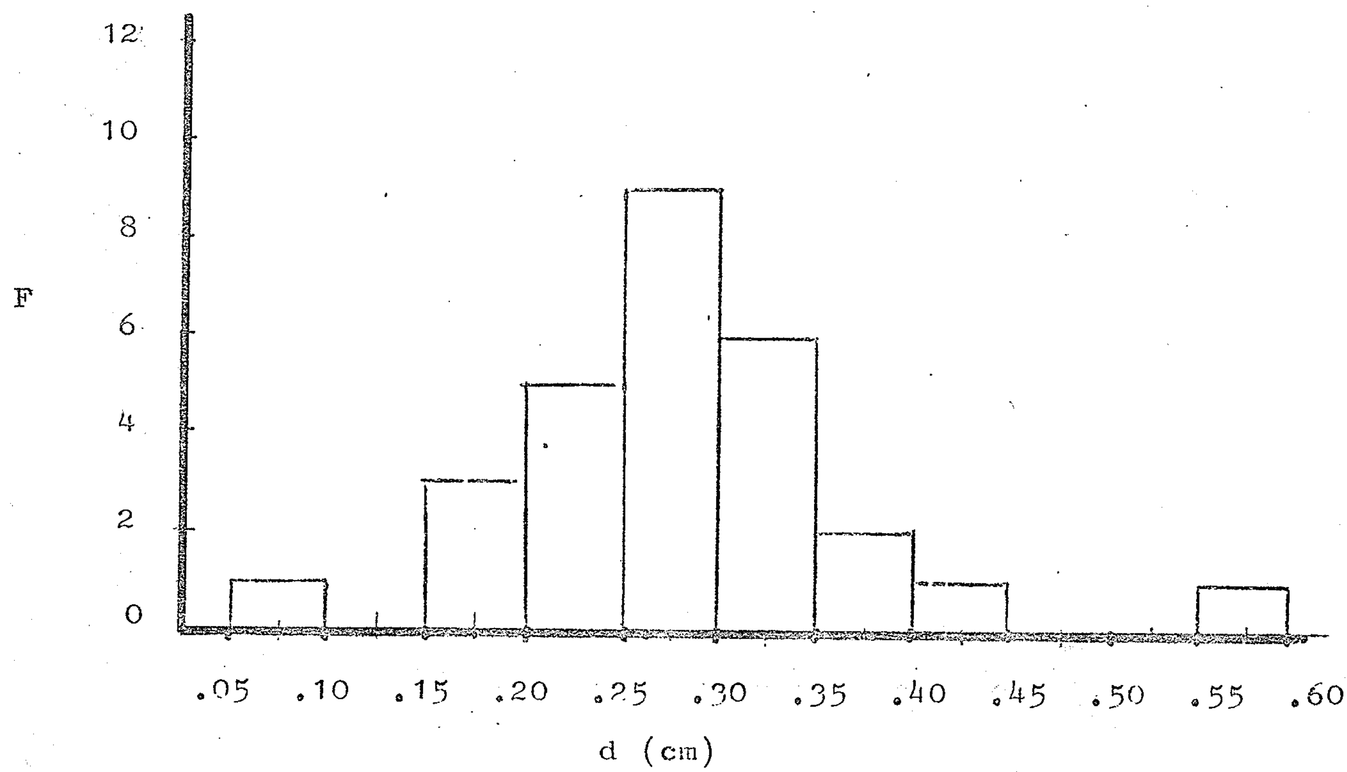

Fig. E.6 Bubble distribution, B=0.021

Fig.E.5,6

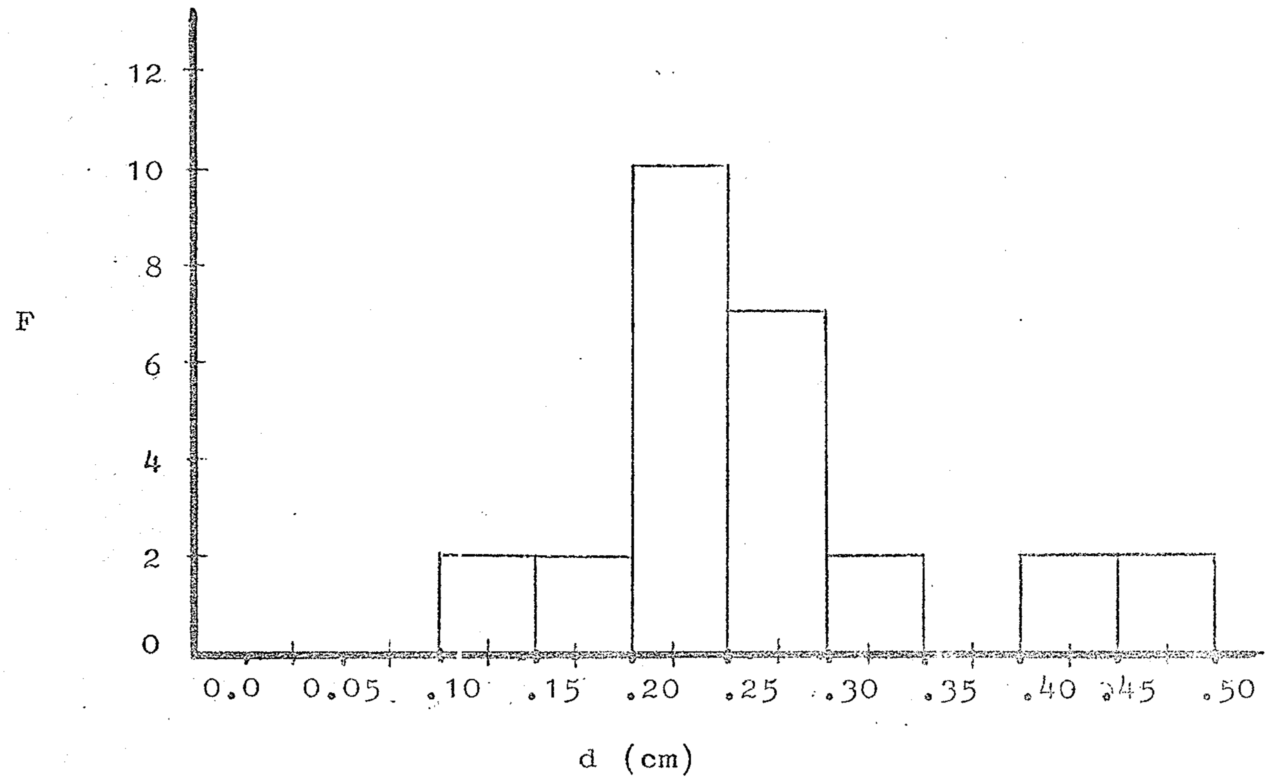

Fig. E.7 Bubble distribution, B=0.023

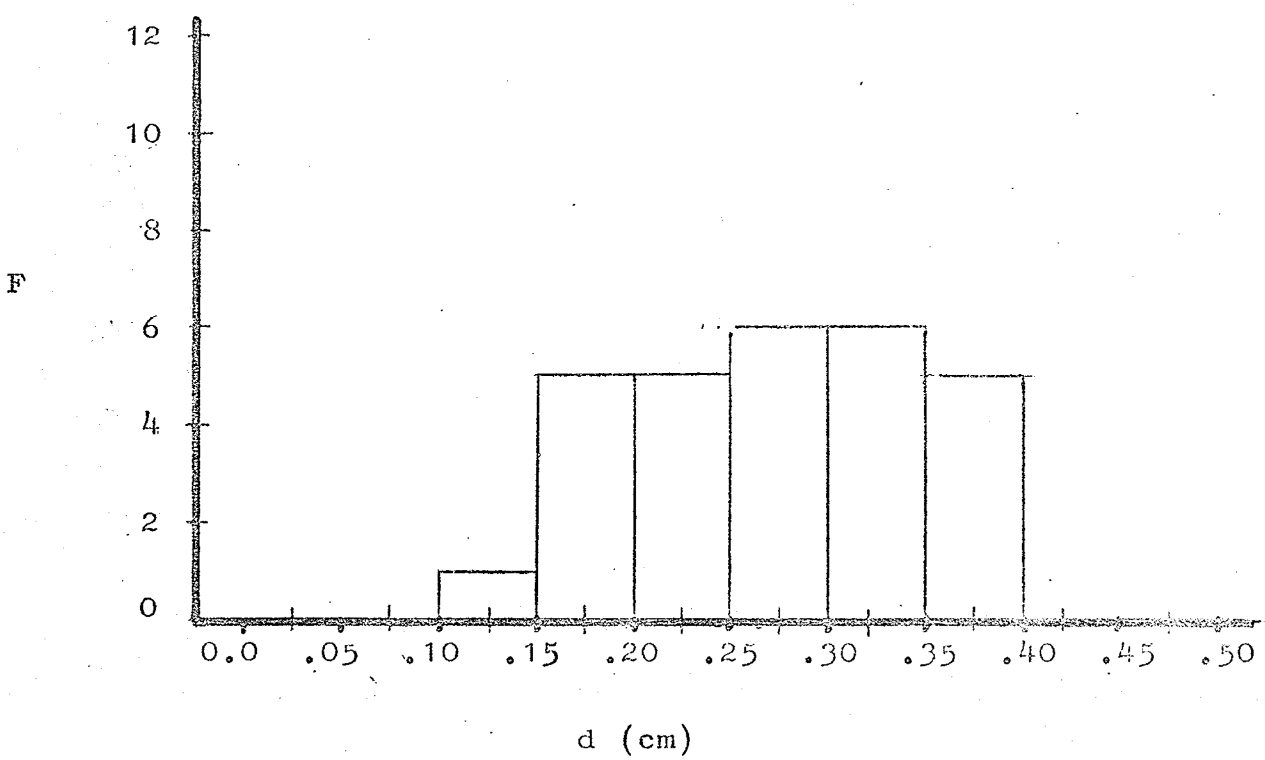

Fig. E.8 Bubble distribution, B=0.027

Fig. E.7,8

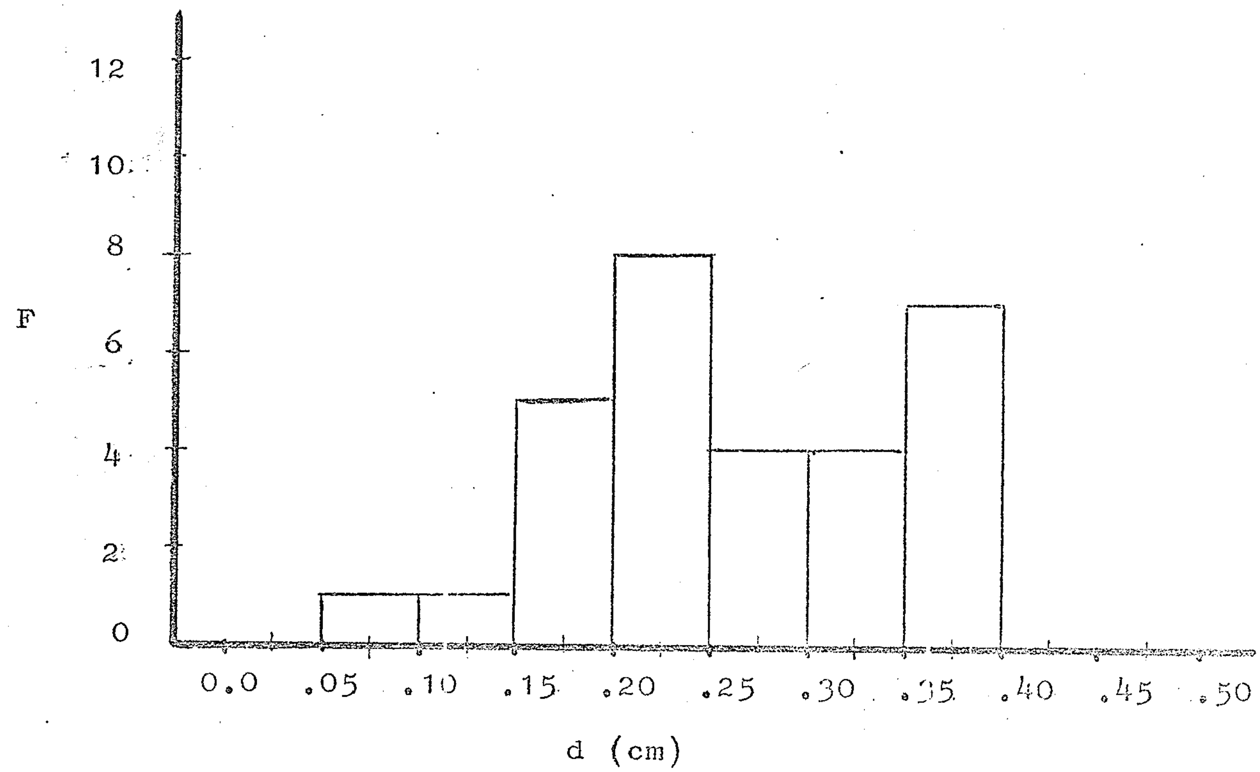

Fig. E.9 Bubble distribution, B=0.031

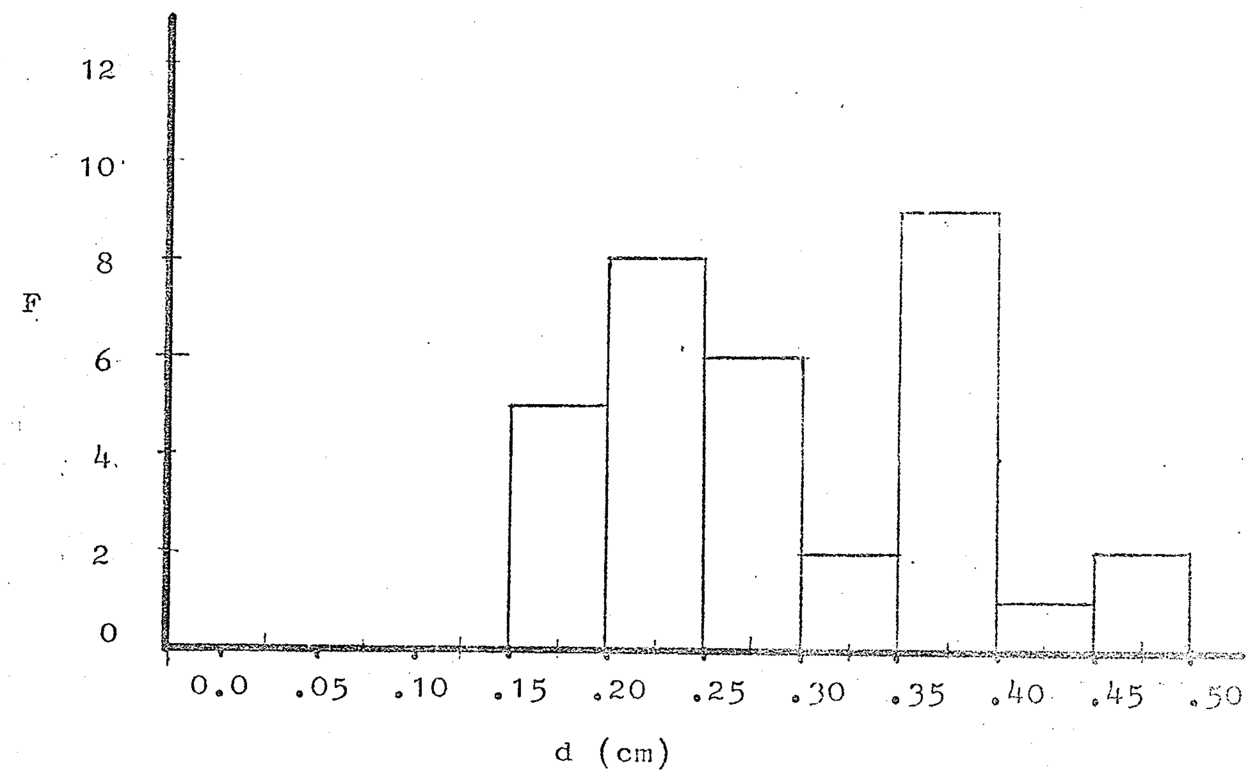

Fig. E.10 Bubble distribution, B=0.039

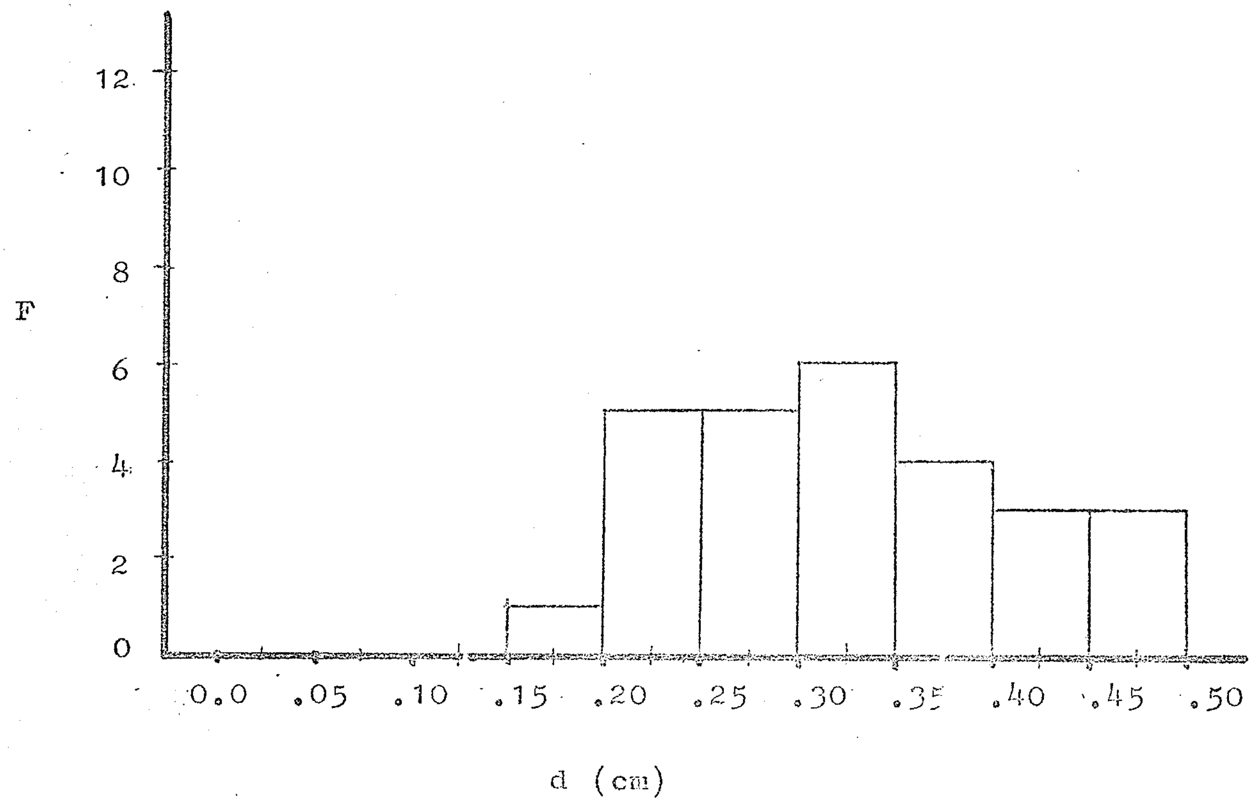

Fig. E.11 Bubble distribution, B=0.042

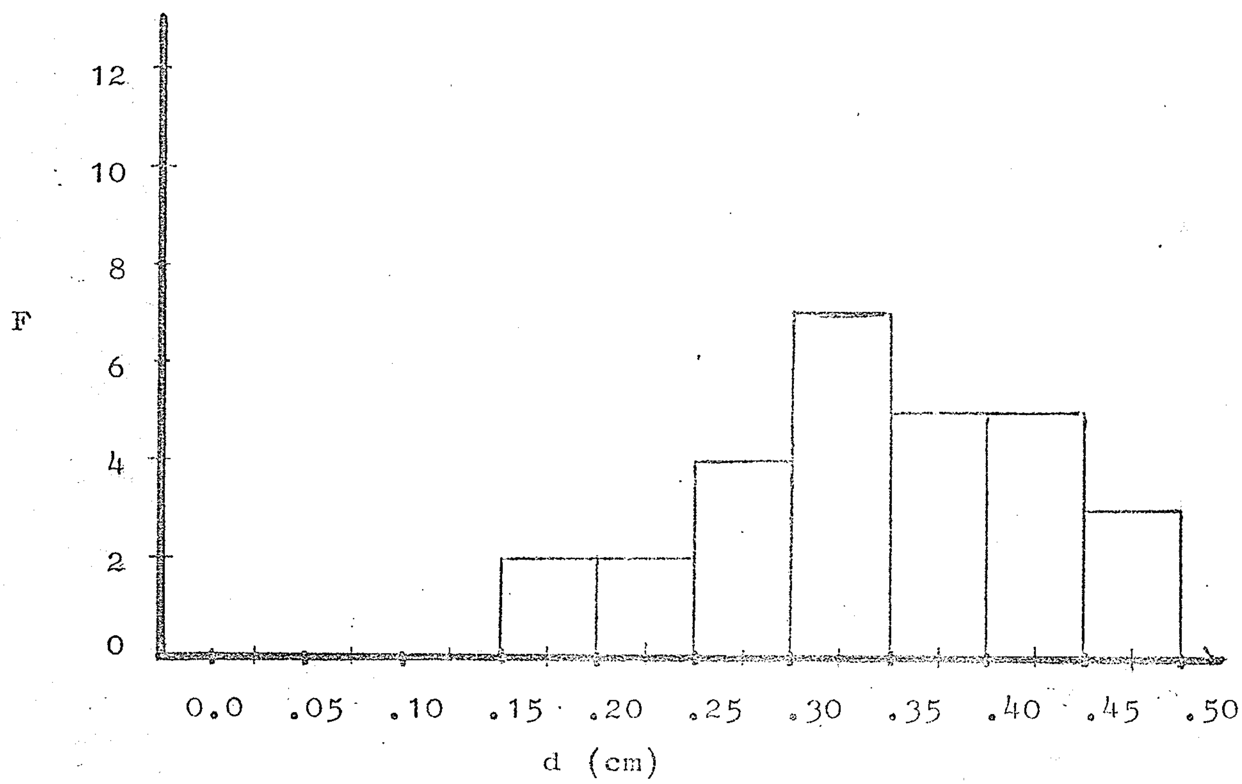

Fig. E.12 Bubble distribution, B=0.044

Fig. E.11,12

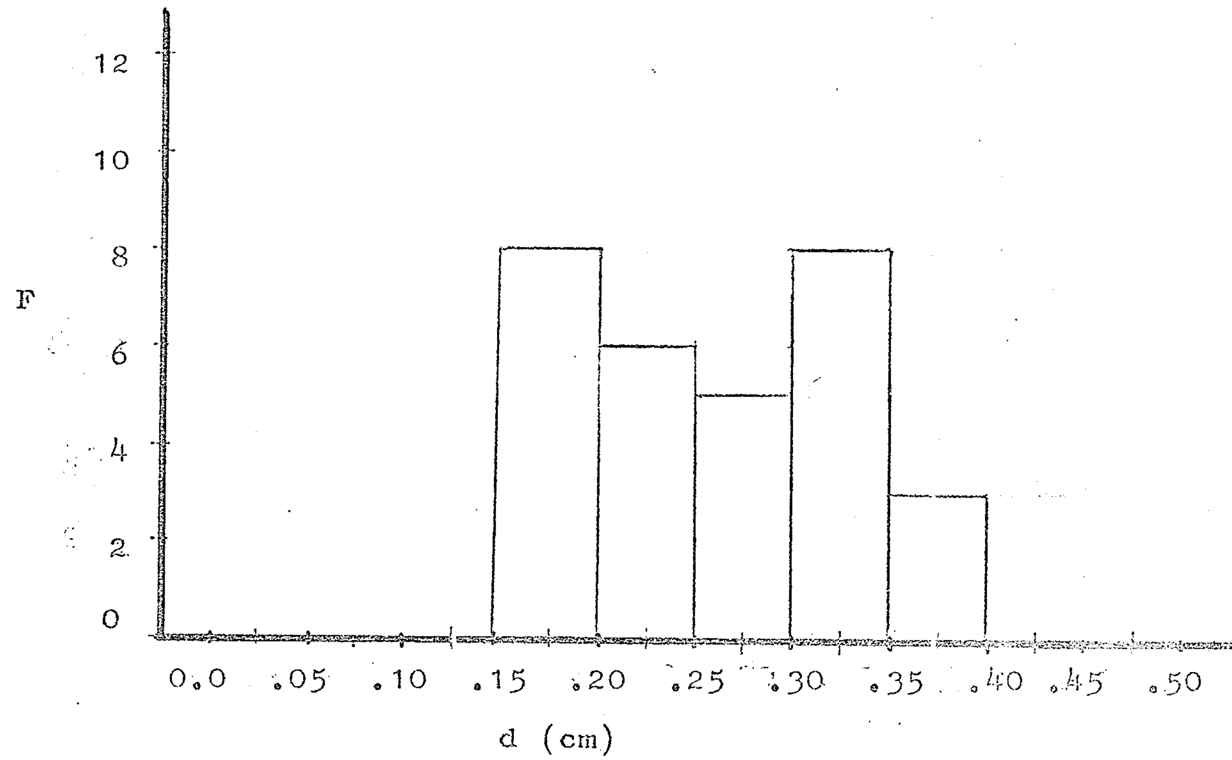

Fig. E.13 Bubble distribution, B=0.047

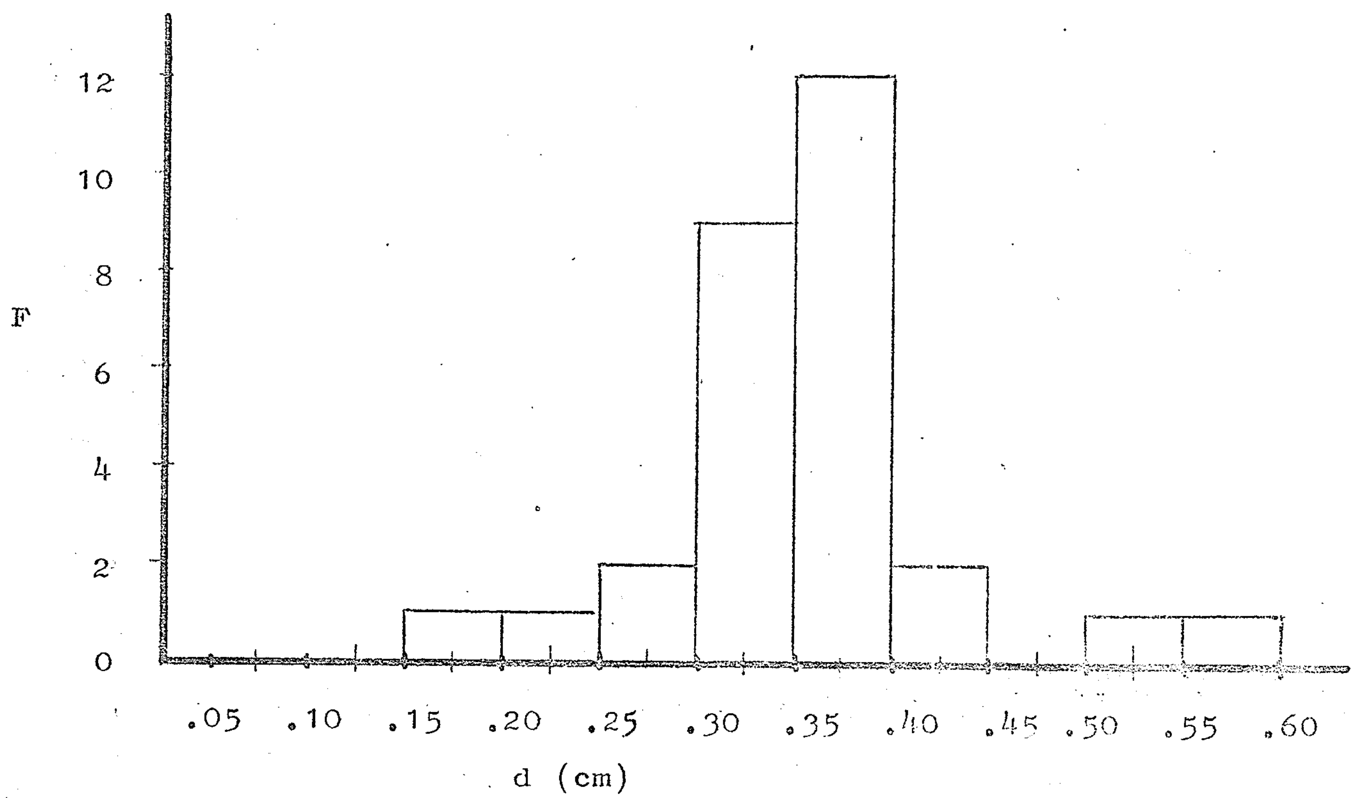

Fig. E.14 Bubble distribution, B=0.053

Fig. E.13,14

APPENDIX F

ESTIMATE OF THE ERROR IN MEASURING THE ACOUSTIC VELOCITY

The errors in measuring the acoustic velocity arise from errors in measurement of the distance between the crystal faces and in measurement of transit times. The former error is estimated at approximately 1%. The errors in measuring the transit times on the oscilloscope may be estimated as approximately 3%, in single phase fluids and low void fraction mixtures and 4% in high void fraction mixtures. (At the high void fractions, the error in measuring the transit time is greater because of distortion of the wave train making the front of the wave train not so well defined compared with single phase and low void fraction conditions.) Combining these errors in the manner prescribed by Kline and McClintock (Mechanical Engineering, vol.37,p.3, 1953) would yield errors in the acoustic velocity of 3.2% for single phase and low void fraction conditions and 4.1% for high void fractions("error" here has the same meaning as "uncertainty interval" in Kline and McClintock with "odds" of approximately 20 to 1).

In the body of the thesis, a comparison was made between acoustic velocities measured in the present work and the corresponding values from the literature. The information appears in Tables 2 and 3. It can be seen there that the maximum deviation from the literature values is 3.6%. The errors estimated above would therefore appear to be realistic.